

Extracellular Signal-Regulated Kinase as an Integrative Synapse-to-Nucleus Signal

by

Shenyu Zhai

Department of Neurobiology  
Duke University

Date: \_\_\_\_\_

Approved:

\_\_\_\_\_  
Ryohei Yasuda, Co-Supervisor

\_\_\_\_\_  
Anne West, Co-Supervisor

\_\_\_\_\_  
Richard Mooney, Chair

\_\_\_\_\_  
Serena Dudek

Dissertation submitted in partial fulfillment of  
the requirements for the degree of Doctor of Philosophy  
in the Department of Neurobiology in the Graduate School of  
Duke University

2013

ABSTRACT

Extracellular Signal-Regulated Kinase as an Integrative Synapse-to-Nucleus Signal

by

Shenyu Zhai

Department of Neurobiology  
Duke University

Date: \_\_\_\_\_

Approved:

\_\_\_\_\_  
Ryohei Yasuda, Co-Supervisor

\_\_\_\_\_  
Anne West, Co-Supervisor

\_\_\_\_\_  
Richard Mooney, Chair

\_\_\_\_\_  
Serena Dudek

An abstract of a dissertation submitted in partial  
fulfillment of the requirements for the degree  
of Doctor of Philosophy in the Department of  
Neurobiology in the Graduate School  
of Duke University

2013

Copyright by  
Shenyu Zhai  
2013

## **Abstract**

The late phase of long-term synaptic potentiation (LTP) at glutamatergic synapses, which is thought to underlie the long lasting memory (at least hours), requires gene transcription in the nucleus. However, it remains elusive how signaling initiated at synapses during induction of LTP is transmitted into the nucleus to commence transcription. Using a combination of two-photon glutamate uncaging and a genetically encoded FRET sensor, I found that induction of synapse-specific LTP at only a few (3-7) dendritic spines leads to pronounced activation of extracellular signal-regulated kinase (ERK) in the nucleus and downstream phosphorylation of transcription factors, cAMP-response element-binding protein (CREB) and E26-like protein-1 (Elk-1). The underlying molecular mechanism of this nuclear ERK activation was investigated: it seems to require activation of NMDA receptors, metabotropic glutamate receptors, and the classical Ras pathway. I also found that the spatial pattern of synaptic stimulation is critical: spatially dispersed stimulation over multiple dendritic branches activated nuclear ERK much more efficiently than clustered stimulation within a single dendritic branch. In sum, these results suggest that biochemical signals could be transmitted from individual spines to the nucleus following LTP induction and that such synapse-to-nucleus signaling requires integration across multiple dendritic branches.

## Contents

<b>Abstract</b> .....	<b>iv</b>
<b>Contents</b> .....	<b>v</b>
<b>List of Figures</b> .....	<b>ix</b>
<b>List of Abbreviations</b> .....	<b>xi</b>
<b>Acknowledgements</b> .....	<b>xv</b>
<b>Chapter 1. Introduction</b> .....	<b>1</b>
1.1 Long-term synaptic plasticity in the hippocampus .....	1
1.1.1 LTP-discovery, characteristics, relationship to learning and memory .....	1
1.1.2 Hippocampus.....	3
1.1.3 Hippocampal CA3-CA1 LTP .....	5
1.2 Extracellular signal-regulated kinase (ERK).....	13
1.2.1 ERK belongs to MAPK family .....	13
1.2.2 Signaling pathways upstream of ERK.....	13
1.2.3 Regulation of ERK signaling by scaffolding proteins .....	15
1.2.4 Overview of functions of ERK in neurons .....	16
1.2.5 ERK in long-term synaptic potentiation (LTP).....	16
1.2.6 Implications in human neurological diseases / human memory.....	26
1.3 Structural plasticity .....	28
1.3.1 Structural features of dendritic spines .....	28
1.3.2 LTP-associated structural remodeling in neurons.....	30

1.3.3 Synaptic plasticity at the level of a single dendritic spine.....	31
1.4 Experimental Rationale and Specific Aims.....	32
<b>Chapter 2. Materials and Methods .....</b>	<b>38</b>
2.1 DNA constructs, antibodies, and reagents .....	38
2.2 Dissociated Culture, Transfection and BDNF stimulation.....	39
2.3 Hippocampal slice culture and gene-gun transfection .....	39
2.4 Two-photon fluorescence lifetime imaging.....	40
2.5 2pFLIM data analyses .....	42
2.6 Two-photon glutamate uncaging and spine enlargement .....	43
2.7 GCaMP imaging and analysis .....	43
2.8 Immunohistochemistry and confocal immunofluorescence imaging.....	44
2.9 Live imaging of mEGFP-ERK2.....	45
2.10 Statistical Analysis.....	46
<b>Chapter 3. ERK activation in the nucleus elicited by LTP induction at individual dendritic spines .....</b>	<b>47</b>
3.1 Introduction.....	47
3.2 Results .....	50
3.2.1 Validation of EKAR in dissociated neuronal culture .....	50
3.2.2 ERK activity during structural plasticity of a single dendritic spine.....	51
3.2.3 Activation of ERK in the nucleus by inducing sLTP at a few dendritic spines	54
3.2.4 Increase in phospho-ERK level in the nucleus following LTP induction at a few dendritic spines.....	58
3.2.5 Nuclear translocation of ERK2 after inducing sLTP at a few dendritic spines	61

3.3 Discussion.....	64
<b>Chapter 4. Molecular mechanisms underlying the nuclear ERK activity increase caused by inducing structural plasticity at a few dendritic spines .....</b>	<b>68</b>
4.1 Introduction.....	68
4.2 Results .....	69
4.2.1 (Differential) molecular mechanisms underlying nuclear ERK activation and sLTP.....	69
4.2.2 GCaMP imaging reveals the spread and source of Ca <sup>2+</sup> evoked by glutamate uncaging .....	73
4.3 Discussion.....	77
4.3.1 NMDAR-dependence and VGCC-independence of nuclear ERK activation...	77
4.3.2 Role of intracellular Ca <sup>2+</sup> release in nuclear ERK activation.....	80
4.3.3 Role of mGluR in nuclear ERK activation.....	83
4.3.4 Calcium-permeable AMPA receptors .....	86
<b>Chapter 5. Spatiotemporal integration of ERK activity .....</b>	<b>87</b>
5.1 Introduction.....	87
5.2 Results .....	88
5.2.1 Relationship between nuclear ERK activation and stimulated spine number .	88
5.2.2 Relationship between nuclear ERK activation and number of stimulated dendrites .....	92
5.2.3 Dendritic ERK activation induced by sLTP induction.....	94
5.2.4 Propagating ERK activity as a synapse-to-nucleus signal.....	97
5.2.5 Integration of ERK activity over time.....	100

5.3 Discussion.....	103
<b>Chapter 6. Nuclear targets for ERK activity increase triggered by sLTP induction at a few spines.....</b>	<b>108</b>
6.1 Introduction.....	108
6.2 Results .....	109
6.2.1 Seven-spine stimulation induces phosphorylation of transcription factors ...	109
6.2.2 Phosphorylation of CREB and Elk-1 is mediated by ERK activity.....	112
6.3 Discussion.....	114
6.3.1 ERK-mediated CREB phosphorylation is triggered by activating a few spines .....	114
6.3.2 ERK-mediated Elk-1 phosphorylation is triggered by activating a few spines .....	117
6.3.3 Future directions.....	119
<b>Chapter 7. General discussions and future directions.....</b>	<b>121</b>
Why ERK activity is long-lasting? .....	122
ERK pathway as a synapse-to-nucleus signal .....	126
<b>References .....</b>	<b>129</b>
<b>Biograpy.....</b>	<b>161</b>

## List of Figures

Figure 1.1 Anatomical structure of the hippocampus viewed in the sagittal plane.....	4
Figure 1.2 Morphology of a hippocampal CA1 neuron. ....	5
Figure 1.3 Signaling pathways upstream of ERK.....	13
Figure 1.4 Regulation of general translation by ERK pathway. ....	22
Figure 3.1 Two-photon glutamate uncaging.....	48
Figure 3.2 Fluorescence lifetime of EKAR as the major readout of ERK activity .....	49
Figure 3.3 Decrease in fluorescence lifetime of EKAR caused by BDNF stimulation in dissociated culture of cortical neurons .....	51
Figure 3.4 EKAR fluorescence lifetime was not altered by inducing structural plasticity at a single dendritic spine .....	53
Figure 3.5 Nuclear ERK is activated by inducing sLTP at a few dendritic spines.....	56
Figure 3.6 EKAR lifetime change in response to sLTP induction at near physiological temperature.....	58
Figure 3.7 Increase in phospho-ERK in the nucleus following stimulation of 7 spines....	60
Figure 3.8 Nuclear translocation of ERK2 was induced by 7-spine stimulation.....	63
Figure 4.1 Pharmacological analysis of nuclear ERK activity increase in response to 7-spine stimulation.....	72
Figure 4.2 Effects of pharmacological agents and genetic manipulation on spine structural LTP (sLTP). ....	73
Figure 4.3 GCaMP3 imaging reveals spread and sources of Ca <sup>2+</sup> transient evoked by glutamate uncaging.....	76
Figure 5.1 Relationship between the number of stimulated dendritic spines and change in fluorescence lifetime of EKAR <sub>nuc</sub> . ....	89

Figure 5.2 Relationship between ERK2 nuclear translocation or nuclear phospho-ERK level and the number of stimulated spines .....	92
Figure 5.3 Relationship between the number of stimulated branches and change in fluorescence lifetime of EKARnuc.....	94
Figure 5.4 Activation of only two spines from a dendritic branch saturates ERK activity contributed by that branch .....	97
Figure 5.5 High level of EKARcyto expression abolishes nuclear ERK activation.....	99
Figure 5.6 Distal stimulation activates nuclear ERK with a delay .....	100
Figure 5.7 Temporally spaced 2-spine stimulations induce nuclear ERK activity increase .....	102
Figure 6.1 Phosphorylation of CREB and Elk-1 triggered by induction of sLTP at 7 spines .....	111
Figure 6.2 Phosphorylation of CREB and pElk-1 induced by 7-spine stimulation depends on ERK activity.....	113

## List of Abbreviations

2-p	Two-photon
ACSF	Artificial cerebrospinal fluid
AMPA	$\alpha$ -amino-3-hydroxy-5-methyl-4-isoxazole-propionic acid receptor
AP	Action potential
APV	2-amino-5-phosphonopentanoate
Arc	Activity-regulated cytoskeleton-associated protein
BDNF	Brain-derived neurotrophic factor
ca-	Constitutively active
CA1	Cornu Ammonis 1
CA3	Cornu Ammonis 3
CaM	Calmodulin
Ca <sup>2+</sup>	Calcium (ion)
CaMK	Calcium/calmodulin-dependent kinase
CaMKII	Calcium/calmodulin-dependent kinase II
CaMKIV	Calcium/calmodulin-dependent kinase IV
CBP	CREB-binding protein
Cd <sup>2+</sup>	Cadmium (ion)
CREB	cAMP response element-binding protein
CPA	Cyclopiazonic acid
DAG	Diacylglycerol
DAPI	4',6-diamidino-2-phenylindole
DG	Dentate gyrus
DMSO	Dimethyl Sulfoxide

dn-	Dominant-negative
EGTA	Ethylene glycol tetraacetic acid
EKAR	ERK activity reporter
Elk-1	E26-like protein-1
E-LTD	Early (phase) long-term synaptic depression
E-LTP	Early (phase) long-term synaptic potentiation
EPSC	Excitatory postsynaptic current
ER	Endoplasmic reticulum
ERK	Extracellular signal-regulated kinase
fEPSP	Field excitatory post-synaptic potential
FLIM	Fluorescence lifetime imaging microscopy
FRET	Forster/Fluorescence resonance energy transfer
GAP	GTPase-activating protein
GDP	Guanosine diphosphate
GEF	Guanine nucleotide exchange factor
GluR	Glutamate receptor
GTP	Guanosine triphosphate
HDAC	Histone deacetylase
HFS	High frequency stimulation
IEG	Immediate early gene
IP <sub>3</sub>	Inositol 1,4,5-triphosphate
LFS	Low frequency stimulation
LTD	Long-term depression
LTP	Long-term potentiation
MAPK	Mitogen-activated protein kinase

MCPG	$\alpha$ -Methyl-4-carboxyphenylglycine
mEGFP	Monomeric enhanced green fluorescent protein
MEK	MAPK/ERK kinase
Mg <sup>2+</sup>	Magnesium (ion)
mGluR	Metabotropic glutamate receptor
MNI-glutamate	4-methoxy-7-nitroindolinyI-caged-L-glutamate
mRFP	Monomeric red fluorescent protein
MSK1	Mitongen- and stress-activated protein kinase 1
NES	Nuclear export signal
NF- $\kappa$ B	Nuclear factor kappa-light-chain-enhancer of activated B cells
NGS	Normal goat serum
NLS	Nuclear localization signal
NMDAR	N-methyl D-aspartate receptor
PIP <sub>2</sub>	phosphatidyl inositol-bisphosphate
PKA	Protein kinase A
PKC	Protein kinase C
PLA2	Phospholipase A2
PLC	Phospholipase C
PP	Protein phosphatase
PSD	Postsynaptic density
RSK	Ribosomal S6 kinase
RyR	Ryanodine receptor
SERCA	Sarco/endoplasmic reticulum calcium ATPase

sER	Smooth endoplasmic reticulum
SRE	Serum response element
SRF	Serum response factor
STC	Synaptic tagging and capture
TBS	Theta burst stimulation
TTX	Tetrodotoxin
UTR	Untranslated region
VGCC	Voltage-gated calcium channel

## Acknowledgements

I would like to express my deepest gratitude towards my thesis advisor, Ryohei Yasuda. Your unwavering support and careful guidance were critical to my academic growth. I have been especially inspired by your wisdom and your enthusiasm for science. Your optimistic attitude and creative ideas always turned seemingly daunting challenges into manageable tasks.

I would also like to thank my former advisor, George Augustine. I will always benefit from the vigorous scientific training you provided at the beginning of my PhD journey, from experimental design and data analysis to presentation and writing.

I am deeply grateful to my thesis committee members, Prof. Serena Dudek, Prof. Richard Mooney, and Prof. Anne West. Without your insightful feedback, fruitful meetings, and intriguing questions, this thesis would not be as strong. I am especially thankful for the guidance on proposal writing from Serena, the zestful discussions with Anne, and the support during lab transition from Rich.

I would like to thank all the past and current members of Yasuda lab for your help and support: Jui-Yun Chang, Lesley Colgan, Nathan Hedrick, Rishabh Kasliwal, David Kloetzer, Seok-Jin Lee, Hideji Murakoshi, Jun Nishiyama, Michael Patterson, Rohit Ramnath, Mikihiro Shibata, Erzsebet Szatmari, Airong Wan, Hong Wang, Jie Wang. My special thanks go to Ana Oliveira who taught me hippocampal slice culture and transfection, and Eugene Park who did some GCaMP experiments in Figure 4.3.

I am also grateful to my wonderful Neurobiology Department family. I'd like to mention a few by name: Ken Berglund, Qing Cheng, Prof. Dona Chikaraishi, Polly Garner, Isamu Gotoh, Jessica Herbst, Lingqing Li, Prof. James McNamara, Jessica Peloquin, Prof. Pate Skene, and Yu Wang. My special thanks go to Keiko Tanaka, for teaching me the best tips in the world for doing whole-cell patch clamp and immunohistochemistry.

Finally, I would like to thank my husband Peng whose love, patience and charm have made my journey so joyful, and my parents who always encourage my dreams while fearlessly pursuing theirs.

## **Chapter 1. Introduction**

### **1.1 Long-term synaptic plasticity in the hippocampus**

#### **1.1.1 LTP-discovery, characteristics, relationship to learning and memory**

Long-term synaptic potentiation (LTP), referring to a long lasting enhancement in the efficacy of excitatory synaptic transmission, was first documented by Bliss and Lømo (Bliss and Lømo, 1973). LTP, as the leading experimental model for learning and memory, has been one of the most extensively investigated areas in neuroscience for the last 30 years (Martin et al., 2000). It is now clear that LTP is a general class of cellular phenomena rather than a unitary event: various forms of LTP have different properties and underlying mechanisms, depending on which synapses are involved, the developmental stage of animal, as well as how they are triggered.

LTP has several characteristics. First, it is input-specific. Potentiation in synaptic efficacy induced at one set of synapses by repetitive stimulation is not arbitrarily spread to other synapses in the same cell. The input-specificity allows each individual neuron to store an enormous amount of information with great specificity. However, there is growing evidence that input specificity breaks down under certain conditions, such as in aging brain or within short distances (Engert and Bonhoeffer, 1997). Second, LTP is associative. Strong stimulation of one pathway will facilitate LTP at another pathway that is stimulated by a weak stimulation within finite time window. Third, LTP is

persistent, lasting from several minutes to many months (Bliss and Collingridge, 1993). All these characteristics have led scientists to consider LTP as the cellular mechanism underlying long-term memory formation.

Despite the fact that LTP has been the most extensively studied model for memory for more than three decades, whether LTP is required for memory has been the subject of active debate. Seminal research by Morris and colleagues provided some of the first evidence that LTP was required for the formation of memories *in vivo* (Morris et al., 1986). Chronic intraventricular infusion of APV, which blocks NMDA receptors (NMDARs) and LTP *in vivo*, caused a selective impairment in spatial learning as shown by Morris water maze test. Later studies showed that perturbation of LTP by selective knockdown of NMDARs or expression of mutant calcium/calmodulin-dependent protein kinase II (CaMKII) in the hippocampus prevented learning while sparing basal synaptic transmission, suggesting hippocampal LTP is required for spatial learning (McHugh et al., 1996; Rotenberg et al., 1996; Silva et al., 1992b; Tsien et al., 1996). However, a more recent study has provided counterevidence: blockade of hippocampal LTP with APV has no effect on spatial learning if animals are pretrained in a different water maze before drug application (Bannerman et al., 1995). Thus, although required for some components of spatial learning, NMDAR-dependent LTP may not be required for encoding the spatial representation of a specific environment. Despite the controversy, LTP (together with LTD) and memory have several parallels. First, they

both can persist for varying periods of time (Squire, 1992). Second, LTP and memory are both consolidated by repeated but spaced induction/learning sessions (Bjork and Allen, 1970; Huang and Kandel, 1994). Third, they are both dependent on de novo protein synthesis (Gold, 2008; Krug et al., 1984) and gene transcription (Bourtchuladze et al., 1994; Jones et al., 2001). Furthermore, LTP, just like memory, is a ubiquitous phenomenon throughout the brain. Therefore, LTP is still considered one of the key neural mechanisms underlying learning and memory.

### **1.1.2 Hippocampus**

This dissertation is primarily focused on the LTP occurring at hippocampal CA3-CA1 synapses, the most extensively studied form of long-term synaptic plasticity.

#### **1.1.2.1 Anatomy of hippocampus**

The hippocampus is a paired brain structure located inside the medial temporal lobe (Figure 1.1). Unlike regions of the neocortex which are connected largely by reciprocal pathways, the hippocampus has a unique set of unidirectional excitatory pathways (Andersen, 2007). The entorhinal cortex (EC), reciprocally connected with many regions of neocortex, is the start of hippocampal circuit. Large stellate pyramidal neurons in layer II of the EC project to dentate gyrus (DG) and less densely, to *Cornu Ammonis* 3 (CA3) region. Granule cells in the DG project unidirectionally to pyramidal neurons in CA3 via axons called mossy fibers. The CA3 neurons, in turn send unreciprocated projections to the CA1 field via the Schaffer collateral axons. The CA1

neurons then form connections with the subiculum. Both CA1 and subiculum project to the deeper layers of the EC, completing the loop. From here on, I will focus on rat CA1 pyramidal neurons which is the cell model employed in this dissertation.

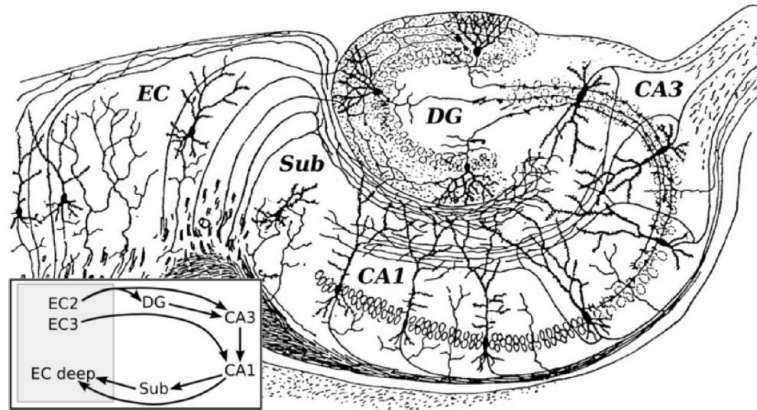


**Figure 1.1 Anatomical structure of the hippocampus viewed in the sagittal plane.**

EC, entorhinal cortex; DG, dentate gyrus; CA3, *Cornu Ammonis* 3; CA1, *Cornu Ammonis* 1; Sub, subiculum. Adapted from (Kerchner and Nicoll, 2008).

### 1.1.2.2 Morphology of CA1 pyramidal neurons

A CA1 pyramidal neuron has a triangular shaped soma and two dendritic trees extending from the soma in opposite directions (Figure 1.2). The smaller dendritic tree occupying the stratum oriens consists of basal dendrites, contributing to ~36% of the entire length of a CA1 pyramidal neuron. The larger dendritic tree transverses two functionally and anatomically distinct regions: the proximal apical dendrites occupy the stratum radiatum and the distal apical dendrites resides in the stratum lacunosum-moleculare (Figure 1.2) (Bannister and Larkman, 1995a; Ishizuka et al., 1995). The apical dendrites in stratum radiatum receive input from CA3 pyramidal neurons whereas

those in stratum lacunosum-moleculare receive direct input via perforant path from entorhinal cortex (Dudman et al., 2007). Dendrites of CA1 neurons are densely studded with dendritic spines, where most excitatory synaptic transmission takes place (Ramon y Cajal, 1904; Bannister and Larkman, 1995b; Megias et al., 2001).

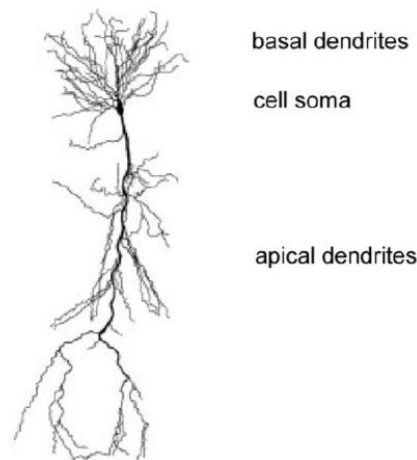


**Figure 1.2 Morphology of a hippocampal CA1 neuron.**  
Adapted from (Spruston, 2008)

### 1.1.3 Hippocampal CA3-CA1 LTP

When a high-frequency train of tetanization is applied to the presynaptic Schaffer collateral fibers, LTP is generated at the CA3-CA1 synapses as evidenced by a sustained increase in the fEPSP amplitude in CA1. Despite that LTP has been the hot spot of neuroscience research for several decades and the subject of thousands of publications, its molecular underpinnings remain unclear. One contributing factor for this ambiguity is that LTP can be induced by multiple intracellular cascades. The importance of an intracellular cascade may vary depending on the LTP induction

protocol, developmental stage, and even the type of hippocampal preparation employed. Given these caveats, we will focus our review to widely accepted molecular mechanisms of CA3-CA1 LTP.

### **1.1.3.1 How is CA3-CA1 LTP induced?**

In a simplified model, high-frequency stimulation (HFS) to Schaffer collaterals causes presynaptic glutamate release and postsynaptic summation of EPSPs. The latter leads to a depolarization of the postsynaptic CA1 neuron and subsequent release of Mg<sup>2+</sup> block of NMDA receptors. Together with glutamate binding, NMDA receptors open and allows entry of Ca<sup>2+</sup>. The resultant elevation in intracellular Ca<sup>2+</sup> concentration, amplified in some cases by voltage-gated calcium channels (VGCCs) and internal stores, is the ultimate trigger for inducing LTP. The critical role of Ca<sup>2+</sup> has been proved beyond doubt. When Ca<sup>2+</sup> elevation was prevented by injection of Ca<sup>2+</sup> chelators in CA1 neurons, high-frequency stimulation failed to induce LTP (Lynch et al., 1983; Malenka et al., 1988). Whereas moderate depolarization paired with EPSP reliably induces LTP, strong depolarization (+20 mV) which suppresses NMDAR-mediated Ca<sup>2+</sup> influx prevents LTP (Malenka et al., 1988). Numerous studies confirmed that Ca<sup>2+</sup> is not only required for LTP, but sufficient for LTP. Elevation of postsynaptic intracellular Ca<sup>2+</sup> concentration, by photolysis of a caged Ca<sup>2+</sup> chelator, alone was sufficient to potentiate EPSP (Malenka et al., 1988). Furthermore, imaging studies have clearly demonstrated that the intracellular Ca<sup>2+</sup> concentration increased within the vicinity of stimulated spines following tetanic

stimulation (Alford et al., 1993; Malinow et al., 1994; Muller and Connor, 1991; Regehr and Tank, 1990). However, the exact magnitude and microdomain location of the  $\text{Ca}^{2+}$  signal required to produce LTP is less well understood, and may vary depending on forms and persistence of LTP (i.e. early-, intermediate-, or late-LTP) (Raymond and Redman, 2002, 2006).

### **1.1.3.2 How is CA3-CA1 LTP expressed?**

Once inside the cytosol,  $\text{Ca}^{2+}$  induces LTP by initiating complicated signal transduction cascades that include protein kinases. The most prominent kinase sensor for  $\text{Ca}^{2+}$  is CaMKII.  $\text{Ca}^{2+}$  binds to calmodulin to form a complex that activates CaMKII. Once bound by  $\text{Ca}^{2+}$ /calmodulin, CaMKII can undergo autophosphorylation at T286, resulting in an active form that persists even after intracellular  $\text{Ca}^{2+}$  drops back to baseline. Mounting evidence suggests that CaMKII is a critical mediator of LTP induction. (Lisman et al., 2002; Lisman et al., 2012). Pharmacological inhibition or genetic deletion of CaMKII prevented LTP induction (Malinow et al., 1989; Silva et al., 1992a). On the other hand, postsynaptic expression of the constitutively active form of CaMKII (ca-CaMKII) enhanced synaptic efficacy and occluded further LTP induction (Pettit et al., 1994). Activated CaMKII translocates to the postsynaptic densities (PSD) and complexes with NMDARs (Gardoni et al., 1998; Otmakhov et al., 2004; Strack and Colbran, 1998). This CaMKII-NMDAR complex plays an important role in LTP induction, as pharmacological interference of complex formation reversed LTP

(Sanhueza et al., 2011). Activated CaMKII phosphorylates a plethora of substrates, including  $\alpha$ -amino-3-hydroxy-5-methyl-4-isoxazole propionic acid receptors (AMPARs). AMPAR phosphorylation is thought to lead to their insertion into the postsynaptic membrane (Hayashi et al., 2000; Rongo and Kaplan, 1999) and their increased channel conductance (Derkach et al., 1999), both of which potentiate synaptic efficacy. Other protein kinases have also been heavily implicated in LTP. For example, in neonatal hippocampus, LTP depends on protein kinase A (or cAMP-dependent protein kinase, PKA) but not CaMKII (Yasuda et al., 2003). Protein kinase C (PKC), yet another kinase that phosphorylates AMPARs, is also critical to LTP expression. Acute phosphorylation by PKC or phosphomimetic mutation drives AMPAR into synaptic membrane whereas blocking PKC-mediated phosphorylation impairs LTP (Boehm et al., 2006). The tyrosine kinase Src also plays an important role in LTP induction (Lu et al., 1998), presumably through upregulation of NMDAR (Yu et al., 1997). Phosphoinositide 3-kinase (PI3K), activated by calmodulin during LTP, is required for LTP expression but not LTP induction (Joyal et al., 1997; Man et al., 2003; Sanna et al., 2002). Therefore, multiple signaling cascades seem to be activated simultaneously during LTP and converge on posttranslational modifications of AMPARs. Their relative importance and crosstalk, however, are poorly understood.

The early phase of LTP (E-LTP) depends on posttranslational modifications of preexisting proteins that result in increased number of AMPARs at postsynaptic

membrane and increased AMPAR channel conductance. This E-LTP, however, does not last and decays back to baseline level with 4 hours after induction if not consolidated.

### **1.1.3.3 How is LTP maintained?**

A hallmark for long-term memory in mammalian brain is that it has different phases, with the maintenance phases depending on protein synthesis and gene transcription (Matthies, 1974, 1989). This is also the case for LTP. LTP can be divided to at least three phases: 1) E-LTP (or LTP1 in some literature) which does not require protein synthesis or gene transcription, 2) LTP2 which requires new protein synthesis but not gene transcription, and 3) LTP3 which is sensitive to inhibition of gene transcription (Bliss and Collingridge, 1993; Frey et al., 1988; Krug et al., 1984; Matthies et al., 1990; Otani et al., 1989). LTP1 is also referred as E-LTP whereas LTP2 and 3 are often collectively referred as late-LTP (L-LTP). The role of protein synthesis in LTP maintenance has been corroborated by many studies. In the presence of protein synthesis inhibitors, synaptic potentiation declines 3-4 hours after tetanization (Frey et al., 1988; Mochida et al., 2001; Otani et al., 1989). The existence of a translation-dependent and transcription-independent phase (i.e. LTP2) was demonstrated by comparing the effects of transcription and translation inhibitors on LTP. Following four trains of tetanic stimulation, the initial 60-90 min of potentiation was impaired by translation inhibitor anisomycin but not by transcription inhibitor actinomycin D (Kelleher et al., 2004a). Interestingly, severing CA1 dendrites from their soma did not

affect LTP until 3 hr post-induction whereas anisomycin impaired LTP had a more immediate impairment on LTP, implying a role of dendritic translation in LTP (Frey et al., 1988). More recent studies confirmed that long-term synaptic plasticity requires protein synthesis that occurs both locally in dendrites and globally in the soma of postsynaptic neurons (Cracco et al., 2005; Steward and Schuman, 2001; Vickers et al., 2005).

Several lines of evidence suggest that LTP also requires gene transcription. First, in the presence of transcription inhibitors LTP was impaired 3-8 hours after tetanization, although the time frame seems to vary among studies (Frey et al., 1996; Nguyen and Kandel, 1997; Otani et al., 1989; Vickers et al., 2005). Second, the transcription factor cAMP-response element binding protein (CREB) has been implicated in LTP and memory. In a knockout mouse with global ablation of  $\alpha$  and  $\beta$  isoforms of CREB, long-term memory was impaired and LTP in CA1 region decayed to baseline within 2 hr (Bourtchuladze et al., 1994). However, the levels of other CREB isoforms increased in these CREB knockout mice as a result of compensatory mechanisms, making it difficult to establish a direct link between CREB and long-term memory based on this study (Blendy et al., 1996). Third, induction of immediate early genes such as *zif268* and *Arc/Arg3.1* is not only associated with but also essential to late-LTP in the dentate gyrus (Cole et al., 1989; Guzowski et al., 2000; Jones et al., 2001; Link et al., 1995; Messaoudi et al., 2007). Last but not least, studies on synaptic tagging and capture (STC) suggest that

some macromolecules critical for maintaining LTP are synthesized globally before being captured and utilized by tagged synapses (Redondo and Morris, 2011). Given the pivotal role of transcription in the maintenance of LTP, a key question arises: which signaling cascades are involved in triggering new gene transcription in the nucleus during LTP?

#### **1.1.3.4 Signaling cascades for LTP maintenance**

How do activated synapses signal to the nucleus to trigger the transcriptional events critical for persistent LTP? One candidate for such synapse-to-nucleus signaling is calcium itself. Calcium may signal to the nucleus through one or more of following ways. First, calcium waves may be generated and propagated to the nucleus (Larkum et al., 2003). Second, calcium-calmodulin complexes may travel from activated synapses to the nucleus (Wu et al., 2001b). Third, somatic and nuclear calcium levels may be directly elevated by opening of VGCCs on the somatic plasma membrane and nuclear membrane (Hardingham et al., 2001). The primary effector of calcium in the nucleus is CaMKIV which phosphorylates and activates transcription factors such as CREB (Sun et al., 1996). Transgenic mice with expression of a dominant-negative form of CaMKIV (dnCaMKIV) in postnatal forebrain showed impairment in CREB phosphorylation and L-LTP, suggesting an important role of CaMKIV in the maintenance of LTP (Kang et al., 2001).

Yet another well-described pathway is through PKA. The role of PKA in L-LTP is evidenced by the facts that PKA inhibitors specifically block L-LTP without affecting the

E-LTP (Matthies and Reymann, 1993), and that application of a PKA agonist alone simulates L-LTP (Frey et al., 1993; Pockett et al., 1993). Moreover, transgenic mice with reduced PKA activity were generated by expressing an inhibitory form of the regulatory subunit of PKA. In these transgenic mice, long-term memory and L-LTP were both impaired whereas basal synaptic transmission and the early phase of LTP were unaffected (Abel et al., 1997). PKA can activate transcription through phosphorylation of transcription factors, resulting in synthesis of new AMPARs required for maintenance of LTP (Nayak et al., 1998). Additional pathways such as postsynaptic CaMKIV, PKC and MAPK act in parallel or in series with PKA to initiate new gene transcription in the neuronal nucleus (Impey et al., 1998; Kang et al., 2001; Roberson et al., 1999).

In addition to transcription-activating pathways, transcription-independent mechanism has been reported to maintain LTP over a period of hours. PKM $\zeta$ , an autonomously active isoform of PKC (Sacktor et al., 1993), was thought to maintain LTP through directly facilitating synaptic incorporation of AMPARs (Yao et al., 2008). PKM $\zeta$ , synthesized locally in the dendrites upon LTP induction (Hernandez et al., 2003; Kelly et al., 2007; Muslimov et al., 2004), was considered both necessary and sufficient to maintain LTP for hours (Ling et al., 2002; Sajikumar et al., 2005; Serrano et al., 2005). Nevertheless, a recent study has showed that transgenic mice lacking PKC $\zeta$  and PKM $\zeta$  exhibited normal LTP and hippocampal-dependent spatial memory. Therefore, PKM $\zeta$  might be dispensable to LTP and its apparent importance in LTP in previous reports

might result from some non-specific effects of the widely used PKM $\zeta$  inhibitor ZIP (Volk et al., 2013).

## 1.2 Extracellular signal-regulated kinase (ERK)

### 1.2.1 ERK belongs to MAPK family

Extracellular signal-regulated kinase (ERK1/2, or p44/p42 MAPK) is an essential component of the signal transduction mechanisms subserving a host of cellular functions, such as cell division, differentiation and survival (Kolch, 2005). ERK, a member of the mitogen-activated protein kinase (MAPK) superfamily, was originally termed based on its ability to respond to growth factors. Other members of the MAPK superfamily include c-Jun N-terminal kinases (JNKs) and the p38 MAPKs (Sweatt, 2001).

### 1.2.2 Signaling pathways upstream of ERK

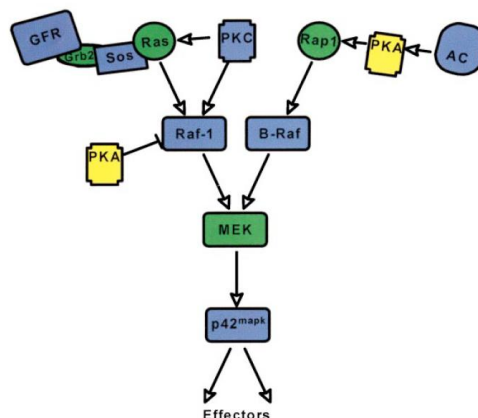


**Figure 1.3 Signaling pathways upstream of ERK**

Adapted from (Sweatt, 2001).

As a prototype of the MAPK signaling cascades, the ERK pathway comprises three serially connected protein kinases that are activated by sequential phosphorylation: the MAP kinase kinase kinase (Raf-1 and B-raf in case of the ERK pathway) phosphorylates and thereby activates the MAP kinase kinase (MEKs in the ERK pathway), which in turn activates MAPK (ERK1/2) by dual-phosphorylation (Canagarajah et al., 1997; Kolch, 2005)(Figure 1.3). In the so-called canonical ERK pathway, Raf-1 is activated by Ras, a small GTPase. Ras switches between active (or GTP-bound) and inactive (or GDP-bound) states as a result of the balance between guanine nucleotide exchange factors (GEFs) and GTPase-activating proteins (GAPs). Ras-GEFs, exemplified by Sos, stimulate release of GDP to allow for GTP binding. On the contrary, Ras-GAPs catalyze the hydrolysis of GTP into GDP by Ras, switching Ras signaling off (Thomas and Huganir, 2004). The Ras/Raf-1 pathway is regulated by crosstalk with other signaling systems. For example, PKC can directly phosphorylate and activate both Ras (Downward et al., 1990) and Raf-1 (Kolch et al., 1993). In addition, cAMP inhibits Raf-1 through PKA-mediated phosphorylation events (Sevetson et al., 1993; Wu et al., 1993). Interestingly, Ras guanine nucleotide-releasing protein (Ras-GRP), a family of Ras-GEFs, is expressed in neurons and contains diacylglycerol (DAG)- and  $\text{Ca}^{2+}$ -binding motifs. Its ability to activate Ras is markedly enhanced by binding of DAG or  $\text{Ca}^{2+}$  (Ebinu et al., 1998; Farnsworth et al., 1995). Therefore, Ras might also be directly activated by second messengers. In the alternative ERK pathway, B-Raf (a counterpart of

Raf-1) is activated by Rap1, a small GTPase analogous to Ras. Rap1 is stimulated by elevated intracellular cAMP, either through a family of cAMP-binding GEFs (de Rooij et al., 1998; Kawasaki et al., 1998), or through activation of PKA (Vossler et al., 1997) (Figure 1.3). In the developing brain, Rap1 is also stimulated by Src-family kinases, presumably through tyrosine phosphorylation of a Rap1-GEF, C3G (Ballif et al., 2004; Sekine et al., 2012).

### **1.2.3 Regulation of ERK signaling by scaffolding proteins**

As discussed above, ERK signaling pathway can be activated by a variety of upstream triggers. How are the upstream activators specifically coupled to ERK pathway? Several recent studies suggest that this might be achieved by compartmentalization of ERK by scaffolding proteins. Krapivinsky et al. demonstrated that NR2B, but not NR2A or NR1 subunits of NMDAR interacts with RasGRF1, a Ras GEF (Krapivinsky et al., 2003). More importantly, disruption of this interaction markedly inhibited NMDAR-dependent ERK activation, without altering NMDAR currents. These results strongly suggest that physical association between RasGRF1 and the NR2B subunit is crucial to ERK activation. Thus, RasGRF1 serves as an NMDAR-dependent regulator of the ERK kinase pathway. Similarly, the postsynaptic scaffold protein PSD-95 has been found to interact with SynGAP, a Ras GAP, in the NMDA receptor complex (Pulido et al., 1998). This association is important for maintaining a

low basal ERK activity (Komiyama et al., 2002). In striatal neurons, dissociation of mGluR5 and the scaffolding protein Homer1b/c significantly inhibited mGluR-mediated ERK activation (Mao et al., 2005b), suggesting that different receptors might employ different scaffolding proteins in coupling to ERK activation.

#### **1.2.4 Overview of functions of ERK in neurons**

Considering its significant role in controlling cell cycle progression, people were at first puzzled by the observation that ERK was abundantly expressed in mature neurons which do not divide nor further differentiate (Thomas and Huganir, 2004). Now, it is clear that neuronal ERK plays a critical role in long-term synaptic plasticity as well as in learning and memory. In addition, ERK is also implicated in neuronal apoptosis and neurodegeneration, which is beyond the scope of our discussion and has been thoroughly reviewed elsewhere (Cheung and Slack, 2004).

#### **1.2.5 ERK in long-term synaptic potentiation (LTP)**

The earliest evidence that ERK is involved in long-term synaptic plasticity was from studies of NMDAR-dependent LTP in hippocampal CA1 neurons. As early as 1996-1997, English and Sweatt discovered that not only is ERK activated during LTP but also necessary for LTP. ERK2, but not ERK1, is activated by high-frequency stimulation that induces LTP in hippocampal CA1 region in a NMDAR-dependent manner (English

and Sweatt, 1996). Preincubation of slices with the MEK inhibitor PD98059 significantly attenuated LTP induction after high-frequency stimulation (English and Sweatt, 1997). This major discovery has later been confirmed by other studies (Atkins et al., 1998; Impey et al., 1998; Winder et al., 1999; Wu et al., 1999). However, the role of ERK is not limited to the “classical” LTP in CA1 neurons. Later studies have demonstrated that ERK is also required for many other forms of synaptic plasticity, including hippocampal NMDAR-independent LTP, hippocampal mGluR-dependent LTD, dentate gyrus LTP, amygdala LTP, cortical LTP, and cerebellar LTD [comprehensively reviewed by (Sweatt, 2001)]. Consistent with these studies, ERK was also found to be necessary for the development of several forms of memory, including contextual fear conditioning, spatial memory, and conditioned taste aversion (Sweatt, 2001). Here, I will focus my literature review mainly on the functions of ERK in NMDAR-dependent hippocampal CA3-CA1 LTP.

How does ERK contribute to hippocampal LTP? Given that ERK is ubiquitously expressed in neurons and has numerous potential cellular targets, it is not surprising that ERK has a pluripotent role in hippocampal LTP, contributing to the establishment of LTP at different spatial and temporal scales.

### **1.2.5.1 ERK and AMPAR trafficking**

As mentioned earlier, AMPAR number at synaptic sites is increased during LTP expression, causing a potentiated postsynaptic response. This process, first demonstrated by Malinow and colleagues, is regulated by Ras-ERK signaling cascade (Zhu et al., 2002). The authors found that hyperactivity of Ras, produced by expression of a constitutively active form of Ras (ca-Ras), potentiated AMPAR-mediated basal transmission by ~80% and this effect was prevented by MEK inhibitor PD98059. Furthermore, increased AMPAR transmission induced by an active form of CaMKII was also blocked by PD98059. These results suggest that CaMKII and Ras, through ERK activation, increase AMPAR transmission for LTP expression. As I discussed earlier (Section 1.1.3.2), CaMKII is crucial to the expression of hippocampal LTP. Hence, Malinow and colleagues provided us with a model: activation of CaMKII is relayed, at least partly, to Ras-ERK pathway for increased AMPAR insertion during LTP. Also reported by Malinow and colleagues, pairing-induced LTP in hippocampal CA1 neurons was abolished by expression of dominant-negative Ras (dnRas) or treatment with the MEK inhibitor PD98059, and occluded by expression of ca-Ras, consolidating a crucial role for proper Ras-ERK signaling in hippocampal LTP (Zhu et al., 2002). The role of ERK in regulating AMPAR trafficking was corroborated by a recent study that monitored AMPAR exocytosis in single spines using two-photon imaging of fluorescently labeled surface AMPARs (Patterson et al., 2010). Upon induction of spine-

specific LTP by glutamate uncaging in single synapses, the rate of AMPAR exocytosis was increased by ~5 fold, as measured in the stimulated spine and nearby dendritic shaft (within ~3  $\mu\text{m}$  of stimulated spine). Blockade of Ras-ERK signaling pathway by application of the MEK inhibitor U0126 or expression of dnRas impaired the increase in exocytosis rate, indicating that LTP-specific AMPAR exocytosis was dependent on Ras-ERK signaling.

#### **1.2.5.2 Regulation of potassium channels**

As discussed in Section 1.1.3.1, LTP induction requires  $\text{Ca}^{2+}$  influx through NMDARs which open upon simultaneous glutamate release and postsynaptic depolarization. Therefore, modulators of postsynaptic electrical responses play a crucial role in LTP induction. Kv4.2, the pore-forming subunit of A-type potassium channels, is densely expressed in the dendrites of CA1 pyramidal neurons and contains many potential phosphorylation sites. Thus, Kv4.2 is an ideal candidate for modulating postsynaptic electrical responses. Johnston and colleagues found that blocking Kv4.2 channels increased dendritic action potential amplitude dramatically and facilitated back propagation of action potentials into dendrites (Hoffman et al., 1997), implying these channels as crucial modulators of dendritic excitability and LTP induction. PKA and PKC activators such as forskolin and PDA are shown to down-regulate channel activation of Kv4.2 and these effects are blocked by the MEK inhibitors U0126 and

PD98059, suggesting that PKA and PKC converge onto ERK in regulating Kv4.2 channels (Hoffman and Johnston, 1998; Yuan et al., 2002). Consistent with these results, several potential phosphorylation sites for ERK has been mapped out within Kv4.2 sequence and ERK-mediated phosphorylation of this channel has been confirmed *in vitro* as well as in hippocampal slices (Adams et al., 2000; Schrader et al., 2006; Varga et al., 2000). In another study, Kandel and colleagues provided more direct evidence for ERK-dependent Kv4.2 inactivation in LTP induction (Morozov et al., 2003). The authors generated transgenic mice with a dominant interfering Rap1 mutant (iRap1). They found that in control slices, LTP stimulation increases phosphorylation of both ERK and Kv4.2. However, in slices with iRap1 mutant, phosphorylation of Kv4.2 channels were markedly reduced at basal condition and there was no increase after LTP stimulation. Taken together, ERK might contribute to LTP induction through inactivating Kv4.2 channels and thereby increasing postsynaptic excitability.

#### **1.2.5.4 Regulation of protein synthesis**

Maintenance of long-lasting synaptic plasticity requires synthesis of macromolecules. Early evidence of the requirement for protein synthesis in LTP was based on studies with pharmacological inhibition of translation (Behnisch et al., 2004; Deadwyler et al., 1987; Frey et al., 1996; Frey et al., 1988; Mochida et al., 2001; Stanton and Sarvey, 1984). More recently, synthesis of reporter proteins was directly visualized

following LTP-inducing stimuli (Behnisch et al., 2004; Kelleher et al., 2004a; Tsokas et al., 2005). How is synaptic activity coupled to activation of the translation machinery? In non-neuronal cells, ERK pathway is known to control multiple translation factors and activate protein synthesis in response to mitogen stimulation (Wang and Proud, 2002). The same mechanism seems to be employed by neurons in the context of long-term synaptic plasticity (Kelleher et al., 2004b). In a study by Kelleher and colleagues, ERK signaling pathway has been demonstrated to be essential for activation of translational machinery and protein synthesis during LTP (Kelleher et al., 2004a). The authors generated transgenic mice that conditionally express dominant-negative MEK1 (dnMEK1) and therefore have impaired ERK signaling. In these dnMEK1 mice, inhibition of L-LTP by the translation inhibitor anisomycin is completely occluded. Moreover, upregulation of protein synthesis and phosphorylation of translation factors that are induced by either neuronal activity (e.g. bicuculline) or LTP-inducing tetanization are significantly blocked by MEK inhibition. In a more physiologically relevant scenario, phosphorylation of translation factors in the hippocampus induced by contextual fear conditioning was markedly diminished in dnMEK1 mouse. Together, these lines of evidence suggest a critical role for ERK in controlling translation during long-term synaptic plasticity and memory. In the current model, general translation is primarily regulated at the step of translation initiation (Figure 1.4) (Kelleher et al., 2004b). In response to synaptic activity and synaptic plasticity, activated ERK leads to

phosphorylation of several translation factors including initiation factor eIF4E, its inhibitory regulator eIF4E-binding protein 1 (4E-BP1), and S6 ribosomal subunit. This causes release of eIF4E from sequestration by 4E-BP1 and allows for mRNA 5' cap recognition and subsequent recruitment of S40 ribosomal subunit. Activity-dependent protein synthesis can then be initiated. As one specific example, ERK has been shown to mediate synthesis of CaMKII after induction of LTP using theta-pulse stimulation paired with beta-adrenergic receptor activation (Giovannini et al., 2001).

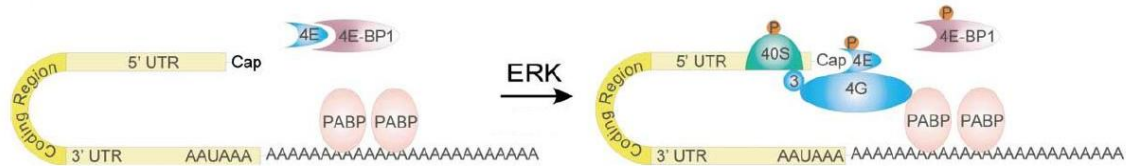


**Figure 1.4 Regulation of general translation by ERK pathway.**

UTR, untranslated region; PABP, poly(A) binding protein, 40S, 40S ribosomal subunit. Adapted from (Kelleher et al., 2004a)

### 1.2.5.5 Regulation of gene transcription via phosphorylation of transcription factors

ERK has been believed for decades to regulate gene transcription which is required for the maintenance of LTP and memory (Thomas and Huganir, 2004). The most prevalent mechanism for ERK-mediated transcriptional regulation is through activation of transcription factors, via direct or indirect phosphorylation. Probably the most extensively studied transcription factor in relation to ERK's role in regulation of gene expression is CREB. CREB is phosphorylated by ribosomal S6 kinase 2 (RSK2) which in turn is a substrate of ERK. Phosphorylation of Ser133 confers CREB its

transcriptional activity. Once activated, CREB recruits the CREB binding protein (CBP) to the initiator complex and thereby drives transcription of a wide range of genes (Sweatt, 2001). The role of ERK as a critical regulator of CREB has been most directly demonstrated in CA1 neurons (Impey et al., 1998) and also documented in dentate gyrus granule cells and striatal neurons (Perkinton et al., 1999; Vanhoutte et al., 1999).

Another prominent example of ERK-activated transcription factor is the ternary complex factor Elk-1 which can be phosphorylated directly by ERK at multiple sites (Besnard et al., 2011). Phosphorylation at Ser 383 is crucial to its transcriptional activity as mutation of this residue completely blocked gene induction by Elk-1 (Gille et al., 1995a). Activated Elk-1 cooperates with serum response factor (SRF) to drive expression of serum response element (SRE)-controlled genes, such as *c-fos*. The strongest evidence for a requirement for ERK-mediated Elk-1 activation in LTP comes from a study in dentate gyrus granule neurons. It was shown that ERK and Elk-1 were activated in a coordinated manner after induction of LTP *in vivo*. Inhibition of ERK phosphorylation by MEK inhibitors prevented Elk-1 phosphorylation and transcriptional upregulation of the immediate early gene *Zif268* (Davis et al., 2000). The *Zif268* gene, containing an SRE site in its promoter sequence, has been shown to be required for the consolidation of cognitive memory (Jones et al., 2001). Therefore, ERK may contribute to LTP by activating transcription factors and upregulating gene expression necessary for maintaining LTP and memory.

### **1.2.5.5 Regulation of gene transcription through epigenetic mechanisms**

Classically, epigenetics refers to heritable alterations in chromatin structure, which in turn regulate gene expression, and is associated with developmental processes such as cell differentiation (Borrelli et al., 2008). In neurobiology, however, epigenetic modifications more typically refer to DNA methylation and histone modifications (including histone acetylation, phosphorylation, methylation and ubiquitylation) occurring in neurons, which are non-dividing, terminally differentiated cells. In recent years, increasing evidence have suggested that epigenetic mechanisms might be utilized to maintain long-term synaptic plasticity and memory by effecting stable, coordinated changes in gene transcription pattern (Levenson and Sweatt, 2006). Acetylation and phosphorylation of histone H3, modifications that favor transcriptional initiation, are markedly upregulated in hippocampal CA1 neurons after contextual fear conditioning (Chwang et al., 2006a; Levenson et al., 2004b). Moreover, strengthening histone acetylation with histone deacetylase (HDAC) inhibitors enhances CA3-CA1 LTP as well as long-term fear memory in vivo (Levenson et al., 2004b). On the other hand, genetic disruption of a histone acetyltransferase CBP impairs late-LTP as well as long-term fear memory (Alarcón et al., 2004; Korzus et al., 2004; Wood et al., 2005).

ERK has been implicated in the epigenetic regulation during long-term synaptic plasticity and memory formation. First of all, inhibition of ERK by injecting animals with MEK inhibitor SL327 prevents both histone acetylation and phosphorylation induced by

contextual fear conditioning (Chwang et al., 2006a; Levenson et al., 2004b; Levenson and Sweatt, 2006). Moreover, activation of ERK *in vitro* by PKC or PKA activators significantly increased histone acetylation and phosphorylation in CA1 neurons (Chwang et al., 2006a; Levenson et al., 2004b). However, ERK might not directly execute these modifications, but rather act through its downstream nuclear substrates. Mice lacking mitogen- and stress-activated protein kinase-1 (MSK1) show impaired contextual fear memory as well as deficient histone acetylation and phosphorylation after training. Slices from MSK1 knockout mice exhibit a deficiency in both histone acetylation and phosphorylation after activation of ERK *in vitro* (Chwang et al., 2007). In sum, ERK plays a crucial role in regulating epigenetic modifications during synaptic plasticity and memory, probably through phosphorylating its nuclear targets.

#### **1.2.5.6 Regulation of structural plasticity**

Long-term synaptic plasticity and memory are accompanied by persistent morphological changes such as new synapse formation, enlarged spines and postsynaptic density [reviewed by (Patterson and Yasuda, 2011)]. Earlier studies revealed the importance of ERK in synaptic growth during 5-HT-induced long-term facilitation (Bailey et al., 1997). Time-lapse imaging studies showed that spaced repetition of depolarization, but not a single or massed depolarization, induces sustained activation of ERK that lasts over 60 min. Interestingly, formation of new

filopodia and spines is induced by repeated stimulation, but not by a single or massed stimulation, revealing a correlation between ERK activity and dendritic morphological changes. More importantly, this formation of new spines and filopodia is completely abolished by MEK inhibitor U0126, indicating an essential role of ERK in structural plasticity (Wu et al., 2001a). Mirroring this finding is another report showing that NMDAR activation induces ERK activation and new spine formation, which were both prevented by MEK inhibitors (Goldin and Segal, 2003). As I will discuss in greater detail later, structural LTP that is induced by repetitive glutamate uncaging at single spines, requires Ras-ERK signaling: the sustained spine enlargement following uncaging was blocked by either MEK inhibitor U0126 or overexpression of dominant-negative Ras (Harvey et al., 2008b). However, the precise mechanism by which ERK mediates structural plasticity remains unclear. It is likely, though, that ERK regulates morphological changes by phosphorylating cytoskeletal proteins, by activating translation of dendritic mRNAs, by inducing transcription of genes related to synaptic remodeling, or by a combination of these processes (Grewal et al., 1999; Thomas and Huganir, 2004).

### **1.2.6 Implications in human neurological diseases / human memory**

Genetic mutations that disrupt the ERK cascades have been linked to cognitive and memory deficits in humans. Neurofibromatosis type I (NF-1) is an autosomal

dominant genetic disease caused by loss-of-function mutations in the *Nf1* gene (McClatchey, 2007). The *Nf1* gene encodes for neurofibromin protein which is a Ras GAP (Silva et al., 1997). Mutations in the *Nf1* gene cause prolonged activation of ERK signaling pathway (Costa et al., 2002). The disease primarily affects tissues that are derived from the neural crest and leads to scoliosis, learning difficulties, eye problems, and epilepsy (McClatchey, 2007). A series of seminal studies by Silva and his coworkers successfully established the link between ERK dysregulation and mental retardation, suggesting that tightly regulated Ras-ERK signaling is essential for human cognitive functions (Costa et al., 2002). Fragile X syndrome (FXS), the most common form of inherited mental retardation, is also associated with dysregulated ERK signaling (Bagni et al., 2012). FXS is caused by expansion of CGG repeats (> 200) in the *FMR1* gene and the resultant loss of fragile X mental retardation protein (FMRP). Although it has been controversial whether the basal level of pERK is elevated in *Fmr1* knockout mice [compare (Hou et al., 2006) with (Hu et al., 2008)], examination of human brain tissue shows that basal levels of activated MEK and ERK are higher in FXS patients compared to age-matched controls (Wang et al., 2012), suggesting that the ERK pathway might be important for the pathophysiology of FXS. Another example of ERK-related neurological disease is Coffin-Lowery syndrome (CLS), a disease caused by mutations in *RSK2* gene (Schneider et al., 2011). This syndrome is associated with impaired motor learning and cognitive function. Finally, an additional example is tuberous sclerosis (TS) which is

caused by mutations in tuberin or hamartin genes. TS is associated with reduced B-Raf and ERK activities (Chévere-Torres et al., 2012). Common symptoms of TS include mental retardation, autism and seizures. To summarize, the activity of the ERK signaling cascade must be tightly balanced for proper cognitive functions in human (Blum and Dash, 2009).

## **1.3 Structural plasticity**

### **1.3.1 Structural features of dendritic spines**

Dendritic spines are tiny membranous protrusions from the plasma membrane of neurons, each consisting of a spine head (volume 0.001–1  $\mu\text{m}^3$ ) and a spine neck (Nimchinsky et al., 2002). Dendritic spines are the sites for more than 90% of excitatory synaptic transmission (Gray, 1959; Harris and Kater, 1994; Nikonenko et al., 2008). Each pyramidal neuron hosts ~ 10,000 dendritic spines (Sheng and Hoogenraad, 2007) which are diverse in their size and shape. Spines are believed to mature from long, thin structures toward enlarged, bulbous ones (Yuste and Bonhoeffer, 2004), and the morphology of a spine is highly correlated with its functional strength [see (Matsuzaki et al., 2001; Smith et al., 2003) but also see (Busetto et al., 2008)]. Irrespective of its size and shape, a dendritic spine contains postsynaptic density (PSD) and some structures. Half of the spines in a hippocampal pyramidal neuron contains smooth endoplasmic reticulum (sER) which is the cellular locale of  $\text{Ca}^{2+}$  release and uptake (Spacek and

Harris, 1997). Spines provide both electrical and biochemical compartmentalizations. Combining patch-clamp recording and glutamate-uncaging, Araya et al. have found that potentials from uncaging at spines are summed linearly whereas potentials from uncaging at shafts cancel each other (Araya et al., 2006a). Moreover, somatic potentials evoked by spine uncaging are inversely correlated with spine neck length (Araya et al., 2006b). These studies strongly suggest that spines serve as electrical isolators in the transmission of membrane potentials. In a more recent study, Magee and colleagues estimated the amount of electrical compartmentalization produced by the spine (Harnett et al., 2012). They show that the spine neck resistance ( $R_{\text{neck}}$ ) is large enough to substantially amplify the spine head depolarization associated with unitary synaptic inputs by ~1.5-45 fold. As a result, the mean unitary dendritic EPSP amplitude of ~0.5 mV under physiological condition (Magee and Cook, 2000) is correspondent to a depolarization of up to ~25 mV within the spine head. This augmented spine head depolarization effectively recruits local active voltage-dependent conductances (such as NMDARs), thereby enhancing electrical interactions among multiple coactive inputs (input cooperativity) (Harnett et al., 2012). Because of their peculiar morphologies, dendritic spines are inherently diffusional barriers, allowing biochemical isolation between inputs and synaptic plasticity at the level of a single spine (Bloodgood and Sabatini, 2005; Lee et al., 2009; Murakoshi et al., 2011; Svoboda et al., 1996).

### **1.3.2 LTP-associated structural remodeling in neurons**

It was proposed more than a century ago that memory formation involved emergence of new synaptic connections and remodeling of existing ones. Since then, a number of studies have reported on the association of new memory formation and morphological changes in the synapses [Reviewed by (Bailey and Kandel, 1993)]. For example, long-term sensitization of the gill withdrawal reflex in *Aplysia* is found to markedly enrich presynaptic varicosities per sensory neuron (Bailey and Chen, 1988). In adult rats, spatial training increases postsynaptic spine volume and density in the basal dendrites of CA1 pyramidal cells (Moser et al., 1997). Most early studies observed no change in the overall synapse density after LTP [reviewed by (Nimchinsky et al., 2002)]. Instead, they found that LTP was associated with selective enrichment of certain spine types, partly due to remodeling of existing spines through increasing spine volume and widening spine neck (Chang and Greenough, 1984; Fifkova and Anderson, 1981; Geinisman et al., 1991; Lee et al., 1980; Sorra and Harris, 1998; Van Harreveld and Fifkova, 1975). The development of two-photon microscopy allows for observation of LTP-associated morphological changes in real time. Using this technique, two studies have clearly demonstrated that LTP in CA1 neurons is associated with new spine formation that only occurs at the activated part of the dendrite (Engert and Bonhoeffer, 1999; Maletic-Savatic et al., 1999).

### 1.3.3 Synaptic plasticity at the level of a single dendritic spine

Structural plasticity can be induced at single dendritic spines (Matsuzaki et al., 2004). Repeated uncaging of caged-glutamate (15-60 pulses between 0.5Hz-1Hz) in Mg<sup>2+</sup> free ACSF results in enlargement of the stimulated spine (i.e. structural LTP or sLTP). The volume of the stimulated spine rapidly increases (100-300% increase) in the first 5-10 minutes and then decays to a sustained plateau (30-100% increase)(Harvey and Svoboda, 2007; Harvey et al., 2008b; Lee et al., 2009; Matsuzaki et al., 2004; Murakoshi et al., 2011; Patterson et al., 2010; Tanaka et al., 2008). This structural plasticity, at least for the first hour, is independent of protein synthesis (Tanaka et al., 2008). When paired with postsynaptic spikes, glutamate uncaging induces a larger increase in spine volume which is followed by little decay. This form of synaptic plasticity is dependent on protein synthesis as well as on BDNF (Tanaka et al., 2008). Protein synthesis-dependent structural plasticity can also be induced by pairing of glutamate uncaging with PKA agonist forskolin (Govindarajan et al., 2011). Structural LTP, often correlated with a potentiation in synaptic efficacy (measured as an increase in EPSC), is closely related to functional LTP regarding pharmacology, amplitude, and time course (Govindarajan et al., 2011; Lee et al., 2009; Matsuzaki et al., 2004; Tanaka et al., 2008). Interestingly, structural LTD (i.e. long-lasting spine shrinkage) can be induced by pairing low-frequency glutamate uncaging with depolarization. The resultant shrinkage of stimulated spines is associated with functional weakening of the synaptic strength and is

dependent on NMDAR and mGluR (Oh et al., 2013). Taken together, these studies demonstrate a dendritic spine is the basic unit of bidirectional synaptic plasticity.

## 1.4 Experimental Rationale and Specific Aims

It is widely accepted that ERK is activated by protocols that induce LTP (Davis et al., 2000; English and Sweatt, 1996, 1997; Impey et al., 1998; Winder et al., 1999). Activated ERK seems to appear throughout the entire neuron, both in the soma and dendrites (Giovannini et al., 2001). However, the LTP protocols used in previous studies usually involve either delivery of strong electrical stimuli or bath application of chemicals, which excite an unknown number of synapses on the postsynaptic neuron. In addition to this complication, synchronized synaptic stimulation typically evokes dendritic spikes and dendritic action potentials that could propagate to the soma (Gasparini et al., 2004; Schiller et al., 2000). The resultant somatic depolarization of a CA1 neuron leads to large  $\text{Ca}^{2+}$  influx through VGCCs at the somatic and dendritic plasma membrane and subsequent widespread activation of ERK (Dudek and Fields, 2002). Therefore, it is difficult, using typical LTP-inducing protocols, to examine the spatiotemporal pattern of ERK activity.

In fact, LTP is known to be input-specific: it can be induced at a single dendritic spine by repetitive uncaging of glutamate (Matsuzaki et al., 2004). Calcium influx through NMDARs is transient ( $\tau_{decay} \sim 20$  ms) and highly compartmentalized in the

uncaged spine (Muller and Connor, 1991; Sabatini et al., 2002; Yuste and Denk, 1995). Its downstream effector Ras, however, is activated for ~5 min and active Ras spreads over a distance of ~10  $\mu\text{m}$  along the dendritic shaft (Harvey et al., 2008b). The spatiotemporal dynamics of ERK, which is downstream of Ras, in response to synapse-specific LTP is largely unknown. Furthermore, it remains unclear whether and how the neuronal nucleus senses and integrates biochemical inputs from individual synapses and dendrites. To address these questions, fine control of synaptic inputs is needed, preferably at single-spine spatial resolution. This can be achieved by using two-photon glutamate uncaging, which was ideal for the purposes of this dissertation. My specific aims are discussed below.

**Aim 1: To probe the spatiotemporal profile of ERK activity upon induction of synapse-specific LTP**

Traditional methods used to measure ERK activity, such as Western blot and immunostaining, fail to provide information with single-spine spatial resolution in a real-time fashion. Therefore, this study employed a genetically encoded, Förster resonance energy transfer (FRET)-based sensor of ERK activity (ERK activity reporter, or EKAR), which selectively and reversibly reports ERK activity with high spatiotemporal resolution (Harvey et al., 2008a). Combining EKAR with two-photon glutamate uncaging, I set out to investigate the spatiotemporal profile of ERK activity during

synapse-specific LTP in CA1 neurons. Particularly, I asked whether nuclear ERK is activated by inducing structural LTP at a few spines, in the absence of action potentials. The EKAR imaging result would be corroborated by immunohistochemistry using antibodies against the active form of ERK. Positive results would support a role for ERK pathway in synapse-to nucleus communication.

**Aim 2: To define the molecular mechanisms underlying the nuclear ERK activation caused by inducing structural plasticity at a few dendritic spines**

The results in Chapter 3 demonstrate that ERK activity is gradually and persistently increased in neuronal nuclei following induction of sLTP at as few as 7 spines without a global calcium rise. However, the underlying molecular mechanism was unclear. To determine which of several possible postsynaptic  $\text{Ca}^{2+}$  sources and biochemical signaling pathways are required, I assessed the effects of different inhibitors on nuclear ERK activation and structural plasticity. In addition, the contribution of various  $\text{Ca}^{2+}$  sources to uncaging-induced  $\text{Ca}^{2+}$  transients was directly determined by imaging  $\text{Ca}^{2+}$  with genetically encoded  $\text{Ca}^{2+}$  indicator GCaMP3 in the presence or absence of different  $\text{Ca}^{2+}$  channel inhibitors.

### **Aim 3: To define the spatiotemporal integration required for nuclear ERK activation**

It is widely appreciated that long-term synaptic plasticity engages signaling from activated spines to the neuronal nucleus, but how biochemical signals triggered at different spines are integrated over space and time is not well understood. I pursued this important question, focusing on ERK. The activity of ERK is increased both in the dendrites and nucleus following LTP induction. More importantly, ERK exerts important yet distinct functions both centrally in the nucleus and peripherally at synaptic contacts (Thomas and Huganir, 2004). It is still unknown how synaptic activity at individual synapses is integrated biochemically and translated into nuclear ERK activation. Two-photon glutamate uncaging allows activation of individual synapses with precise spatial and temporal control and so is ideal for investigating ERK integration across different dendritic locations and over time.

First, I asked what spatial pattern of synaptic activation was required for nuclear ERK activation. To determine the minimum number of spines needed for nuclear ERK activation, I monitored ERK activity in the nucleus by EKAR imaging while inducing sLTP at varied numbers of spines at a fixed density. To determine which of sparse and clustered stimulations is more effective in triggering nuclear ERK activation, I compared nuclear EKAR signals produced by sLTP induction at 7 spines that are located on 7 different branches or on the same branch.

Second, I set out to determine whether nuclear ERK and synaptic ERK represent spatially distinct pools of ERK, or propagation of ERK activity from the activated dendrites to the nucleus underlies nuclear ERK activation. To distinguish the two possibilities, I determined whether cytoplasmic overexpression of EKAR, which is an intrinsic ERK buffer, impairs nuclear EKAR signal in response to sLTP induction at 7 spines. Moreover, to determine the continuity of ERK activity, ERK activity was monitored along the path from stimulated synapses to the nucleus by EKAR imaging.

Third, I asked whether ERK activation could be integrated over time. Specifically, I tested whether temporally spaced stimuli, each alone subthreshold, can still trigger nuclear ERK activation.

**Aim 4: To define the biological significance of nuclear ERK activation triggered by sLTP induction at a few spines**

Consolidation of long-term synaptic plasticity and long lasting memory depends on new gene transcription in the neuronal nucleus (Adams and Dudek, 2005). The best-known function of ERK in the nucleus is to phosphorylate transcription factors, either directly or through intermediate kinases, and these phosphorylation events are essential for subsequent transcriptional activation (Thomas and Huganir, 2004). The results from Chapter 3 demonstrate that ERK is activated in the nucleus following induction of structural LTP at a few dendritic spines in the absence of action potentials. This

observation, together with the well-known nuclear function of ERK, leads to the hypothesis that transcription factors are phosphorylated in response to sLTP induction at 7 spines in an ERK-dependent manner. To test this hypothesis, I first asked whether transcription factors are phosphorylated following sLTP induction at a few spines. Specifically, I measured the levels of phosphorylated transcription factors CREB and Elk-1 by immunohistochemistry following repetitive glutamate uncaging (sLTP protocol) at 7 spines. Next, I asked whether this phosphorylation of transcription factors was mediated by ERK. Toward this end, I determined whether ERK inhibitor prevented elevations in pCREB and pElk-1 levels in response to 7-spine stimulation. Answers to these questions would shed light on the functional relevance of ERK-mediated synapse-to-nucleus communication.

## **Chapter 2. Materials and Methods**

### **2.1 DNA constructs, antibodies, and reagents**

#### **DNA constructs**

Plasmids pCI-EKARnuc, pCI-EKARcyto, pCI-dnRas (Ras S17N), EGFP-ERK2, monomeric red fluorescent protein (mRFP)-MEK1 were generously given by Dr. Karel Svoboda. Plasmid pmEGFP-C1 is available at Clontech. GCaMP3 was a gift from Dr. Guoping Feng.

#### **Antibodies**

Primary antibodies used in this study were anti-phospho-ERK1/2 (Thr202/Tyr204) rabbit monoclonal antibody (Cell Signaling, #4370), anti-phospho-CREB (Ser133) rabbit monoclonal antibody (Cell Signaling, #9198), and anti-phospho-Elk-1 (Ser383) rabbit polyclonal antibody (Cell Signaling, #9181). The secondary antibody used is Alexa Fluor® 568 F(ab')<sub>2</sub> fragment of goat anti-rabbit IgG (Invitrogen, A-21069).

#### **Reagents**

Pharmacological compounds used in this study include the following: tetrodotoxin (TTX, ENZO), the ERK inhibitor FR180204 (Calbiochem), an NMDA receptor antagonist D-AP5 (Tocris), CdCl<sub>2</sub> (Sigma), mGluR antagonists (S)-MCPG (Tocris) and NPS 2390 (Tocris), the MEK inhibitor U0126 (Tocris), and U0124 (Calbiochem).

## **2.2 Dissociated Culture, Transfection and BDNF stimulation**

For validation of sensors, dissociated cultures of cortical neurons were prepared from postnatal day 0 Sprague Dawley rats and grown on 35-mm dishes coated with poly-D-lysine as previously described (Habas et al., 2006). Briefly, the culture medium consists of Basal Medium Eagle (BME) supplemented with 10% heat-inactivated fetal bovine serum, 35 mM glucose, 1 mM L-glutamine, 100 U/ml of penicillin and 0.1 mg/ml streptomycin. Cells were seeded at a density of  $2 \times 10^6$  per 35-mm plate and maintained at 37°C with 95% O<sub>2</sub> and 5% CO<sub>2</sub>. Cultures were treated with cytosine arabinoside (2.5 μM) on the second day after seeding (DIV 2) to inhibit proliferation of non-neuronal cells. Additional glucose (4.5 mM) was added on DIV 2 and then on DIV 4. The cortical neuron cultures were kindly prepared by Dr. Erzsebet Szatmari.

Cortical neurons were transfected with EKARnuc or EKARcyto on DIV 4 using the Lipofectamine 2000 reagent (Invitrogen) as described previously (Hetman et al., 2002). Cells were used for experiments on DIV 6 or DIV 7. Imaging was performed in the growth medium. Brain-derived neurotrophic factor (BDNF; Millipore, #GF029) was pre-diluted with BME and added to the neurons at a final concentration of 100 ng/ml.

## **2.3 Hippocampal slice culture and gene-gun transfection**

Hippocampal slice cultures were prepared from postnatal day 6 or 7 Sprague Dawley rats, as described previously (Stoppini et al., 1991). All animal handling in this

study was conducted in accordance with the animal care and use guidelines of the Duke University Medical Center. Rat pups were anesthetized with isofluorane, decapitated, and the brains quickly placed in ice-cold dissection medium containing: 1 mM CaCl<sub>2</sub>, 5 mM MgCl<sub>2</sub>, 10 mM glucose, 4 mM KCl, 26 mM NaHCO<sub>3</sub> and 248 mM sucrose. The hippocampi were then dissected out and cut into slices of 350 μm thickness by a McIlwain tissue chopper (Campden). Individual slices were then placed onto membranes (PICM0RG50, Millipore) interfacing tissue medium (pH 7.4 and mOsm 300) containing: 0.0084 g/ml HEPES base MEM, 20% horse serum, 1 mM L-glutamine, 1 mM CaCl<sub>2</sub>, 2 mM MgSO<sub>4</sub>, 12.9 mM D-glucose, 5.2 mM NaHCO<sub>3</sub>, 30 mM HEPES, 0.075% ascorbic acid, and 1 μg/ml insulin. Cultured slices were incubated at 35 °C, with 97% O<sub>2</sub> and 3% CO<sub>2</sub>. The culture medium was changed every 2-3 days.

After 8-14 days *in vitro*, biolistic transfection of slices was performed using a Helios gene gun (Bio-Rad) loaded with bullets (McAllister, 2000; O'Brien and Lummis, 2006). Bullets were prepared using 9-11 mg gold particles (1.0 μm diameter) coated with a total of 50 μg of cDNA. After 1-3 days of transfection, positive CA1 pyramidal neurons at a depth of 15-50 μm from the tissue surface were used for experiments.

## **2.4 Two-photon fluorescence lifetime imaging**

Fluorescence resonance energy transfer (FRET) imaging was performed using a custom-built 2-photon fluorescence lifetime imaging microscope (2pFLIM) (Murakoshi

et al., 2008; Yasuda et al., 2006). EKAR sensor was excited with a Ti:Sapphire laser (Maitai; Spectra-Physics, Fremont, CA) tuned to a wavelength of 920 nm. The laser intensity was controlled using an electro-optical modulator (Pockels cells, Conoptics). Emitted fluorescence from mEGFP- and mRFP-tagged sensors was collected by an objective (60x, numerical aperture 0.9, Olympus), divided by a dichroic mirror (565 nm; Chroma) and detected by two separated photoelectron multiplier tubes (PMTs) placed after wavelength filters (HQ510/70-2p for green and HQ620/90-2p for red, Chroma). For fluorescence lifetime imaging in the green channel, PMT with low transfer time spread (H7422-40p; Hamamatsu) was used. Fluorescence lifetime images were obtained using a time-correlated single photon counting board (SPC-140; Becker & Hickl) controlled with custom MATLAB-based program ScanImage (Pologruto et al., 2003; Yasuda et al., 2006).

Unless otherwise specified, all experiments were performed at room temperature (25-27 °C) and the bathing solution was Mg<sup>2+</sup>- free artificial cerebral spinal fluid (ACSF) containing the following: 4.0 mM CaCl<sub>2</sub>, 1 μM TTX and 2.0 mM 4-methoxy-7-nitroindolyl (MNI)-caged-L-glutamate (Tocris), which was continuously aerated with 95% O<sub>2</sub> and 5% CO<sub>2</sub>. To maintain the osmotic pressure (~310 mosmol kg<sup>-1</sup>) of the bathing solution for a long experiment (> 1 hr), distilled water was slowly added (1-2 μl min<sup>-1</sup> into 7 ml at room temperature, or 10 μl min<sup>-1</sup> into 10 ml at 34 °C). CA1 pyramidal neurons were identified based on their morphology and location within the hippocampal slice (Andersen, 2007).

## 2.5 2pFLIM data analyses

The mean fluorescence lifetime averaged over multiple populations  $\tau_m$  was measured from the mean photon arrival time  $\langle t \rangle$  as follows (Yasuda et al., 2006):

$$\tau_m = \langle t \rangle - t_0 = \frac{\int dt \cdot tF(t)}{\int dt \cdot F(t)} - t_0 \quad (\text{Eq. S1})$$

where  $F(t)$  is the fluorescence decay curve after a short laser pulse,  $t$  is time, and  $t_0$  is the time offset. The offset  $t_0$  was estimated before each experiment by fitting fluorescence decay curve with double exponential function and comparing  $\langle t \rangle$  with the fluorescence lifetime averaged over two populations as follows:

$$t_0 = \frac{\int dt \cdot tF(t)}{\int dt \cdot F(t)} - \tau_m \sim \frac{\int dt \cdot tF(t)}{\int dt \cdot F(t)} - \frac{P_1\tau_1^2 + P_2\tau_2^2}{P_1\tau_1 + P_2\tau_2}, \quad (\text{Eq. S2})$$

where  $P_1$  and  $P_2$  are the fraction and  $\tau_1$  and  $\tau_2$  are fluorescence lifetime of EKAR in open and closed conformations obtained by fitting. Change in fluorescence lifetime is independent of  $t_0$ , thereby independent of model and curve fitting.

Basal  $\tau_m$  and  $P_2$  of EKAR<sub>nuc</sub> were  $2.35 \pm 0.04$  ns and  $21.6 \pm 5\%$  (mean  $\pm$  SD), respectively. Neurons with high basal EKAR<sub>nuc</sub> FRET ( $\tau_m < 2.29$  or  $P_2 > 30\%$ ) were discarded from further analyses due to the saturation of FRET signal.

## 2.6 Two-photon glutamate uncaging and spine enlargement

A second Ti:Sapphire laser tuned at a wavelength of 720 nm was used to uncage MNI-caged glutamate at the tip of the spine of interest (see Figure 3.1). Uncaging experiments were performed in artificial cerebral spinal fluid (ACSF) containing: 127 mM NaCl, 2.5 mM KCl, 4 mM CaCl<sub>2</sub>, 25 mM NaHCO<sub>3</sub>, 1.25 mM NaH<sub>2</sub>PO<sub>4</sub> and 25 mM glucose) containing zero Mg<sup>2+</sup>, 1 μM TTX and 2 mM MNI-caged L-glutamate aerated with 95% O<sub>2</sub> and 5% CO<sub>2</sub> at 25-27 °C. The uncaging protocol applied to induce structural plasticity consisted of 60 uncaging pulses (720 nm, 6 mW) with 4-6 ms duration at 1Hz.

Spine volume was estimated by quantifying the fluorescence intensity of mEGFP from EKAR sensor, GFP-ERK2, or individually expressed mEGFP protein. The changes in spine volume upon uncaging were represented by the fractional change in fluorescence light intensity ( $[F-F_0]/F_0$ ). The transient volume change was calculated as the difference between the peak volume at 1-2 min after uncaging and the baseline volume, normalized to the baseline. The sustained volume change was estimated as the spine volume at a later time (25-30 min for immunostaining experiments and 60-70 min in EKAR imaging) minus the baseline volume, normalized to the baseline.

## 2.7 GCaMP imaging and analysis

Hippocampal organotypic slices were transfected with GCaMP3 with biolistic gene transfer as described above. 36-48 hr after transfection, imaging and uncaging were

performed at the same setup used for 2pFLIM. Images were acquired at the frame-scan mode (128 x 128 pixels, 1ms/line). Time series were reported as  $\Delta F/F = (F-F_0)/F_0$  where  $F$  is the raw fluorescence and  $F_0$  is the mean fluorescence in a baseline period of 32 frames (about 4 s) prior to uncaging stimuli. Image analysis was performed with ImageJ (NIH).

## **2.8 Immunohistochemistry and confocal immunofluorescence imaging**

Neurons in organotypic hippocampal slice culture were transfected with monomeric enhanced green fluorescent protein (mEGFP) using biolistic gene transfer (McAllister, 2000). Slices with at least two mEGFP-expressing CA1 neurons were subjected to experiments, and at least one mEGFP CA1 neuron in the slice was not stimulated and used as control. Following stimulation, the slices were incubated in imaging solution for an additional 45-90 min and then fixed in 4% paraformaldehyde in phosphate buffered saline (PBS) at 4°C for >16 hours. The slices were next permeabilized and blocked at 4°C for 1 hr in PBS containing 5% normal goat serum and 0.2% Triton-X100 (NGS/PBST). Primary antibody staining was performed for 16 hr at 4°C using rabbit anti-phospho-ERK, anti-phospho-CREB, or anti-phospho-Elk-1 antibodies (Cell Signaling) diluted in NGS/PBST (1:100, v/v). After 6 washes (5 min each) in NGS/PBST, the slices were incubated with Alexa Fluor 568-conjugated anti-rabbit goat secondary antibody (Invitrogen). Both NGS/PBST and PBS were supplemented with phosphatase inhibitors NaF (5 mM) and Na<sub>3</sub>VO<sub>4</sub> (1 mM). To label the nucleus, slices were incubated

with 4',6-diamidino-2-phenylindole (DAPI, 1  $\mu$ M; Invitrogen) diluted in PBS for 5 min. Slices were mounted between a coverslip and a glass slide with VectaShield mounting medium (Vector Laboratories, #H-1000).

Confocal images of fixed tissues were acquired by a Leica TCS SP5 laser scanning confocal microscope with a 40x 1.25 N.A. oil objective. DAPI, mEGFP and Alexa Fluor 568 were excited by a 405 nm Diode laser, a 488 laser line of an Argon laser, and a 561 nm diode laser, respectively. An acousto-optical beam splitter (AOBS) served as tunable dichroic for all lasers. PMTs were adjusted to allow sufficient separation between different channels. Images were acquired with averaging 6 lines at a resolution of 1024x1024 pixels.

Confocal images were analyzed using ImageJ. Briefly, the nucleus region (marked by DAPI fluorescence) of a neuron was manually delineated as an ROI in the blue channel. The mean intensity of each ROI in the red channel (Alexa Fluor 568) was then measured. The result of each target neuron (identified by mEGFP signal in the green channel) was normalized to the average of five random surrounding untransfected neurons.

## **2.9 Live imaging of mEGFP-ERK2**

CA1 pyramidal neurons in organotypic hippocampal slices were co-transfected with mEGFP-ERK2 and mRFP-MEK1 at DNA amount ratio of 1:3 using biolistic gene

transfer. Time-lapse imaging of mEGFP-ERK2 was performed 1-3 days after transfection with the same two-photon imaging system used for 2pFLIM. Analysis of fluorescence intensity in different cellular compartments was performed by ScanImage (Pologruto et al., 2003). Neurons with nuclear/somatic ratio of mEGFP-ERK2 intensity  $> 0.3$  under basal condition were regarded as basally activated and therefore excluded from analysis.

## **2.10 Statistical Analysis**

Unless otherwise stated, error bars represent standard errors of the means (SEM). Statistical analyses were performed by one-way ANOVA followed by post-hoc using the least significance difference.

## Chapter 3. ERK activation in the nucleus elicited by LTP induction at individual dendritic spines

### 3.1 Introduction

It is widely accepted that ERK is activated following LTP induction (Davis et al., 2000; English and Sweatt, 1996, 1997; Impey et al., 1998; Winder et al., 1999). Activated ERK seems to appear throughout the whole cell, both in the soma and dendrites (Giovannini et al., 2001). However, the LTP protocols used in previous studies usually involve delivery of electrical stimuli or bath application of chemicals that excite an unknown number of synapses on the postsynaptic CA1 neuron. In addition to this complication, synchronized synaptic stimulation typically evokes dendritic spikes and dendritic action potentials that could propagate to soma (Gasparini et al., 2004; Schiller et al., 2000). The resultant somatic depolarization of the CA1 neuron leads to large  $\text{Ca}^{2+}$  influx through voltage-gated calcium channels (VGCCs) at the somatic and dendritic plasma membrane and subsequent widespread activation of ERK (Dudek and Fields, 2002). Therefore, using conventional LTP protocols, it is difficult, if ever possible, to determine the ERK activity pattern in response to defined synaptic activity.

LTP is known to be input-specific: it can be induced at a single dendritic spine by repetitive uncaging of glutamate (Matsuzaki et al., 2004). Calcium influx through NMDARs is transient ( $\tau_{decay} \sim 20$  ms) and highly compartmentalized in the uncaged spine (Muller and Connor, 1991; Sabatini et al., 2002; Yuste and Denk, 1995). A downstream

effector of calcium, Ras, is activated for ~5 min and active Ras spreads over a distance of ~10  $\mu\text{m}$  along the dendritic shaft (Harvey et al., 2008b). The spatiotemporal dynamics of ERK, which is downstream of Ras, in response to synapse-specific LTP is largely unknown. To address this question, I needed fine control of synaptic inputs, preferably at single-spine spatial resolution. This was enabled by two-photon glutamate uncaging (Figure 3.1) (Matsuzaki and Kasai, 2011).

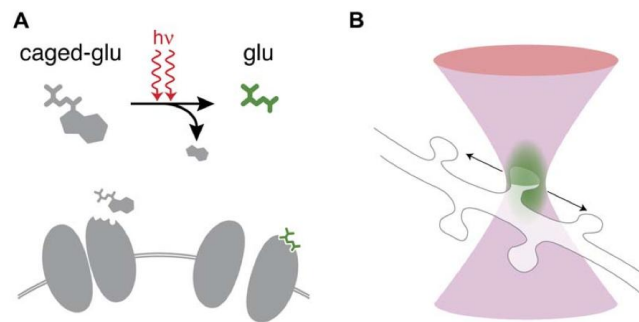


**Figure 3.1 Two-photon glutamate uncaging**

(A) Simultaneous absorption of two infrared photons cleaves off the chemical cage on glutamate, generating the bioactive neurotransmitter.  
(B) Photolysis of caged glutamate occurs with single-spine precision. Adapted from (Judkewitz et al., 2006).

Traditionally, ERK activity is detected by Western blotting or immunostaining for phosphorylated, active ERK. However, these methods fail to provide information with fine spatial resolution in a real-time fashion. Therefore, this study employed a genetically encoded, FRET-based sensor of ERK activity (ERK activity reporter, or EKAR) (Harvey et al., 2008a). As illustrated in Figure 3.2A, EKAR consists of a FRET pair (EGFP and mRFP) flanking a phospho-binding WW domain, a substrate peptide

and an ERK docking domain. Upon ERK activity increase, the substrate peptide becomes phosphorylated by ERK and binds to the phospho-binding domain, leading to a conformational change in the sensor protein. As a result, the EGFP and mRFP are brought into proximity, causing an increase in FRET. This increase in FRET can be detected by 2pFLIM as a decrease in the lifetime (or  $\tau$ ) of EGFP (Figure 3.2B, also see Materials and Methods). Epidermal growth factor (EGF)-induced decrease in EKAR lifetime is completely reversed by the MEK inhibitor U0126, indicating the selectivity and reversibility of this sensor (Harvey et al., 2008a). I used two forms of EKAR: 1) EKAR<sub>nuc</sub>, which is mainly localized in the nucleus due to the presence of a putative nuclear localization signal (NLS) in its phospho-binding domain; and 2) EKAR<sub>cyto</sub>, which is exclusively expressed in the cytosol due to inclusion of a nuclear-export signal (NES) in its sequence (Harvey et al., 2008a).

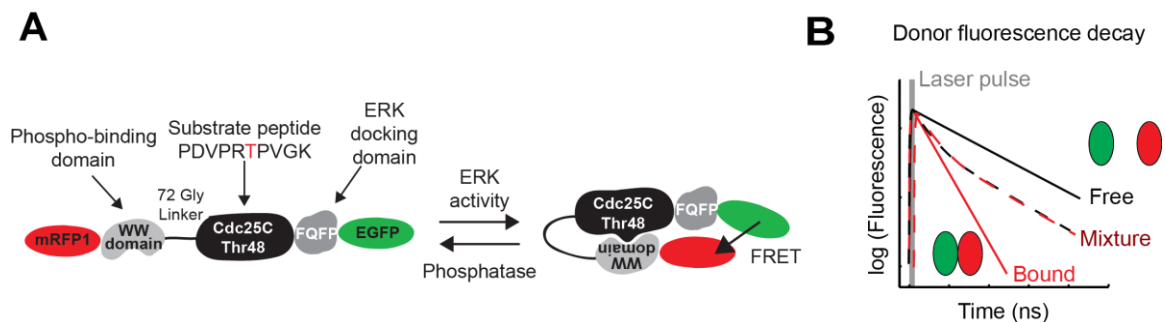


**Figure 3.2 Fluorescence lifetime of EKAR as the major readout of ERK activity**

(A) Design of EKAR. FRET is increased upon phosphorylation of substrate peptide by ERK [Adapted from (Harvey et al., 2008a)]

(B) An increase in FRET is measured as a decrease in the fluorescence lifetime of the donor [Adapted from (Yasuda, 2006)].

With these tools, I set out to investigate the spatiotemporal profile of ERK during in synapse-specific LTP. Specifically, I asked whether ERK in the nucleus could be activated by inducing LTP at individual synapses, without eliciting a somatic depolarization. In this Chapter, I present experimental results supporting the hypothesis that Ras-ERK signaling pathway subserves a synapse-to-nucleus messenger in response to LTP.

## **3.2 Results**

### **3.2.1 Validation of EKAR in dissociated neuronal culture**

To determine the maximum possible signal of EKAR in neurons, BDNF was used to strongly activate ERK in neuronal cultures. Dissociated cortical neurons were transfected with EKARnuc or EKARcyto. As shown in Figure 3.3 A, EKARnuc is highly concentrated in the nucleus whereas EKARcyto is excluded from the nucleus, consistent with previously reported subcellular distribution of these sensors (Harvey et al., 2008a). Bath application of BDNF (100 ng/ml) immediately decreased the fluorescence lifetime ( $-0.033 \pm 0.007$  ns for EKARnuc,  $n = 8$ ;  $-0.030 \pm 0.003$  ns for EKARcyto,  $n = 6$ ; averaged over 40-60 min), whereas vehicle application had no effect on EKAR lifetime ( $0.0011 \pm 0.005$  ns for EKARnuc,  $n = 8$ ;  $-0.0061 \pm 0.004$  ns for EKARcyto,  $n = 4$ ; averaged over 40-60 min, Figure 3.3). This result suggests that both forms of EKAR reliably report ERK activity in a real-time manner. It also informed us the near-maximum lifetime change of EKAR, which would serve as a reference in interpreting later results.

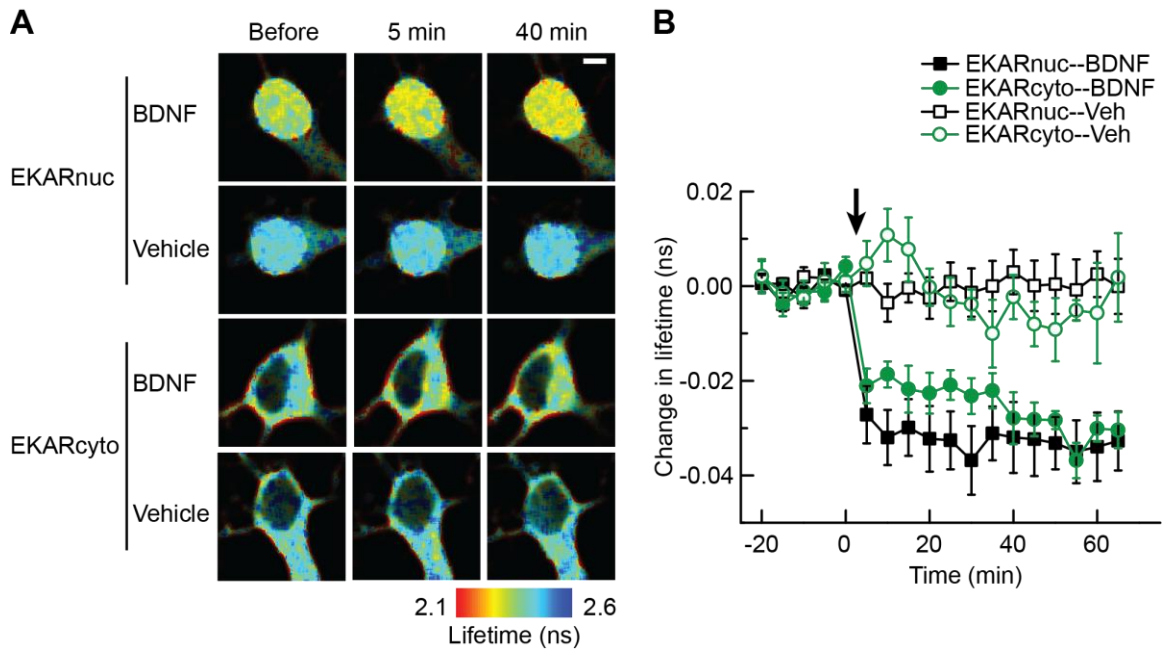


**Figure 3.3 Decrease in fluorescence lifetime of EKAR caused by BDNF stimulation in dissociated culture of cortical neurons**

(A) Fluorescence lifetime images of the soma region of EKARnuc- or EKARcyto-expressing cortical neurons. Decreases in EKAR lifetime upon BDNF application indicate ERK activation. Scale bar = 5  $\mu$ m.

(B) Time course of EKAR fluorescence lifetime. The arrow indicates bath application of BDNF (100 ng/ml) or vehicle.

### 3.2.2 ERK activity during structural plasticity of a single dendritic spine

Firstly, I examined the kinetics of ERK activity during structural plasticity of a single dendritic spine. CA1 pyramidal neurons in organotypic hippocampal slices were sparsely transfected with EKAR using ballistic gene transfer, and imaged using 2pFLIM. In order to obtain a strong fluorescence signal and avoid photobleaching from using high imaging laser power, imaging of the dendritic segments was performed in EKARcyto-expressing neurons whereas imaging of neuronal nuclei in EKARnuc-expressing neurons. A train of two-photon uncaging laser pulses (60 pulses at 1 Hz, 4-6

ms each, 4-6 mW) was applied to a spine separated from neighboring spines in ACSF containing 4 mM  $\text{Ca}^{2+}$ , 0 mM  $\text{Mg}^{2+}$ , 1  $\mu\text{M}$  TTX and 2 mM MNI-glutamate (Lee et al., 2009; Matsuzaki et al., 2004; Murakoshi et al., 2011). This repetitive glutamate uncaging caused a transient phase of dramatic spine enlargement followed by a sustained phase of moderate enlargement for at least an hour (Figure 3.4 A), indicating that structural LTP (sLTP) was induced at the stimulated spine. However, there was no change in EKAR fluorescence lifetime at the stimulated spine, ~10-15  $\mu\text{m}$  dendritic segment bearing the stimulated spine, or the nucleus (Figure 3.4 B-E). Since ERK is thought to be required for the sustained phase of sLTP (Harvey et al., 2008b), this negative result suggests at least three possibilities: 1) ERK activation during sLTP induced at a single spine was below the detection threshold of EKAR; 2) ERK was activated in regions that were not captured in this imaging experiment; or 3) sLTP required the baseline levels of ERK activity but did not produce further ERK activation.

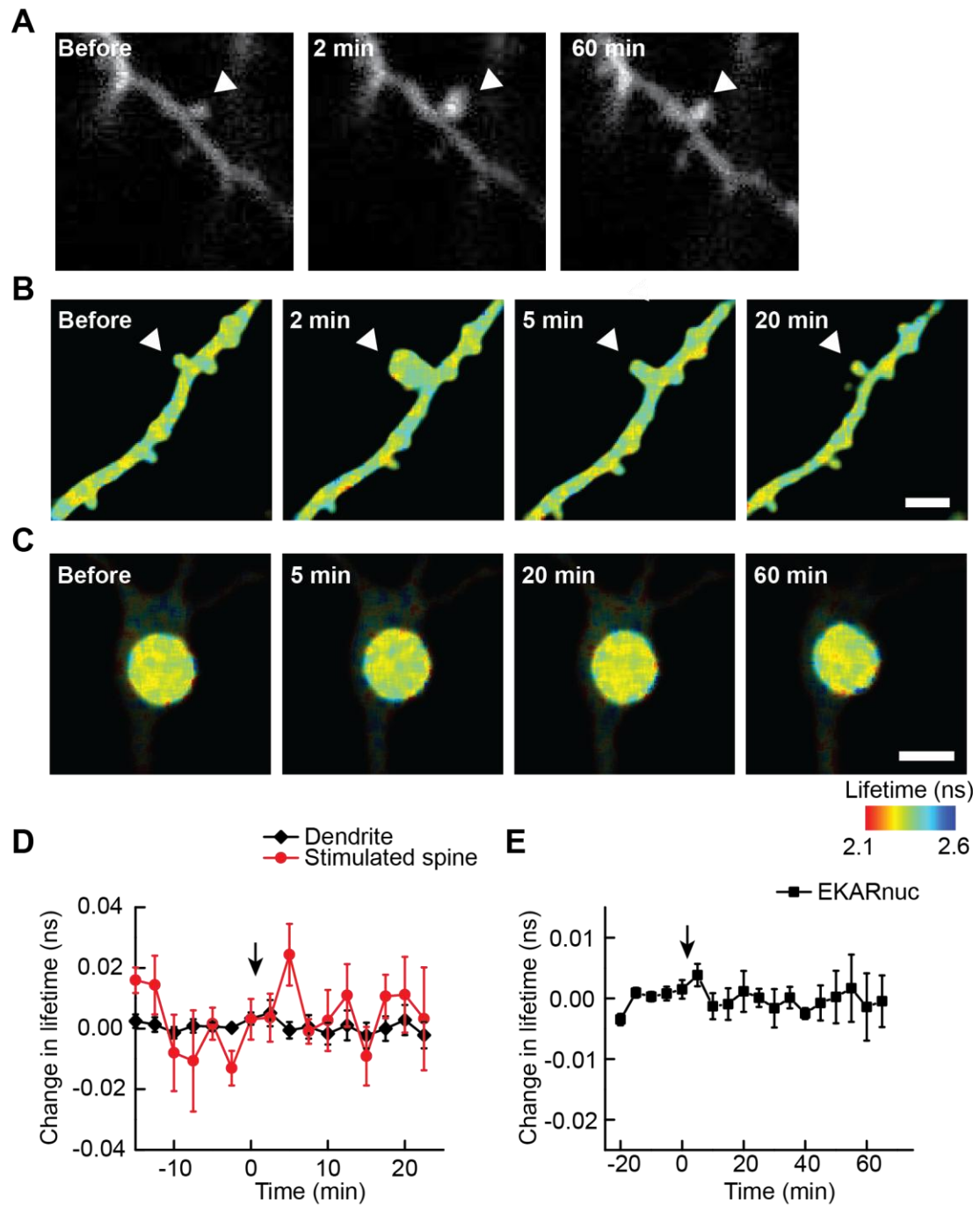


Figure 3.4 EKAR fluorescence lifetime was not altered by inducing structural plasticity at a single dendritic spine

- (A) Stimulation of a single spine (indicated by arrowhead) by repetitive two-photon glutamate uncaging (1Hz, 60s) induced structural plasticity (sLTP) that persisted for more than 1 hr.
- (B) Fluorescence lifetime images of an EKARcyto-expressing dendrite during induction of sLTP at a single spine (arrowhead). Scale bar = 3  $\mu\text{m}$ .
- (C) Fluorescence lifetime images of an EKARnuc-expressing nucleus during induction of sLTP at a single dendritic spine. Scale bar = 10  $\mu\text{m}$ .
- (D) Time course of EKAR fluorescence lifetime in the stimulated spine (red dots) and nearby dendritic shaft (~10-15  $\mu\text{m}$ , black diamonds). The black arrow indicates induction of sLTP at a single spine. n = 5.
- (E) Time course of EKAR fluorescence lifetime changes in the nucleus of a CA1 neuron that was stimulated by inducing sLTP at a single spine (black square). The black arrow indicates sLTP induction. n = 7.

### **3.2.3 Activation of ERK in the nucleus by inducing sLTP at a few dendritic spines**

As detected by EKAR, nuclear ERK is activated by a global LTP protocol--theta burst stimulation (Harvey et al., 2008a), but not by inducing sLTP locally at a single dendritic spine (shown above, Figure 3.4). It is unknown whether nuclear ERK can be activated by inducing sLTP in a few dendritic spines. To address this question, the nucleus of an EKARnuc-expressing CA1 neuron was imaged by 2pFLIM. sLTP was induced successively at 7 spines that were distributed over the proximal dendritic region (1-2 spines per dendritic branch, > 10  $\mu\text{m}$  in between, all within 200  $\mu\text{m}$  to the soma, Figure 3.5 A-B). Structural plasticity was also monitored by imaging weak EKARnuc fluorescence in the cytosol. As shown in Figure 3.5 C & E, sLTP was induced at the stimulated spines in EKARnuc neurons to a degree similar to that in mEGFP neurons (transient volume change:  $275 \pm 18\%$  in EKARnuc neurons and  $293 \pm 41\%$  in

mEGFP neurons; sustained volume change:  $61 \pm 4\%$  in EKARnuc neurons and  $64 \pm 11\%$  in mEGFP neurons), confirming that expression of the sensor did not disrupt structural plasticity. The magnitude of structural plasticity observed here was also consistent with previous studies (Harvey et al., 2008b; Lee et al., 2009; Matsuzaki et al., 2004; Murakoshi et al., 2011). Following this 7-spine stimulation, the fluorescence lifetime of EKARnuc in the nucleus gradually declined ( $-0.022 \pm 0.002$  ns from binning of 40-70 min,  $n = 7$ ; Figure 3.5 F, G: Ctrl), indicating that a slow and sustained elevation of ERK activity in the nucleus was produced by sLTP induction at 7 spines. This decrease in EKARnuc lifetime was completely blocked by the ERK inhibitor FR180204 ( $-0.00053 \pm 0.00042$  ns from binning of 40-70 min,  $n = 7$ ; Figure 3.5 F, G: FR), confirming that lifetime change of EKARnuc specifically reports the activity of ERK. Notably, the finding that nuclear ERK was activated by 7 spines, but not at a single spine, was successfully reproduced at  $\sim 34^\circ\text{C}$  (Figure 3.6), implying a physiological relevance of this finding.

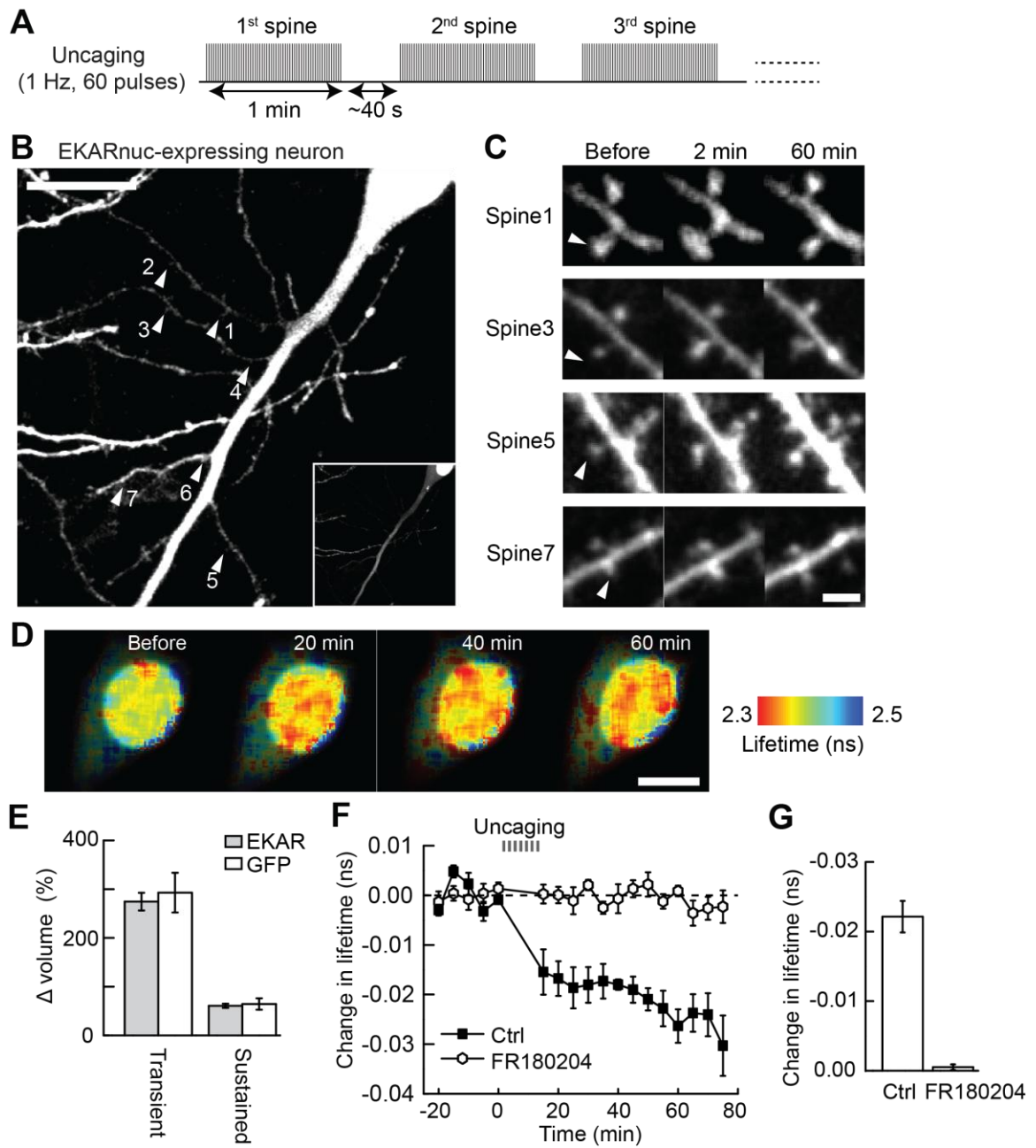
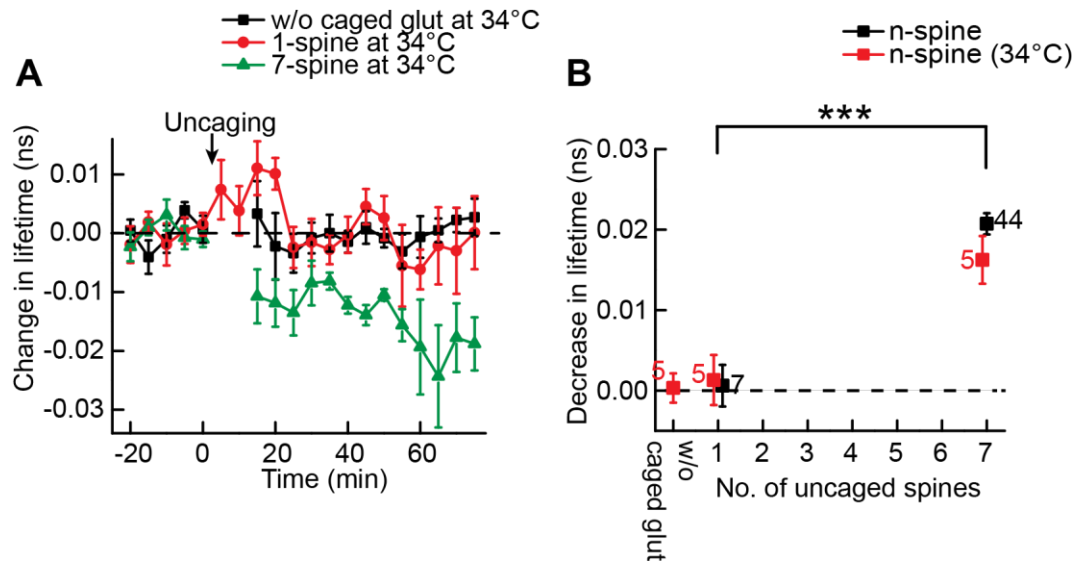


Figure 3.5 Nuclear ERK is activated by inducing sLTP at a few dendritic spines

- (A) Schematic for 7-spine stimulation.
- (B) Image of a neuron expressing EKARNuc. The white arrowheads indicate the locations of 7 stimulated spines. Scale bar, 20  $\mu\text{m}$ .
- (C) Images of spine structural long-term potentiation (sLTP) induced by two-photon glutamate uncaging in the neuron shown in (B). Scale bar, 5  $\mu\text{m}$ .
- (D) Fluorescence lifetime images of EKARNuc before and after (20, 40 and 60 min) 7-spine stimulation in the same neuron as in (B) and (C). Scale bar, 10  $\mu\text{m}$ .
- (E) Quantification of the transient (1-2 min) and sustained (30-70 min) phases of sLTP following 7-spine stimulation in EKARNuc neurons and mEGFP neurons (n = 38 for EKARNuc neurons and n = 16 for mEGFP neurons).
- (F) Time course of EKARNuc fluorescence lifetime following 7-spine stimulation (Ctrl; solid squares). EKAR lifetime in the paired experiments with ERK inhibitor FR180204 (50  $\mu\text{M}$ ) is also shown (open hexagons). n = 7 for both conditions. Error bars are SEM.
- (G) Changes in EKARNuc fluorescence lifetime averaged over 40-70 min from the results shown in (F).



**Figure 3.6 E KAR lifetime change in response to sLTP induction at near physiological temperature**

(A) Time course of E KAR fluorescence lifetime change in the nucleus at near physiological temperature ( $\sim 34^{\circ}\text{C}$ ). E KAR-expressing CA1 neurons were stimulated by repetitive uncaging pulses (sLTP protocol) delivered to a single spine (“1-spine at  $34^{\circ}\text{C}$ ”), 7 spines (“7-spine at  $34^{\circ}\text{C}$ ”), or 7 spines in the absence of caged glutamate (“w/o caged glut at  $34^{\circ}\text{C}$ ”).  $N = 5$  for all groups.

(B) Quantification of E KAR fluorescence lifetime change at  $34^{\circ}\text{C}$  (red) compared with that at room temperature (black, data same as in Figure 5.1). Data were binned over 40-70 min following 7-spine stimulation and 30-60 min following 1-spine stimulation. Numbers of samples are indicated next to the data points. Data are means  $\pm$  SEM.  $***P < 0.01$ , ANOVA followed by post-hoc test using the least significant difference.

### 3.2.4 Increase in phospho-ERK level in the nucleus following LTP induction at a few dendritic spines

The results shown above suggest that nuclear ERK could be activated by inducing sLTP at as few as 7 spines. To confirm this intriguing finding, I measured nuclear ERK activation by an alternative method: immunostaining for ERK phosphorylated at the sites essential for ERK activation (Thr-202 and Tyr-204 for ERK1 and Thr185 and Tyr187 for ERK2) (Canagarajah et al., 1997). Firstly, organotypic slices

were transfected with monomeric enhanced green fluorescent protein (mEGFP). Next, mEGFP-expressing CA1 neurons were stimulated by uncaging at 7 spines and the slices fixed and subjected to immunostaining with anti-phospho-ERK antibody. The level of phosphorylated ERK in the nucleus was then quantified by measuring the immunofluorescence in the nucleus of the transfected neuron normalized to the average fluorescence in nuclei of 5 surrounding untransfected neurons. As shown in Figure 3.7, the level of nuclear phospho-ERK was significantly higher at 45 min and 75 min after 7-spine stimulation compared to unstimulated mEGFP-expressing neurons in the same slices ( $P < 0.05$ , one-way ANOVA followed by post-hoc test using the LSD). Thus, consistent with EKARnuc imaging results shown in Figure 3.5, the immunostaining data indicate that activation of 7 spines induced a slow and sustained activation of ERK in the nucleus.

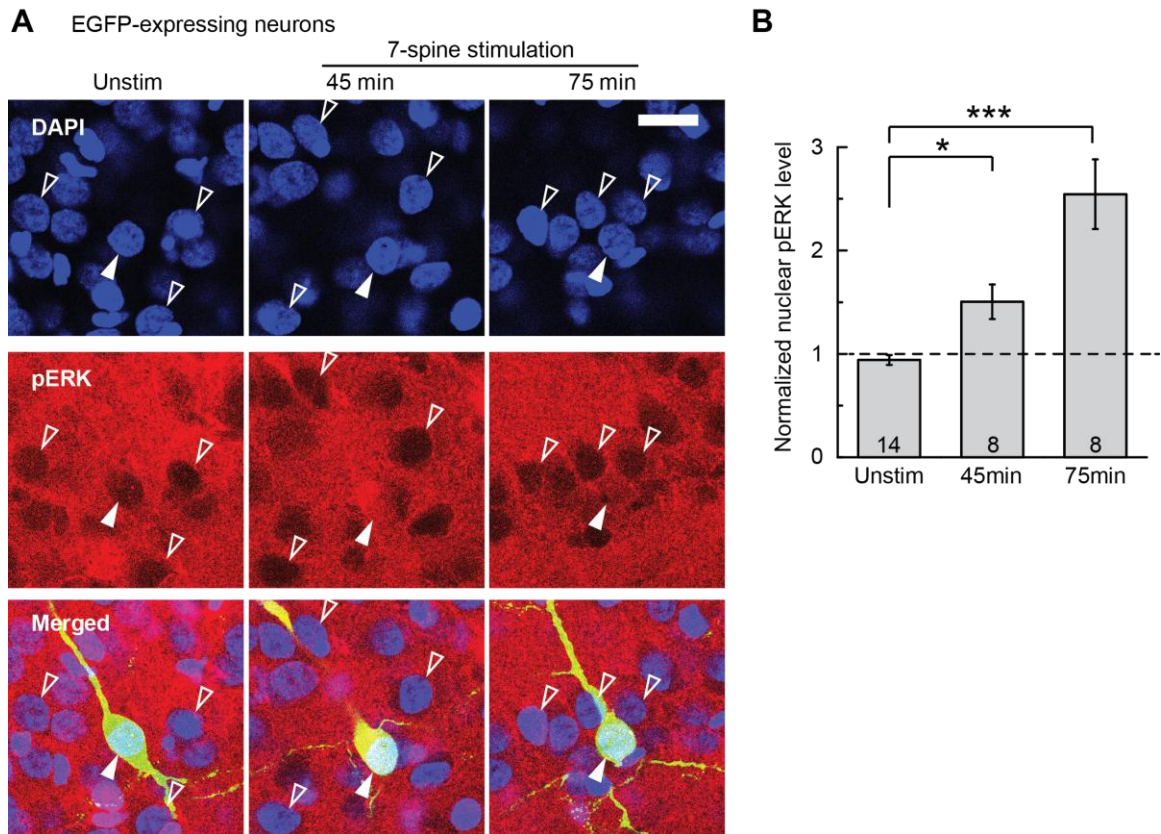


**Figure 3.7 Increase in phospho-ERK in the nucleus following stimulation of 7 spines**

(A) Immunofluorescence images of phospho-ERK (red) in neurons expressing mEGFP (green). Shown are an unstimulated neuron (“Unstim”; left) and neurons fixed 45 min (middle) or 75 min (right) after 7-spine stimulation. Nuclei were stained with nucleus dye DAPI (blue). All three neurons shown were from the same slice. Filled arrowheads, mEGFP-expressing neurons (either unstimulated or uncaged); open arrowheads, examples of surrounding neurons. Scale bar, 20  $\mu$ m.

(B) Quantification of the immunofluorescence of phospho-ERK in the nuclei. The immunofluorescence in the nucleus (identified with DAPI staining) of an mEGFP-expressing neuron was normalized to the averaged immunofluorescence in the nuclei of 5 surrounding untransfected neurons. Stimulated neurons were always paired with unstimulated neurons in the same slices (see Materials and Methods). The numbers of samples are indicated at the bottom the graph. Data are means  $\pm$  SEM. \* $P < 0.05$ , \*\*\* $P < 0.001$ , ANOVA followed by post-hoc test using the least significance difference.

### 3.2.5 Nuclear translocation of ERK2 after inducing sLTP at a few dendritic spines

At basal state, ERK is mainly localized in the cytoplasm (Ortiz et al., 1995). Since its upstream kinase MEK is primarily localized in the cytoplasm due to an NES in its sequence (Fukuda et al., 1996), ERK is presumably activated in the cytoplasm. To exert its role in regulating gene transcription, ERK must translocate to the nucleus. Indeed, previous studies have shown that during LTP, activation of nuclear ERK is associated with translocation of active ERK2 into the nucleus (Impey et al., 1998). To determine if nuclear ERK translocation also occurs in response to synapse-specific LTP induction in a few spines, I performed live imaging of mEGFP-tagged ERK2. CA1 neurons in organotypic slices were co-transfected with mEGFP-ERK2 and mRFP-MEK1. Co-expression of MEK1 is required for retaining overexpressed ERK2 in extra-nuclear region under basal condition, probably due to one-to-one stoichiometry of the mEGFP-ERK2 interaction with mRFP-MEK1 (Burack and Shaw, 2005; Fukuda et al., 1997; Horgan and Stork, 2003; Wiegert et al., 2007). Before stimulation, mEGFP-ERK2 was localized predominantly to the cytoplasm (Figure 3.8 A). Following 7-spine stimulation, mEGFP-ERK2 slowly accumulated in the nucleus and reached a plateau after ~60 min (normalized nuc/soma ratio:  $140 \pm 4\%$ , averaged over 60-70 min,  $n = 9$ , Figure 3.8). The time course was consistent with that of the nuclear ERK activity increase measured with EKARnuc (Figure 3.5) and immunostaining for phospho-ERK (Figure 3.7). This result suggests that nuclear translocation is responsible, at least in part, for increased ERK

activity in the nucleus. Without caged glutamate in the bath solution, the same stimulation protocol failed to induce any increase in the nuclear fraction of mEGFP-ERK2 (nuc/soma ratio:  $96 \pm 7\%$ , averaged over 60-70 min,  $n = 7$ ; Figure 3.8), indicating that the observed nuclear accumulation of ERK2 is not an artifact resulting from photodamage by uncaging and imaging lasers or long period of chamber incubation.

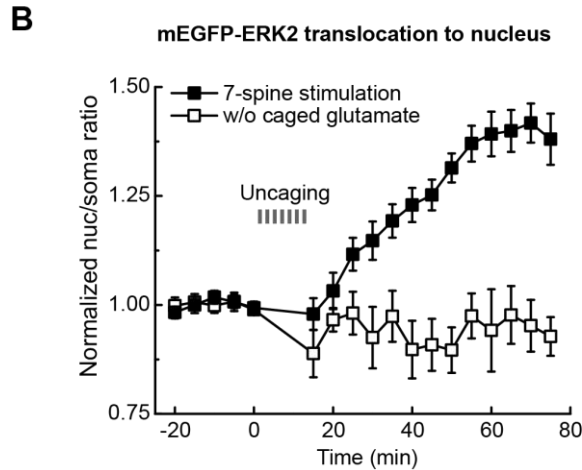
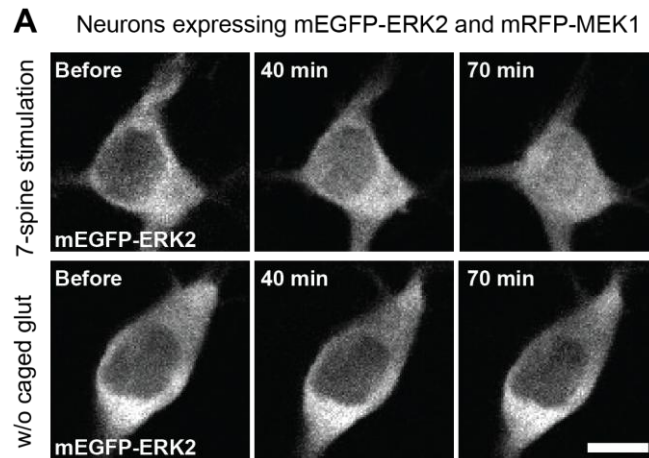


**Figure 3.8 Nuclear translocation of ERK2 was induced by 7-spine stimulation**

CA1 pyramidal neurons expressing mEGFP-ERK2 and mRFP-MEK1 were identified and stimulated by glutamate uncaging at 7 spines on proximal apical dendrites, same protocol used in Figures 3.5 - 3.7.

(A) Two-photon imaging of mEGFP-ERK2 in hippocampal neurons with 7 spines stimulated with uncaging laser pulses in the presence (“7-spine stimulation”) or absence of caged glutamate (“w/o caged glut”), respectively. Representative images of mEGFP-ERK2 are shown for time points prior to uncaging (Before), at 40 and 70 min after uncaging (40 min, 70 min). Scale bar: 10  $\mu$ m.

(B) Time course of nuclear translocation of mEGFP-ERK2 in response to 7-spine stimulation in the presence (n = 9) or absence (n = 7) of caged glutamate. The fraction of mEGFP-ERK2 in the nucleus (i.e. nuclear/somatic ratio) was normalized to the baseline (-20 min ~ 0min). Data are means  $\pm$  SEM.

### 3.3 Discussion

ERK has long been implicated in LTP and it is activated by many different LTP-inducing protocols, such as high-frequency stimulation (Dudek and Fields, 2001; English and Sweatt, 1996), theta burst stimulation (Dudek and Fields, 2001; Harvey et al., 2008a; Schmitt et al., 2005), BDNF (Wiegert et al., 2007), and forskolin application (Selcher et al., 2003). ERK is also considered to be activated during structural plasticity (sLTP) in a single dendritic spine—the smallest unit of LTP, since blocking Ras-ERK signaling pathway impairs sLTP (Harvey et al., 2008b; Patterson et al., 2010). But what is the spatiotemporal kinetics of ERK when a single synapse is undergoing synaptic plasticity? Particularly, is ERK activity in the nucleus elevated by inducing sLTP locally at individual synapses? To address these questions, I monitored ERK activity primarily using FRET-based sensor EKAR while inducing sLTP at individual dendritic spines with repetitive glutamate uncaging. I have demonstrated that inducing sLTP sequentially at 7 spines by glutamate uncaging caused a sustained decrease in the fluorescence lifetime of EKAR (Figures 3.5-3.6) and an increase in phospho-ERK immunoreactivity in the nucleus (Figure 3.7). This sustained increase in nuclear ERK activity was accompanied by translocation of ERK2 from the cytoplasm to the nucleus (Figure 3.8). These results suggest that ERK is activated in the nucleus for at least 1 hr following 7-spine stimulation. As each CA1 pyramidal neurons have roughly 10,000 synapses, our results indicate that activation of only a tiny fraction ( $< 0.1\%$ ) of synapses can activate nuclear

signaling. More importantly, as action potentials were blocked by TTX in the imaging solution, these results suggest that information is transmitted from activated synapses into the nucleus through biochemical signals and that Ras-ERK signaling cascade might play a role in such synapse-to-nucleus communication.

The absolute change in EKAR lifetime elicited by 7-spine stimulation (i.e. -0.022ns) was smaller than a typical signal from CaMKII sensor or Ras sensor (Harvey et al., 2008b; Lee et al., 2009). However, several lines of evidence suggest that it might have profound significance. First, the EKAR lifetime change induced by 7-spine stimulation is ~67% of that induced by BDNF application, a near-maximum response (Figure 3.3). Second, the decrease in EKAR lifetime induced by 7-spine stimulation (Figure 3.5) is similar to that induced by electrical theta-burst stimulation [ $\sim -0.02$  ns, (Harvey et al., 2008a)]. Third, the same 7-spine stimulation produced a 1.5-fold increase in phospho-ERK level in the nucleus (Figure 3.7), a change comparable to the that produced by BDNF or KCl treatment shown by previous studies (Impey et al., 1998; Schmitt et al., 2005; Wiegert et al., 2007). Fourth, the same 7-spine stimulation produced an ~40% increase in the nuc/soma ratio of ERK2 (Figure 3.8), which is half of amount induced by action potential bursting (Wiegert et al., 2007). Taken together, inducing sLTP successively at 7 spines leads to a marked increase of ERK activity in the nucleus that might have physiological relevance.

My results also showed that inducing sLTP at one spine did not affect the lifetime of EKAR in the stimulated spine or dendritic segment (Figure 3.4). This is surprising because ERK was believed to be activated in or near the stimulated spine during sLTP based on the previous findings that: (1) Ras is activated in the stimulated spine during sLTP and invades ~10  $\mu\text{m}$  of the dendrite shaft; and (2) blocking the Ras-ERK pathway abolishes sLTP (Harvey et al., 2008b; Patterson et al., 2010). This contradiction could be explained by any of the three possible scenarios. First, the basal level of ERK activity in the dendrites is adequately high, thus preventing any further increase by inducing sLTP at a single spine. Indeed, as shown by immunohistochemistry, the basal level of phospho-ERK in the cytoplasm was much higher than that in the nucleus (Figure 3.7). Nevertheless, a certain degree of ERK activity is necessary to structural plasticity, since complete blockade of ERK kinase signaling impaired the sLTP (Harvey et al., 2008b; Patterson et al., 2010). A second possible scenario is that ERK is activated at the stimulated spine but the signal is too small to be detected by EKAR. A newly improved version of EKAR (Komatsu et al., 2011), which has a signal that is 2-3 times higher than the original EKAR, might be used in the future to probe dendritic ERK activity during sLTP in a single spine. Because ERK is evidently activated in the nucleus by inducing sLTP at 7 spines (Figures 3.5 - 3.7), it is of great interest to understand how signals from different synapses are integrated and possibly amplified. Finally, a third possibility is that ERK is activated in regions that

were not captured by the EKAR experiment, such as in the primary dendritic trunk. This possibility was tested in Chapter 5 where the spatiotemporal dynamics of ERK activity was addressed in a more detailed and systematic way.

## **Chapter 4. Molecular mechanisms underlying the nuclear ERK activity increase caused by inducing structural plasticity at a few dendritic spines**

### **4.1 Introduction**

As shown in the previous chapter, ERK activity in the nucleus is elevated after inducing sLTP at as few as 7 dendritic spines while action potentials are inhibited. This nuclear ERK activity increase was attributable, at least in part, to translocation of the phosphorylated kinase molecule from the cytoplasm into the nucleus. However, it is unknown how synaptic stimulation, in the form of glutamate uncaging, is translated into ERK phosphorylation. In this Chapter, I present experimental results that have identified the molecular pathway(s) making this connection.

ERK is activated ultimately by an increase in intracellular  $\text{Ca}^{2+}$  concentration in response to synaptic excitation (Thomas and Huganir, 2004). The  $\text{Ca}^{2+}$  rise could result from  $\text{Ca}^{2+}$  entry via NMDARs (Bading et al., 1995), VGCCs (Bading et al., 1993),  $\text{Ca}^{2+}$ -permeable AMPARs (Jonas et al., 1994), or from  $\text{Ca}^{2+}$  release from intracellular calcium stores (Hagenston et al., 2008; Watanabe et al., 2006). It is unknown which calcium sources are required for nuclear ERK activation triggered by inducing sLTP at a few spines.

As described in Chapter 1 (Section 1.2.2), ERK is activated through two small GTPase pathways. In the classical pathway, small GTPase Ras is activated as a result of

Ca<sup>2+</sup>-dependent inactivation of Ras GAPs and activation of Ras GEFs, activation of receptor tyrosine kinases, or PKC activation. Ras then activates Raf-1. In the novel pathway, PKA activates small GTPase Rap-1, which then activates B-Raf. Both Raf-1 and B-Raf converge on MEK, the kinase that directly phosphorylates and activates ERK (Sweatt, 2001; Sweatt, 2004). The Ras and Rap pathways might serve different roles: Ras mediates AMPAR synaptic delivery during LTP while Rap is thought to mediate AMPAR removal during LTD (Zhu et al., 2002). Ras appears indispensable for structural plasticity, as expression of dominant-negative Ras (dnRas) prevents sustained enlargement of stimulated spines (Harvey et al., 2008b). Here, I hypothesize that the Ras-ERK signaling pathway is required for nuclear ERK activation induced by glutamate uncaging at 7 spines.

## **4.2 Results**

### **4.2.1 (Differential) molecular mechanisms underlying nuclear ERK activation and sLTP**

To address the question of which calcium sources are involved, I determined the effects of different pharmacological inhibitors on the lifetime change of EKARNuc. Inhibition of *N*-methyl-D-aspartate-type glutamate receptors (NMDARs) with 2-amino-5-phosphonopentanoic acid (APV, 50  $\mu$ M) completely prevented nuclear ERK activation ( $P < 0.001$ , Figure 4.1, A and G) as well as sLTP ( $P < 0.001$ , Figure 4.2) (Matsuzaki et al., 2004). In contrast, blockade of VGCCs with CdCl<sub>2</sub> (200  $\mu$ M) did not prevent nuclear ERK

activation ( $P = 0.87$ , Figure 4.1 A and G), although it partially inhibited the sustained phase of sLTP ( $P < 0.05$ , Figure 4.2). Inhibition of type I metabotropic glutamate receptors (mGluRs) with  $\alpha$ -methyl-4-carboxyphenylglycine (MCPG, 1 mM) or NPS 2390 (20  $\mu$ M) attenuated the nuclear ERK activation (both  $P < 0.05$ ; Figure 4.1, B, C and G). Nuclear ERK activation was also partially inhibited when the intracellular  $\text{Ca}^{2+}$  stores were depleted by preincubating slices with cyclopiazonic acid (CPA, 20  $\mu$ M), an inhibitor of sarco/endoplasmic reticulum  $\text{Ca}^{2+}$ -ATPase (SERCA) for more than 40 min prior to the experiments ( $P < 0.05$ ; Figure 4.1, D and G). Inhibition of neither mGluRs nor intracellular  $\text{Ca}^{2+}$  stores affected sLTP (Figure 4.2) (Harvey et al., 2008b; Matsuzaki et al., 2004). These results suggest that nuclear ERK activation requires  $\text{Ca}^{2+}$  influx through NMDARs but not VGCCs. Activation of mGluRs is also required, possibly in an  $\text{Ca}^{2+}$  release-dependent manner. Noticeably, although essential for nuclear ERK activation, mGluRs are dispensable for spine enlargement (Matsuzaki et al., 2004). Therefore, compared to local structural plasticity in the stimulated spines, nuclear ERK activation seems to require additional calcium source and signaling cascades.

Next, I tested the hypothesis that the classical Ras-MEK pathway is required for ERK activation in the nucleus. Expression of a dominant-negative form of Ras (dnRas, Ras S17N) completely abolished nuclear ERK activation whereas expression of an empty vector did not ( $P < 0.001$ ; Figure 4.1, E and G). Also, the MEK inhibitor U0126 (40  $\mu$ M), but not its non-functional analog U0124 (40  $\mu$ M), markedly reduced nuclear ERK

activation ( $P < 0.05$ ; Figure 4.1, F and G). DnRas and U0126 inhibited the sustained phase of sLTP ( $P < 0.05$  for dnRas and  $P < 0.001$  for U0126; Figure 4.2), consistent with previous studies (Harvey et al., 2008b; Patterson et al., 2010). Taken together, these results indicate that both nuclear ERK activation and sLTP are mediated by Ras-MEK signaling pathway.

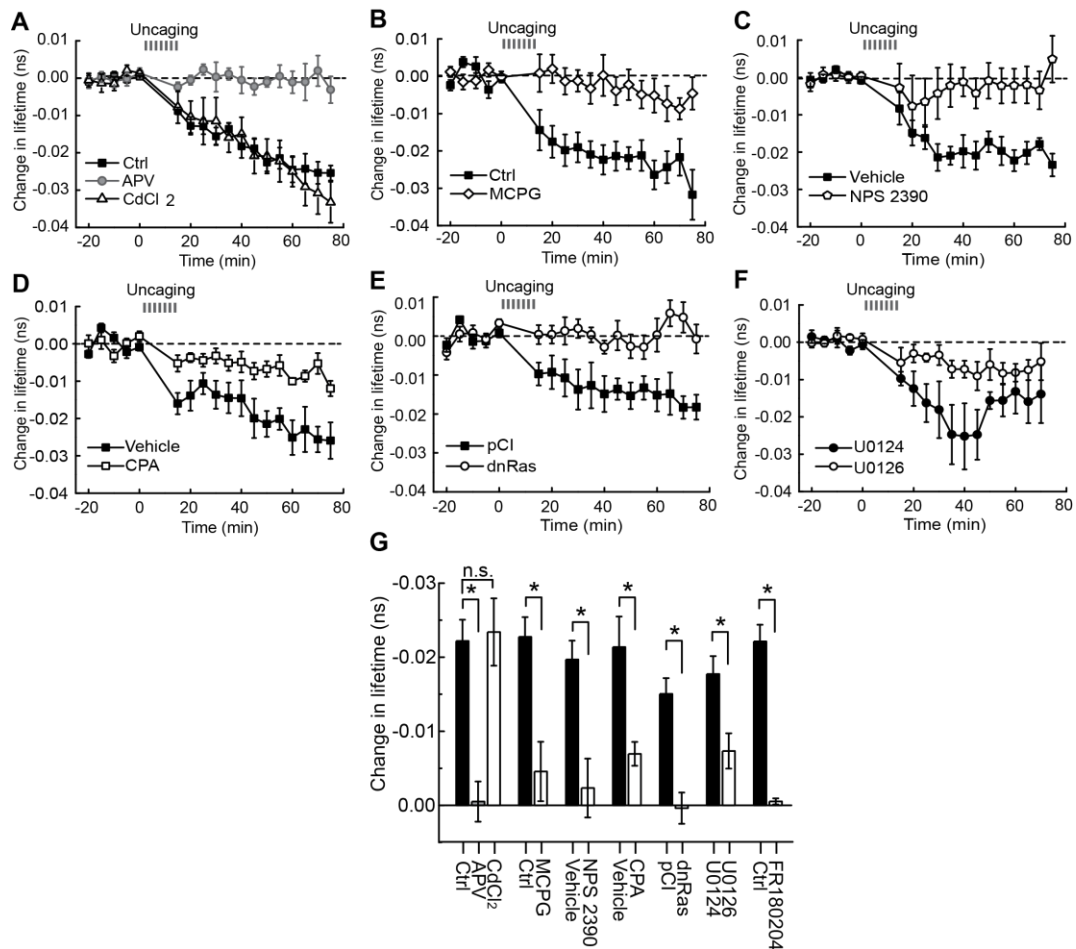


**Figure 4.1 Pharmacological analysis of nuclear ERK activity increase in response to 7-spine stimulation**

(A to F) Effects of pharmacological agents and genetic manipulation on the time course of EKARnuc lifetime change following 7-spine stimulation. The paired control experiments (black filled symbols) were performed with no vehicle in (A) and (B), 0.05% dimethyl sulfoxide (DMSO) as vehicle control in (C) and (D), or non-functional analog U0124 in (F). For (E), EKARnuc together with dnRas or empty vector pCI was delivered biolistically to neurons.  $n = 14$  for Ctrl and 7 for APV and CdCl<sub>2</sub> in (A), 6 for Ctrl and MCPG in (B), 6 for Vehicle and NPS 2390 in (C), 6 for Vehicle and CPA in (D), 7 for pCI and 8 for dnRas in (E), and 7 for U0124 and U0126 in (F).

(G) Sustained fluorescence lifetime change of EKARnuc averaged over 40-70 min (The data are from the same neurons as in A-F and Figure 3.5 G). Data are means  $\pm$  SEM. Asterisks denote statistical significance ( $*P < 0.05$ , ANOVA followed by post-hoc test using the least significant difference).

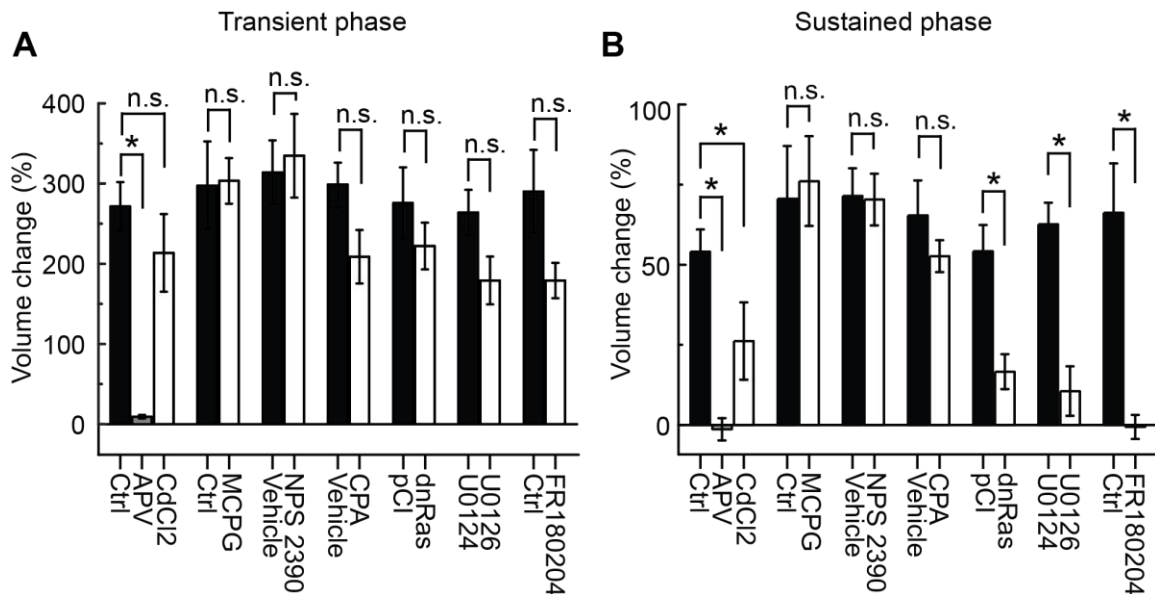


**Figure 4.2 Effects of pharmacological agents and genetic manipulation on spine structural LTP (sLTP).**

Quantification of the transient (1-2 min; **A**) and sustained (~70 min; **B**) phases of sLTP following 2-p glutamate uncaging. The data are from the same neurons as in Figure 4.1 G. Data are means  $\pm$  SEM. n.s., no statistical significance; \* $P < 0.05$ ; ANOVA followed by post-hoc test using the least significance difference.

#### 4.2.2 GCaMP imaging reveals the spread and source of $Ca^{2+}$ evoked by glutamate uncaging

To study the synaptic  $Ca^{2+}$  transient evoked by sLTP protocol, I performed  $Ca^{2+}$  imaging using the genetically encoded calcium indicator GCaMP3 (Tian et al., 2009). In organotypic hippocampal slices, GCaMP3 was delivered by biolistic transfection (see Chapter 2 Materials and Methods). Due to the improved fluorescence intensity of GCaMP3 compared to previous versions of GCaMP, dendritic structures including dendritic spines could be visualized under baseline conditions. Spines of GCaMP3-expressing neurons were stimulated by repetitive glutamate uncaging (1 Hz for 60 s) to

induce sLTP. Secondary dendritic segments bearing the stimulated spines were imaged at a speed of 128ms/frame. In a few experiments (n = 6 spines), the branching point on primary dendritic trunk was close to the stimulated spine and therefore imaged for later analysis. As shown in Figure 4.3 A, repetitive glutamate uncaging produced strong elevations in GCaMP3 fluorescence intensity ( $\Delta F/F$ ) in the stimulated spines (red trace). The fluorescence elevation was much less pronounced, if at all, in adjacent regions (black, blue, grey and green traces). Due to the slow kinetics of the GCaMP3 fluorescence response (rise  $t_{1/2} = 83 \pm 2$  ms, decay  $t_{1/2} = 610 \pm 32$  ms)(Tian et al., 2009), GCaMP3 fluorescence intensity usually peaked at the second acquisition (i.e. 256 ms) following the onset of an uncaging pulse (see the enlarged area of Figure 4.3 A). The baseline of spine GCaMP3 fluorescence was gradually increased during sLTP protocol and did not return to the initial baseline after the uncaging protocol ceased (Figure 4.3 A). This was mostly likely due to induction of structural plasticity in the stimulated spine (Figure 4.3 B). To avoid this complication caused by spine enlargement, the first peak (256 ms) was used in later analysis.

Brightness of region of interests (ROIs) at various locations relative to the stimulated spine was analyzed to reveal the spread of uncaging-evoked  $Ca^{2+}$  transient (Figure 4.3 C). The peak  $\Delta F/F$  of GCaMP3 was  $290 \pm 21$  %,  $161 \pm 23$  %,  $140 \pm 20$  %,  $52 \pm 10$  %,  $9 \pm 3$  %,  $0 \pm 2$  %,  $83 \pm 21$  %,  $2 \pm 3$  % for the stimulated spine, spine base (0  $\mu m$ ), 0-2  $\mu m$ , 2-4  $\mu m$ , 4-6  $\mu m$ , 6-8  $\mu m$  on the dendritic shaft, adjacent spine, and primary trunk branch

point, respectively. These results suggest that uncaging-evoked  $\text{Ca}^{2+}$ , although highly concentrated in the stimulated spine, spills over to as far as 3-4  $\mu\text{m}$  away from the stimulated spine. This spread of  $\text{Ca}^{2+}$  along the axis of a dendritic shaft was consistent with that measured with a low affinity  $\text{Ca}^{2+}$  indicator OGB-5N (length constant  $\lambda = 1.6 - 2.4 \mu\text{m}$ ) (Noguchi et al., 2005). Noticeably, the response in adjacent spines was similar to that in the dendritic shaft at the same distance from the stimulated spine, indicating that adjacent spines were not excited directly by glutamate uncaging.

To study the contributions of various  $\text{Ca}^{2+}$  sources to uncaging-evoked  $\text{Ca}^{2+}$  transient, GCaMP3 imaging was carried out in the presence of different pharmacological inhibitors (Figure 4.3 D). APV completely abolished the GCaMP3 signal triggered by glutamate uncaging, suggesting that NMDAR is the predominant, if not exclusive,  $\text{Ca}^{2+}$  source evoked by the sLTP protocol evident in spines. None of  $\text{CdCl}_2$ , CPA or MCPG affected GCaMP3 signal, suggesting that VGCC and intracellular  $\text{Ca}^{2+}$  stores do not contribute to the spine-specific  $\text{Ca}^{2+}$  transient triggered by sLTP protocol.

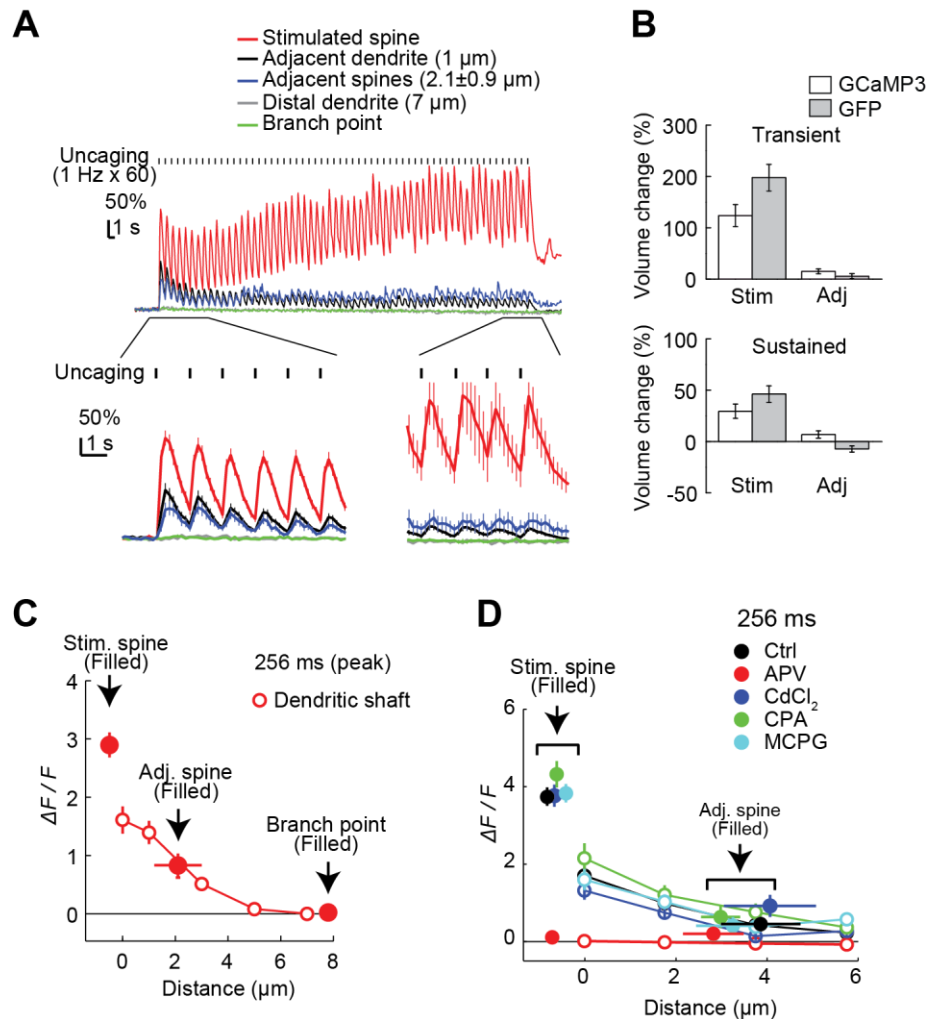


**Figure 4.3 GCaMP3 imaging reveals spread and sources of  $\text{Ca}^{2+}$  transient evoked by glutamate uncaging**

(A) GCaMP3 fluorescence signal ( $\Delta F/F$ ) in response to sLTP protocol (glutamate uncaging at 1 Hz for 60 s). Error bars represent SEMs.

(B) Quantification of the transient (1-2 min) and sustained (~30 min) phases of structural plasticity in GCaMP3 neurons in comparison to GFP neurons. GCaMP3, due to its inherent calmodulin-containing structure, may compete with endogenous calmodulin for  $\text{Ca}^{2+}$  and therefore tends to reduce structural plasticity. This effect is not statistically significant ( $P > 0.05$  for both phases in the stimulated neuron).

(C) Quantification of GCaMP3 fluorescence intensity (at 256 ms) elicited by glutamate uncaging in the stimulated spine [Stim. spine,  $n$  (spine/neuron) = 42/6], adjacent spine [Adj. spine, 2.1  $\pm$  0.9  $\mu\text{m}$  (mean  $\pm$  SD) away from the stimulated spine,  $n$  (spine/neuron) = 41/6], branching point on the primary dendrite [branch point, 7.8  $\pm$  3.3  $\mu\text{m}$  (mean  $\pm$  S.D.) away from the stimulated spine,  $n$  (spine/neuron) = 6/4], and dendritic

shaft at various distances to the stimulated spine [n (spine/neuron) = 42/6 for 0-2  $\mu\text{m}$ , 2-4  $\mu\text{m}$ , and 4-6  $\mu\text{m}$ ; n (spine/neuron) = 23/6 for 6-8  $\mu\text{m}$ ].

(D) Effects of pharmacological inhibitors on the GCaMP3 fluorescence intensity across different ROIs. Spine numbers are 48, 32, 35, 26, 35 for Ctrl, APV, CdCl<sub>2</sub>, CPA and MCPG, respectively). These pharmacology GCaMP3 data were obtained by Eugene Park.

## **4.3 Discussion**

### **4.3.1 NMDAR-dependence and VGCC-independence of nuclear ERK activation**

Calcium signaling has been extensively studied using calcium imaging techniques (Sabatini et al., 2001). Global calcium signal results from opening of VGCCs by back-propagating action potentials or suprathreshold synaptic stimulation, and can be detected in the dendrites and spines (Koester and Sakmann, 1998; Yuste and Denk, 1995). On the other hand, synapse-specific calcium signals arises mostly from NMDARs, since spine Ca<sup>2+</sup> is substantially blocked by NMDAR antagonists and has the voltage-dependence characteristic of NMDARs (Emptage et al., 1999; Koester and Sakmann, 1998; Kovalchuk et al., 2000; Regehr and Tank, 1990; Schiller et al., 1998; Yuste and Denk, 1995; Yuste et al., 1999).

Both NMDARs and VGCCs are required in LTP induced by high frequency stimulation (HFS) (Cavus and Teyler, 1996), although the relative contribution of each calcium source to the long-lasting LTP seems species-dependent [compare (Impey et al., 1996) with (Reymann et al., 1989)]. Moreover, both types of channels contribute to somatic ERK activation in response to high-frequency stimulation, as evidenced by the

finding that both APV and nifedipine (L-type channel blocker) reduce phospho-ERK (Dudek and Fields, 2001; Zhao et al., 2005). However, NMDAR-mediated portion of ERK activation could be fully substituted by eliciting sufficient action potentials (Dudek and Fields, 2002; Zhao et al., 2005). These studies suggest that NMDARs contribute indirectly to ERK phosphorylation in HFS-LTP, through facilitating action potentials and opening of VGCCs, and that VGCCs alone are sufficient to induce ERK activation in the soma. However, the possibility of ERK activation induced by NMDAR-mediated  $\text{Ca}^{2+}$  influx was not excluded. Indeed, it has been shown that ERK is activated by a  $\text{Ca}^{2+}$  microdomain near the mouth of NMDAR, in the absence of a global calcium increase (Hardingham et al., 2001).

Structural plasticity induced by 2-p glutamate uncaging at single spines is NMDAR-dependent, since the NMDAR antagonist APV completely abolishes both the transient and sustained phases of structural plasticity (Harvey et al., 2008b; Matsuzaki et al., 2004; Murakoshi et al., 2011). In line with these previous reports, the present study showed that APV completely blocked structural plasticity at all 7 spines stimulated by repetitive glutamate uncaging (Figure 4.2). Furthermore, GCaMP imaging in this study (Figure 4.3 D) suggests that NMDAR is the predominant source for the  $\text{Ca}^{2+}$  signal evoked by glutamate uncaging, consistent with a previous study (Noguchi et al., 2005). Taken together, my results strongly suggest that NMDAR is a  $\text{Ca}^{2+}$  source essential for uncaging-induced spine structural plasticity and nuclear ERK activation.

A novel  $\text{Ca}^{2+}$ -independent mechanism of ERK activation by NMDAR and mGluR5 has been found in striatal neurons (Yang et al., 2004). Remarkably, ERK phosphorylation induced by NMDA and mGluR agonists is significantly attenuated by disrupting the interaction between NMDAR and PSD95, but not by the NMDAR channel blocker MK-801. To my knowledge, such a  $\text{Ca}^{2+}$ -independent mechanism has not been reported in hippocampal neurons. The possibility of a  $\text{Ca}^{2+}$ -independent NMDAR action in the present study can be easily determined by comparing the effects of APV and MK801 on EKAR time course. If nuclear ERK activation is still triggered in the presence of MK801 (which blocks  $\text{Ca}^{2+}$  flow through NMDAR), a  $\text{Ca}^{2+}$ -independent NMDAR function is involved.

It has been shown that glutamate uncaging elicits  $\text{Ca}^{2+}$  influx through both NMDARs and VGCCs (Bloodgood et al., 2009). However, the significance of VGCCs in structural plasticity has not been reported previously. This study showed that  $\text{Cd}^{2+}$  did not affect the transient phase of sLTP but partially inhibited the sustained phase (Figure 4.2), suggesting a role for VGCCs in structural plasticity. In contrast, uncaging-induced nuclear ERK activation was independent of VGCCs, as the non-selective VGCC blocker  $\text{Cd}^{2+}$  did not affect EKAR lifetime change (Figure 4.1 A). These results suggest that VGCCs may play a role in maintaining structural plasticity, but does not contribute to ERK activation in the absence of action potentials.

GCaMP imaging in this study showed that uncaging-evoked  $\text{Ca}^{2+}$  transient was unaffected by  $\text{Cd}^{2+}$  (Figure 4.3), indicating that the spine  $\text{Ca}^{2+}$  influx mediated by VGCCs is negligible compared to that mediated by NMDARs under our condition (i.e. zero  $\text{Mg}^{2+}$ ). In the present study, TTX in the imaging solution inhibits generation of action potentials, excluding the possibility of a VGCC-induced global calcium signal. It should be noted that  $\text{Cd}^{2+}$ , although widely used, is not a selective VGCC blocker. It has been recently documented that prolonged  $\text{Cd}^{2+}$  treatment opens permeability transition pores on mitochondria, induces  $\text{Ca}^{2+}$  elevation, and activates CaMKII (Chen et al., 2011; Li et al., 2003). In addition,  $\text{Cd}^{2+}$  has been reported to partially antagonize NMDAR's channel function (Legendre and Westbrook, 1990; Mayer et al., 1989), although our GCaMP imaging showed no such effect (Figure 4.3). In the future, the role of VGCC in structural plasticity and in nuclear ERK activation will need to be confirmed with more selective VGCC blockade, such as a cocktail of VGCC antagonists (nimodipine,  $\omega$ -conotoxin-MVIIC, SNX-482, mibefradil, and nickel) (Bloodgood et al., 2009).

#### **4.3.2 Role of intracellular $\text{Ca}^{2+}$ release in nuclear ERK activation**

Unlike NMDAR and VGCC, the role of intracellular  $\text{Ca}^{2+}$  release in conventional LTP/LTD is less well defined. Early studies using pharmacological inhibitors have proposed that  $\text{Ca}^{2+}$  release is required for some forms of LTP, because inhibition of ryanodine- or  $\text{IP}_3$ -sensitive calcium stores abolishes LTP induced by weak stimuli but

not does not affect LTP induced by strong tetanization (e.g. 8X TBS) (Behnisch and Reymann, 1995; Raymond and Redman, 2002). This simple model was complicated by later studies using transgenic mice. Mice mutants lacking some isoforms of ryanodine receptors or IP<sub>3</sub> receptors exhibit facilitated LTP and impaired LTD (Fujii et al., 2000; Futatsugi et al., 1999; Nishiyama et al., 2000). Taken together, fine control of Ca<sup>2+</sup> release from intracellular stores is crucial for bidirectional synaptic plasticity.

Intracellular Ca<sup>2+</sup> release is another major source of Ca<sup>2+</sup> transients in neurons. Repetitive synaptic stimulation leads to Ca<sup>2+</sup> release from intracellular stores in CA1 pyramidal neurons, through activation of mGluR and IP<sub>3</sub> receptors (Nakamura et al., 1999; Watanabe et al., 2006). The resultant Ca<sup>2+</sup> waves spread over large regions of apical dendritic trunk, but barely invade oblique secondary branches or spines (Nakamura et al., 2002). This is probably because of concentrated distribution of IP<sub>3</sub>Rs and RyRs in the primary dendritic trunk (Jacob et al., 2005). However, the contribution of intracellular Ca<sup>2+</sup> release to synapse-specific Ca<sup>2+</sup> signal is more controversial. Synaptically evoked spine Ca<sup>2+</sup> transients has been attributed to calcium release from ryanodine-sensitive stores induced by NMDAR activation (i.e. calcium-induced calcium release, or CICR) in cultured hippocampal slices (Emptage et al., 1999), but such CICR in spines has not been found by other groups (Kovalchuk et al., 2000; Nakamura et al., 1999; Yuste et al., 1999). This discrepancy may be due to differences in tissue preparation and stimulation protocols (Sabatini et al., 2001). In line with the majority of previous evidence, the

present study indicated that intracellular  $\text{Ca}^{2+}$  release did not contribute to local  $\text{Ca}^{2+}$  transients evoked by glutamate uncaging (Figure 4.3 D). Moreover, intracellular  $\text{Ca}^{2+}$  release was also dispensable for structural plasticity (Figure 4.2), in good agreement with previous finding that blocking  $\text{Ca}^{2+}$  influx with low extracellular  $\text{Ca}^{2+}$  completely abolishes structural plasticity and Ras activation (Harvey et al., 2008b). Interestingly, intracellular  $\text{Ca}^{2+}$  release seems to be required for nuclear ERK activation induced by 7-spine stimulation (Figure 4.1B), suggesting that nuclear ERK activation requires additional  $\text{Ca}^{2+}$  sources compared to structural plasticity. It would be interesting to test whether localized  $\text{IP}_3$  uncaging, alone or coupled to sLTP induction at a single spine, is sufficient to induce nuclear ERK activation.

Although EKAR imaging with CPA treatment implies that intracellular  $\text{Ca}^{2+}$  release was evoked by induction of sLTP at a series of 7 spines, the release site should be spatially separated from the stimulated spine. GCaMP imaging failed to detect a CPA-sensitive component of  $\text{Ca}^{2+}$  signal in the vicinity of the stimulated spines, even in the primary trunk near the stimulated spines ( $\sim 11 \mu\text{m}$  away; Figure 4.3). Intracellular  $\text{Ca}^{2+}$  release evoked by induction of sLTP at a few spines might occur in the “hot spots” along the primary dendrite where  $\text{IP}_3$  receptors are clustered (Fitzpatrick et al., 2009; Power and Sah, 2002).

An alternative explanation should be ruled out before accepting this conclusion. CPA, as an inhibitor of sarcoendoplasmic reticulum  $\text{Ca}^{2+}$ -ATPase (SERCA), depletes

intracellular  $\text{Ca}^{2+}$  store by inhibiting the intake of  $\text{Ca}^{2+}$  into internal stores. Therefore, it could elevate  $\text{Ca}^{2+}$  and activate ERK by itself (Chao et al., 1992; Chung et al., 2001). Therefore, the failure of nuclear ERK activation in the presence of CPA (Figure 4.1 D) could merely be resulted from saturation of ERK or EKAR prior to glutamate uncaging. In the future,  $\text{Ca}^{2+}$  imaging covering the dendritic tree and soma should be performed simultaneously with 7-spine stimulation, in order to study whether and where intracellular  $\text{Ca}^{2+}$  release is evoked. Any possible acute effect of CPA application on EKAR lifetime should also be examined.

#### **4.3.3 Role of mGluR in nuclear ERK activation**

Type I metabotropic glutamate receptors (mGluR1 and mGluR5) are implicated in bidirectional synaptic plasticity and memory formation (Bortolotto et al., 1999; Kotecha et al., 2003). In particular, HFS-LTP at CA1 synapses and spatial learning are impaired by pharmacological inhibitors or genetic knockout of type I mGluRs (Balschun et al., 1999; Neyman and Manahan-Vaughan, 2008). Moreover, mGluR activation induces long-term synaptic depression at CA3-CA1 synapses in an NMDAR-independent way (mGluR LTD)(Oliet et al., 1997). It plays diverse functions. For example, mGluR activates synthesis of new proteins that help sustain LTP (Raymond et al., 2000). Moreover, mGluR activation leads to increased DNA binding activity of NF- $\kappa$ B, which is crucial to the late phase but not the early phase of mGluR-LTD (O'Riordan et al., 2006). However, mGluR is not essential in structural plasticity at a single spine

induced by glutamate uncaging, at least for the first hour (Matsuzaki et al., 2004). The present study suggests that type I mGluR is required for nuclear ERK activation triggered by uncaging at a few spines (Figure 4.1 B, C), while confirming that it is not required for sLTP (Figure 4.2). The differential requirements for mGluR indicate that compared to local structural plasticity, nuclear ERK activation requires additional signaling mechanism.

Remaining unclear is how mGluR activation contributes to nuclear ERK activity increase. There are at least five possible mechanisms. First, mGluR activates PKC through phospholipase C (PLC) and diacylglycerol (DAG)(Niswender and Conn, 2010). In turn, PKC can activate ERK through activating Ras and/or Raf (Sweatt, 2001). A positive feedback loop consisting of ERK and PKC has been found in cerebellar LTD, which produces a sustained activation of these kinases (Tanaka and Augustine, 2008; Yamamoto et al., 2012). Such a positive feedback mechanism might also operate in CA1 neurons to produce sustained ERK activity. Second, mGluR activation leads to production of IP<sub>3</sub> by PLC. IP<sub>3</sub> and Ca<sup>2+</sup> synergistically activates IP<sub>3</sub> receptors (IP<sub>3</sub>R) which are calcium channels on the ER (Niswender and Conn, 2010). The resultant calcium release from intracellular stores might lead to an amplified ERK activation. Third, in striatal neurons, it has been found that mGluR activation results in inactivation of protein phosphatase 2A (PP2A) through tyrosine phosphorylation, which in turn leads to strengthened ERK activity (Mao et al., 2005a). Fourth, mGluR is physically associated

with Homer scaffold proteins in the postsynaptic complexes in striatal neurons. Selective disruption of mGluR5-Homer1b/c interaction leads to significant reduction in mGluR-mediated ERK activation, suggesting that ERK is activated in a  $Ca^{2+}$ -independent Homer-dependent pathway following mGluR activation (Mao et al., 2005b). However, such phosphatase-dependent and scaffold-dependent mechanisms of mGluR-mediated ERK activation have not yet been reported in hippocampal neurons. Fifth, mGluR activation has been reported to potentiate NMDAR currents (Fitzjohna et al., 1996), potentially leading to a larger NMDAR-mediated  $Ca^{2+}$  influx in response to glutamate uncaging. However, this scenario is highly unlikely since my GCaMP imaging did not detect any effect of mGluR inhibitor on the APV-sensitive  $Ca^{2+}$  transient (Figure 4.3). The first four possible mechanisms can be tested in the future. Given that PKC is required for sLTP, the possibility of a PKC-ERK positive feedback loop could be tested by selectively disrupting the loop by PLA<sub>2</sub> inhibitor or delayed application of PKC inhibitor (Tanaka and Augustine, 2008). As discussed above, the potential contribution of an mGluR- and IP<sub>3</sub>R-dependent  $Ca^{2+}$  release need to be studied by integrating individual spine uncaging and neuron-wide  $Ca^{2+}$  imaging. The potential roles of PP1A and Homer1/b in mGluR-mediated ERK activation should first be determined in hippocampal neuron system, and then in the present paradigm (i.e. uncaging-induced nuclear ERK activation).

#### **4.3.4 Calcium-permeable AMPA receptors**

GluA2-lacking, calcium-permeable AMPA receptors (CP-AMPA receptors) constitute an additional source of spine  $\text{Ca}^{2+}$  in some types of neurons. In CA1 pyramidal neurons, its basal postsynaptic expression is very low or nonexistent (Adesnik and Nicoll, 2007; Plant et al., 2006; Wenthold et al., 1996). Their possible role in conventional LTP has been in debate (Adesnik and Nicoll, 2007; Gray et al., 2007; Plant et al., 2006). Given that the NMDAR antagonist APV completely abolishes structural plasticity and activation of Ras-ERK signaling cascade (Figures 4.1-4.3) (Harvey et al., 2008b; Matsuzaki et al., 2004; Murakoshi et al., 2011), the contribution of CP-AMPA receptors should be negligible in these processes and was not examined in this study. This would need to be confirmed in future experiments using CP-AMPA receptor-specific inhibitors.

## Chapter 5. Spatiotemporal integration of ERK activity

### 5.1 Introduction

A widely appreciated idea is that long-term synaptic plasticity engages synapse-to-nucleus signaling, but it is not well understood how signaling cascades triggered at different spines are integrated over space and time. To explore this important question, I focused on the protein kinase ERK. The activity of ERK is increased both in the dendrites and nucleus following LTP induction. More importantly, ERK exerts important yet distinct functions both centrally in the cell nucleus and peripherally at synaptic contacts (Thomas and Huganir, 2004). Remaining unknown is how synaptic activity at individual synapses is integrated and translated into nuclear ERK activation.

Two-photon glutamate uncaging allows activation of individual synapses with precise spatial and temporal control and thus is ideal for investigating signal integration among different dendritic locations and over time.

In this part, three directions were pursued. First, I asked what spatial pattern of synaptic activation is required for nuclear ERK activation. To this end, I first determined the minimum number of spines needed for nuclear ERK activation. I then determined which of sparse and clustered stimulations is more effective in triggering nuclear ERK activation. Second, I asked whether nuclear ERK and synaptic ERK represent spatially distinct pools of ERK, or whether propagation of ERK activity from the activated

dendrite to the nucleus underlies nuclear ERK activation. Third, I asked whether ERK activation could be integrated over time. Specifically, I tested whether temporally spaced stimuli, each alone subthreshold for ERK activation, trigger nuclear ERK activation.

## **5.2 Results**

### **5.2.1 Relationship between nuclear ERK activation and stimulated spine number**

The results shown in Figures 3.5-3.7 indicate that nuclear ERK activity is increased by sLTP induction sequentially at a few spines, but not by sLTP at a single spine. This leads to the interesting question of how many synapses are required for nuclear ERK activation. Therefore, in this section, I determined the relationship between nuclear ERK activation and the number of stimulated spines. Organotypic slices were transfected with EKARnuc and positive CA1 pyramidal neurons were used for the experiments. Repetitive glutamate uncaging, the sLTP protocol, was delivered sequentially to different numbers of spines at a fixed density (total 1-7 spines, 1-3 spines/dendritic branch, separated by more than 10  $\mu\text{m}$ ; for 2- and 3-spine stimulation, spines from 2 dendritic branches were stimulated). The fluorescence lifetime of EKARnuc in the nucleus was recorded by 2-p FLIM. As shown in Figure 5.1, glutamate uncaging at a single spine failed to cause any detectable change in nuclear ERK activity ( $-0.00061 \pm 0.003$  ns), whereas glutamate uncaging at 3 spines led to a significant

decrease in EKARnuc lifetime ( $-0.015 \pm 0.003$  ns). The amplitude of EKARnuc signal induced by 3-spine stimulation was close to that induced by 7-spine stimulation ( $P = 0.11$ , Figures 5.1 and 3.5), or electrical theta-burst stimulation [ $\sim -0.02$  ns, see (Harvey et al., 2008a)]. Glutamate uncaging at 2 spines distributed over 2 branches induced a moderate decrease in EKAR lifetime ( $-0.00806 \pm 0.004$  ns), although the signal was not statistically different from that induced by 1-spine or 3-spine stimulation ( $P = 0.12$  and  $0.16$ , respectively). These results suggest that activation of as few as 3 spines is sufficient to trigger ERK activation in the neuronal nucleus.

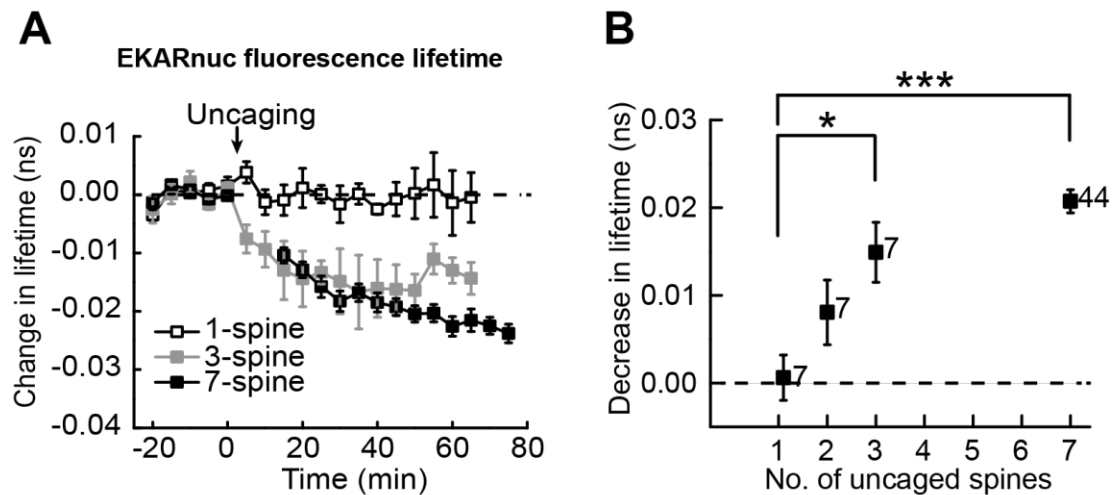


**Figure 5.1 Relationship between the number of stimulated dendritic spines and change in fluorescence lifetime of EKARnuc.**

(A) Time course of fluorescence lifetime change of EKARnuc following sequential stimulation of varied numbers of spines at a fixed density (1-3 spines per dendritic branch, separated by more than  $10 \mu\text{m}$ ).

(B) Quantification of the sustained fluorescence lifetime change (averaged over 40-70 min for 7-spine stimulation and 30-60 min for other stimulations). The numbers of samples are indicated next to the data points. Data are means  $\pm$  SEM.  $*P < 0.05$ ,  $***P < 0.001$ , ANOVA followed by post-hoc test using the least significant difference.

Translocation of ERK from cytoplasm to the nucleus underlies nuclear ERK activation in response to neuronal activity, BDNF stimulation (Wiegert et al., 2007), or glutamate uncaging at 7 spines (Figure 3.8). In this study, I also determined how many synapses are needed for inducing ERK2 nuclear translocation. Similar to that described previously (Figure 3.8), CA1 neurons in organotypic slices were transfected with mEGFP-ERK2 and mRFP-MEK1 (at a ratio of 1:3). The nuclear fraction of mEGFP-ERK2 was monitored while the neuron was stimulated by uncaging at varied numbers of spines at a fixed density (Figure 5.2). Inducing sLTP at a single spine failed to cause any detectable nuclear accumulation of mEGFP-ERK2 (normalized nuc/soma ratio =  $91 \pm 7\%$ ), compared to the sham-treated neurons that were radiated by uncaging laser pulses without caged glutamate (normalized nuc/soma ratio =  $96 \pm 7\%$ ; Figure 5.2). However, stimulation of 3 spines was sufficient to drive a significant increase in the nuclear fraction of mEGFP-ERK2 (normalized nuc/soma ratio =  $119 \pm 9\%$ ,  $P < 0.05$ ; Figure 5.2). Stimulation of 7 spines resulted in even more pronounced accumulation of mEGFP-ERK2 in the nucleus ( $140 \pm 4\%$ ,  $P < 0.001$ ; Figures 3.5 and 5.2).

The relationship between nuclear ERK activation and number of activated spines was further confirmed by immunostaining, an alternative assay for ERK activity. Neurons-expressing mEGFP were subject to sLTP induction at 1, 3, or 7 spines, or sham treatment (i.e. 7-spine stimulation protocol without caged glutamate). As negative control (i.e. 1 fold), some mEGFP neurons in the same slices were not stimulated

(stimulated spine number = 0). Slices were fixed at 1 hr after uncaging and immunostained using anti-phospho-ERK antibody. Consistent with earlier results (Figure 3.7), stimulation of 7 spines led to a profound increase in pERK level in the nucleus ( $2.48 \pm 0.22$  fold), compared to unstimulated control ( $P < 0.001$ ; Figure 5.2B). Remarkably, stimulation of 3 spines also produced a significant increase in nuclear pERK ( $1.72 \pm 0.5$  fold,  $P < 0.05$ ; Figure 5.2 B). In contrast, pERK level in the nucleus was unaltered by stimulation of a single spine ( $1.06 \pm 0.2$  fold) or uncaging laser pulses alone ( $0.94 \pm 0.07$  fold) (Figure 5.2 B). Taken together, these results indicate that nuclear ERK activity is significantly increased by activating as few as 3 spines. Considering the large size difference between spines and the nucleus ( $> 2000$  fold) (Adams and Dudek, 2005) and high basal phosphatase activity in neurons, these results suggest that an amplification mechanism must be employed in nuclear ERK activation.

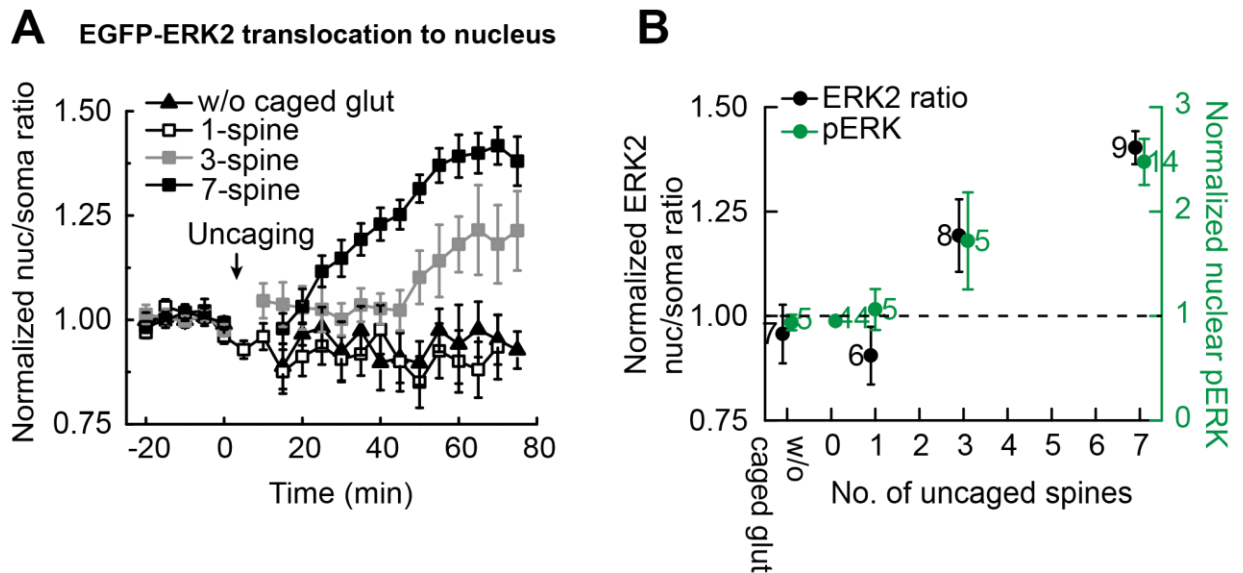


**Figure 5.2 Relationship between ERK2 nuclear translocation or nuclear phospho-ERK level and the number of stimulated spines**

(A) Time course of nuclear accumulation of mEGFP-ERK2 in response to stimulation of varied numbers of spines. The nuclear accumulation was quantified as nuclear/somatic (nuc/soma) ratio of green fluorescence intensity normalized to baseline. The data of 7-spine stimulation in the presence (“7-spine”) or absence of caged glutamate (“w/o caged glut”) are the same as in Figure 3.8.

(B) Quantification of the EGFP-ERK2 nuclear translocation (black) and phospho-ERK level (green) induced by stimulating varied numbers of spines. The nuc/soma ratio was averaged over 55-70 min for 1-spine stimulation and 60-75 min for other groups. As a sham control, uncaging laser pulses were delivered to 7 spines in the absence of caged glutamate (“w/o caged glut”). For pERK immunohistochemistry (green), the immunofluorescence in the nucleus of an mEGFP-expressing neuron was normalized to the averaged fluorescence in the nuclei of 5 surrounding untransfected neurons. Stimulated neurons were always paired with unstimulated neurons in the same slices (see Materials and Methods). Data are means  $\pm$  SEM. The numbers of samples are indicated next to the data points.

### 5.2.2 Relationship between nuclear ERK activation and number of stimulated dendrites

Next, I asked which of clustered or sparse inputs is more effective in triggering ERK activation in the nucleus. To address this question, I varied the number of dendritic

branches on which the 7 stimulated spines reside. Notably, clustered stimulation of all 7 spines on a single branch failed to induce any nuclear ERK activity increase (Figure 5.3). In contrast, sparse stimulation of 7 spines that were distributed over 7 different branches (i.e. one spine per branch) resulted in activation of nuclear ERK (Figure 5.3). I also grouped previous data from 7-spine stimulation (Figure 5.1) based on the number of dendrites involved. Given the total number of stimulated spines was 7, stimulation of 3, 4, 5, or 7 dendritic branches resulted in similar magnitudes of nuclear ERK activation (Figure 5.3 B). Moreover, stimulation of 3 spines that were distributed on 2 branches led to significant nuclear ERK activity increase (Figure 5.1). Taken together, these results suggest that signal integration across multiple dendritic branches is required to induce nuclear activation of ERK.

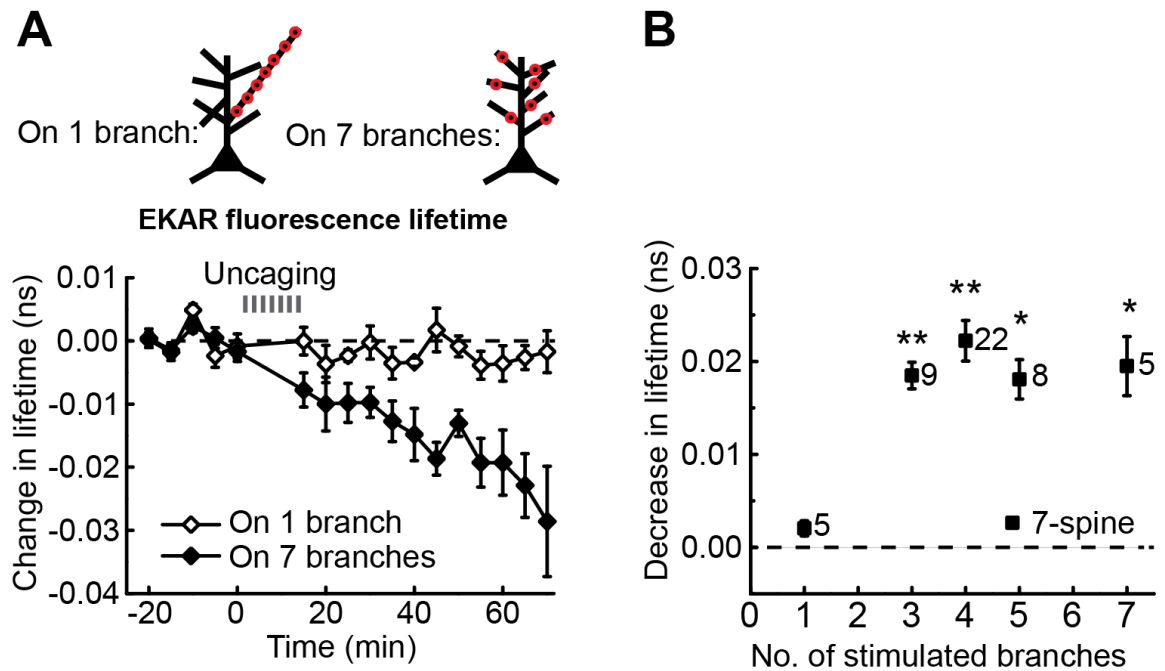


**Figure 5.3 Relationship between the number of stimulated branches and change in fluorescence lifetime of EKARnuc**

(A) Time course of fluorescence lifetime change of EKARnuc following stimulation of 7 spines that reside on the same branch or on 7 different branches.

(B) Quantification of EKAR fluorescence lifetime change (averaged over 40-70 min) following stimulation of varied numbers of dendritic branches. Data are means  $\pm$  SEM. The numbers of samples are indicated next to the data points. Asterisks indicate significant difference compared to the “7-spines-on-1-branch” group ( $*P < 0.01$ ,  $**P < 0.001$ , ANOVA followed by post-hoc test using the least significance difference).

### 5.2.3 Dendritic ERK activation induced by sLTP induction

The finding that activation of 3 spines spreading over 2 branches is more effective than activation of 7 spines on the same branch in inducing nuclear ERK activation was unexpected yet intriguing. One model is that dendritic branches are non-linear, saturable structure for ERK activity. To test this hypothesis, dendrites, especially

the branching areas on the primary dendrite that receives inputs from branches, were monitored following stimulation of different numbers of spines from the same dendritic branch. Organotypic slices were biolistically transfected with EKARcyto and EKARnuc at a ratio of 1:3. Co-expression of EKARnuc was utilized to lower the expression level of EKARcyto, thus avoiding the intrinsic buffering effect of EKAR on ERK activity (also see Figure 5.6). Three different regions were simultaneously imaged from EKAR-expressing CA1 neurons: 1) the branching area where a secondary dendrite extends off, 2) the proximal trunk within 40  $\mu\text{m}$  from the soma, and 3) the stimulated dendritic branch (Figure 5.4 A). Neurons were stimulated by inducing sLTP in 1, 2, or 3 spines on the same dendritic branch (a neuron stimulated at 2 spines from the same branch was shown in Figure 5.4 A as an illustration). I found that ERK activity in the branching area was nearly unaffected by stimulation of a single spine (EKAR lifetime change:  $-0.0029 \pm 0.004$  ns), whereas it was markedly and persistently increased by stimulation of two spines from the same branch (EKAR lifetime change:  $-0.017 \pm 0.003$  ns,  $P < 0.05$ ; Figure 5.4 B-D). Interestingly, inducing sLTP at one additional spine from the same dendrites did not further elevate ERK activity in the branching area (EKAR lifetime change:  $-0.018 \pm 0.005$  ns; Figure 5.4 D). ERK activity in the proximal trunk and dendritic branch exhibited the same trend (Figure 5.4 E-F), although there was no statistical significance between the same-branch, 1-spine, and 2-spine stimulations. These results suggest that ERK activity of a dendritic branch is saturated by sequentially activating only 2 spines.

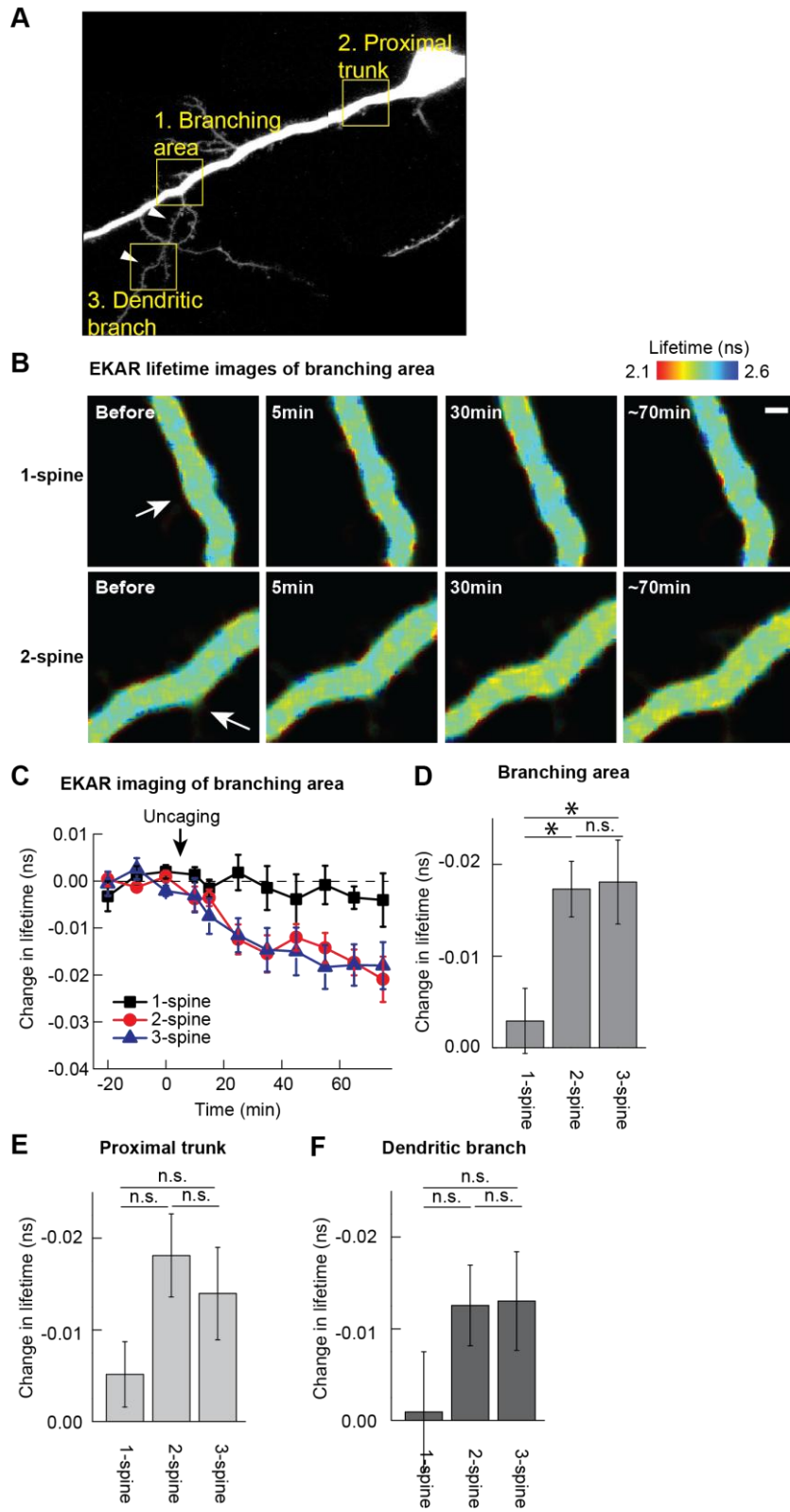


**Figure 5.4 Activation of only two spines from a dendritic branch saturates ERK activity contributed by that branch**

(A) Illustration of the experimental design. In a neuron expressing EKARcyto together with EKARnuc, FLIM imaging was performed every 10 min at three different locations (marked by the yellow squares). Glutamate uncaging was delivered to induce sLTP sequentially in two spines (indicated by the white arrowheads) residing on a dendrite that branches off at the branching area.

(B) Examples of FLIM images of the branching areas in response to same-branch 1-spine or 2-spine stimulation. Scale bar = 2  $\mu\text{m}$ .

(C) Time course of EKAR lifetime in the branching area in response to same-branch 1-spine, 2-spine or 3-spine stimulation (n = 6 for each group).

(D) Amplitude of EKAR lifetime change in the branching area averaged over 55-75 min. Data were the same as in (C). \* $P < 0.05$ ; n.s., not significant; ANOVA followed by post-hoc test using the least significance difference

(E) Amplitude of EKAR lifetime change in the proximal dendritic trunk.

(F) Amplitude of EKAR lifetime change in the stimulated dendritic branch.

#### **5.2.4 Propagating ERK activity as a synapse-to-nucleus signal**

The observation that nuclear ERK activity was elevated by sLTP induction at a few spines in the absence of action potentials (Figures 3.5-3.7) suggests that a biochemical signal was conveyed from the activated synapse to the nucleus. Also, activation of ERK in the primary dendrite was observed following inducing sLTP at 2 spines. Therefore, it is very likely that 7-spine stimulation triggers cell-wide, not only nuclear, ERK activation. To test this possibility, the ERK activity was measured simultaneously in one of the stimulated secondary dendrites, the primary dendritic trunk and the nucleus following 7-spine stimulation. For this purpose, organotypic slices were transfected with both nuclear and cytosolic forms of EKAR (DNA amount of EKARnuc/EKARcyto = 1:1). EKAR-expressing CA1 neurons were imaged by FLIM and stimulated by inducing sLTP sequentially at 7 spines (i.e. 7-spine stimulation: 60 pulses

at 1 Hz, 4-6 ms pulse duration, at a density of 1-3 spines per dendrite for a total of 7 spines). Interestingly, EKAR responses varied from cell to cell. EKAR signal, especially in the nucleus, was negatively correlated with the level of EKARcyto expression ( $r = -0.76$ ,  $P < 0.01$ ; Figure 5.5 A). Therefore, the neurons were grouped based on the level of EKARcyto, although the boundary between high and low levels was arbitrarily chosen (expression index = 100, Figure 5.5 A). In neurons with high expression level of EKARcyto (EKARnuc + high EKARcyto, Figure 5.5 B), EKAR lifetime change was most profound in the stimulated secondary dendrite, moderate in the primary dendrite, and negligible in the nucleus. On the other hand, EKAR lifetime change was similar in all three compartments in neurons with low EKARcyto level (EKARnuc + low EKARcyto, Figure 5.5 C). The design of EKAR sensor provides an explanation to this difference in EKAR response. With a docking site for ERK, EKAR sensor protein is an intrinsic ERK buffer. Therefore, at high concentration EKAR might prevent spreading of ERK from the dendrites to the nucleus. The result from low EKARcyto neurons suggests that ERK is activated neuron-wide. Taken together, these results suggest that spreading of activated ERK from dendrite to nucleus might underlie nuclear ERK activation in response to 7-spine stimulation.

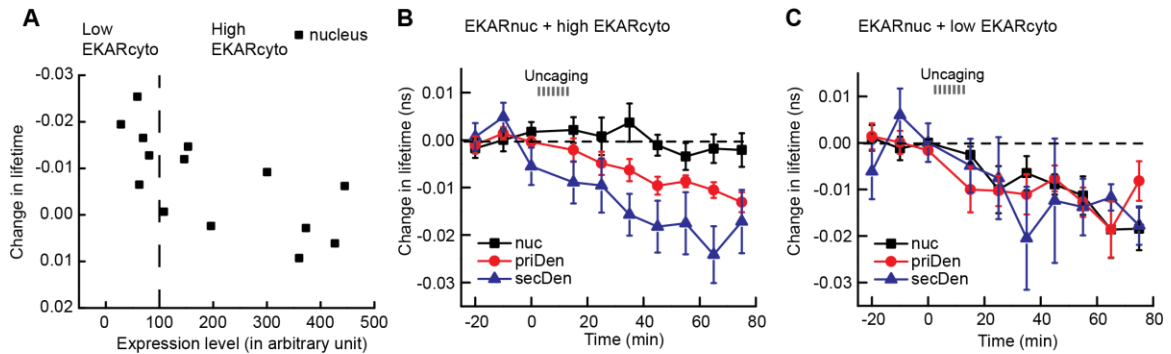


**Figure 5.5 High level of EKARcyto expression abolishes nuclear ERK activation.**

(A) Correlation between ERK activation in the nucleus (averaged over 55-75 min) and EKARcyto expression level. The dashed line represents an arbitrary criterion for defining EKARcyto level.

(B) Time course of EKAR fluorescence lifetime in response to 7-spine stimulation in neurons with a high level of EKARcyto expression. FLIM images were taken every 10 min in the nucleus (“nuc”), proximal primary dendritic trunk (“priDen”), and secondary dendrite (“secDen”). n = 9.

(C) Time course of EKAR fluorescence lifetime in response to 7-spine uncaging in CA1 neurons with a moderate level of EKARcyto expression. n = 5.

To further confirm that dendrite-to-nucleus propagation of ERK underlies nuclear ERK activation, I examined nuclear ERK activity in response to stimulating 7 spines that were located distally (> 200  $\mu\text{m}$  from the nucleus). In support of the ERK propagation model, I found that stimulation of 7 distal spines activated nuclear ERK with an obvious delay (Figure 5.6 A). But the stabilized activity was similar to that induced by the typical 7-spine stimulation in which 7 proximal spines (50-200  $\mu\text{m}$ ) are uncaged ( $P = 0.27$ , Figure 5.6 B).

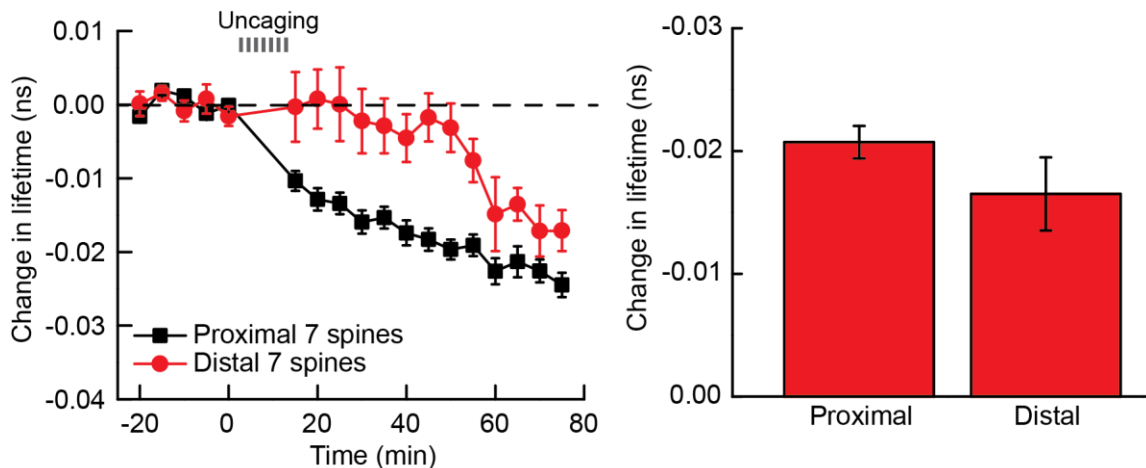


**Figure 5.6 Distal stimulation activates nuclear ERK with a delay**

(A) Time course of EKAR<sub>nuc</sub> lifetime change in the nucleus following sLTP induction at 7 spines that are located distally (> 200  $\mu\text{m}$ , red,  $n = 7$ ), or proximally (50 - 200  $\mu\text{m}$ , black, data from Figure 5.1,  $n = 44$ )

(B) Quantification of EKAR lifetime change in the nucleus in response to distal or proximal stimulation shown in (A) (averaged over 70-75 min for distal and 40-70 min for proximal).

### 5.2.5 Integration of ERK activity over time

Stimulation of spines distributed over two or more dendrites produces significant nuclear ERK activation (Figures 5.1-5.2), whereas stimulation of spines on a single dendrite does not (Figure 5.3). However, stimulation of spines (2-3) on a single dendrite leads to dendritic ERK activation that persists for over 1 hr (Figure 5.4). Therefore, an interesting question is whether ERK signals from different dendrites can still effectively integrate when temporally spaced. To answer this question, I monitored nuclear ERK activity in response to two temporally spaced stimulations, each consisting of sLTP induction at 2 spines from one branch. The second stimulation was applied 30

min after the first stimulation, to a different branch (“Different branches”, Figure 5.7 A). As a control, the second stimulation was applied to the same branch (“Same branch”, Figure 5.7 A). As expected for uncaging at spines in a single dendrite, the first 2-spine stimulation did not change EKAR lifetime in the nucleus (Figure 5.7 B). The second stimulation, when applied to a different branch, induced a significant decrease in nuclear EKAR lifetime (Figure 5.7 B). This result suggests that dendritic ERK can be integrated over at least 30 min for inducing nuclear ERK activation. Two temporally spaced stimulations, when applied on the same dendrite, failed to activate ERK (Figure 5.7 B), suggesting that temporal spacing alone cannot integrate subthreshold signals to induce nuclear ERK. This result also confirms that ERK input from a branch is saturated by activation of two spines (see Figure 5.4). Interestingly, ERK activation produced by the second stimulation on a different branch varied among trial to trial. Upon close examination, a strong negative correlation between ERK signal and distance between branching points was found ( $r = -0.71$ ;  $P < 0.01$ ). When grouped based on the distance between branching points (30  $\mu\text{m}$  was arbitrarily set as the criterion), the present data show that spaced stimulation of two dendrites within 30  $\mu\text{m}$  is much less effective in inducing nuclear ERK activity than spaced stimulation of two dendrites separated by more than 30  $\mu\text{m}$  (Figure 5.7 C).

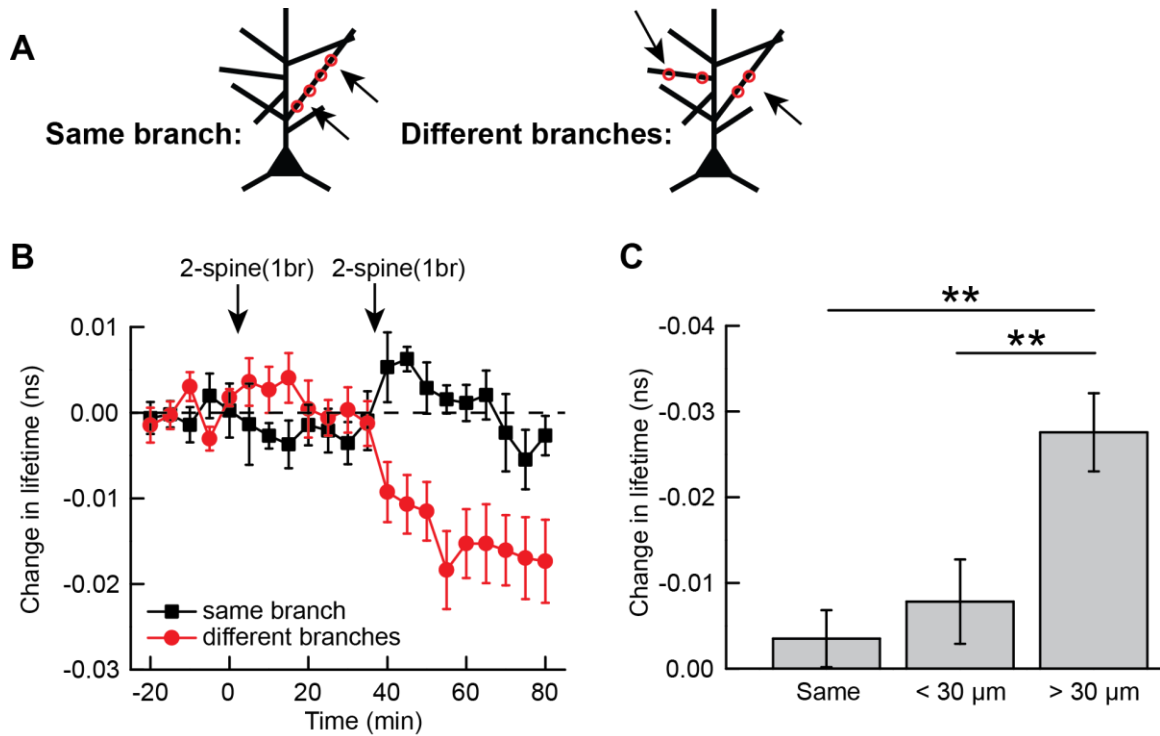


**Figure 5.7 Temporally spaced 2-spine stimulations induce nuclear ERK activity increase**

(A) Cartoon illustration of temporally spaced 2-spine stimulations. Each 2-spine stimulation, represented by a black arrow, consists of sLTP induction at two spines (red circles) from a single branch. The second 2-spine stimulation was either applied to the same branch (“Same branch”) or to a different branch (“Different branches”).

(B) Time course of EKAR lifetime change in the nucleus in response to spaced 2-spine stimulations applied to the same branch (black,  $n = 6$ ), or to two different branches (red,  $n = 11$ ).

(C) Mean EKAR lifetime change averaged over 70-80 min in neurons subject to spaced 2-spine stimulations. The second stimulation was applied to the same branch (“Same”), to a different branch with  $< 30 \mu\text{m}$  between two branching points (“ $< 30 \mu\text{m}$ ”,  $n = 6$ ), or to a different branch with  $> 30 \mu\text{m}$  between two branching points (“ $> 30 \mu\text{m}$ ”,  $n = 6$ ). \*\* $P < 0.01$ , ANOVA followed by post-hoc test using the least significance difference.

### 5.3 Discussion

Dendrites are both electrical and biochemical inputs of the neuron. Integration of electrical inputs from different dendrites, usually referred as dendritic integration, has been extensively studied by electrophysiological approaches (Magee, 2000). However, our understanding of how biochemical signals from different dendrites orchestrate to inform the nucleus has been limited, probably to due to lack of a high-resolution, real-time readout. During the past few years, a large number of genetically encoded FRET sensors for enzyme activity have been developed (Miyawaki, 2003). Combining a FRET sensor for ERK and two-photon glutamate uncaging, the present study set out to investigate the spatiotemporal activity of ERK in neurons. In this Chapter, three aspects of the ERK activity integration were studied: spatial summation and pattern, amplitude of unitary synaptic/dendritic ERK signal, and temporal summation.

I found that nuclear ERK activation and translocation were triggered by inducing sLTP at as few as 3 spines distributed over 2 dendritic branches (Figures 5.1-5.2). Interestingly, inducing sLTP at 7 spines distributed on the same dendritic branch failed to trigger nuclear ERK activation (Figure 5.3). One possible mechanism is that each dendritic branch acts as a biochemical signaling unit and can emit only a limited amount of biochemical signal to the nucleus irrespective of the number of stimulated spines. This model was corroborated by the observation that ERK activity at the branching area in the primary dendrite was almost saturated by stimulation of 2 spines on the same

branch (Figure 5.4). Indeed, it has been well established that stimulation of a single spine can induce signal transduction in surrounding spines and dendritic shaft over 5-50  $\mu\text{m}$  (Govindarajan et al., 2011; Harvey et al., 2008b; Murakoshi et al., 2011). Therefore, clustered spines have both spine-specific signals, as exemplified by Cdc42 (Murakoshi et al., 2011) and overlapping or even shared biochemical signaling pools, as exemplified by Ras (Govindarajan et al., 2011; Harvey et al., 2008b; Murakoshi et al., 2011).

One-to-one topographical organization of synaptic inputs onto a dendritic branch has not been found in mammalian brain region (Branco and Häusser, 2010). In pyramidal neurons, nearby spines on the same dendritic branch are innervated by different axons (Kleindienst et al., 2011). However, functional clustering of synaptic inputs has been reported. Synapses that are located within 8-16  $\mu\text{m}$  on the same dendritic branch are much more likely to be coactive during spontaneous activity in both developing and mature hippocampal neurons (Kleindienst et al., 2011; Takahashi et al., 2012). This was further confirmed in live animals. Spontaneous co-activity is more likely to occur in clustered spines (< 6  $\mu\text{m}$ ) in the barrel cortex of anaesthetized mice (Takahashi et al., 2012).

Several lines of evidence suggest that synaptic plasticity, like spontaneous activity, is clustered on the dendrite. First, LTP induced by theta-burst stimulation (TBS) induces new spine formation preferentially in the proximity of activated spines (De Roo et al., 2008). Second, sensory experience induces synaptic enhancement in a clustered

manner ( $< 8 \mu\text{m}$ ) in the barrel cortex *in vivo* (Makino & Malinow, 2011). Moreover, after LTP is induced at a single spine by two-photon glutamate uncaging, LTP could be induced at a nearby spine by a subthreshold stimulus that by itself is normally too weak to induce LTP. The LTP induction threshold is lowered for 10 min over a  $10 \mu\text{m}$  dendritic segment (Harvey and Svoboda, 2007). These forms of clustered plasticity can be explained by 1) spreading of signaling molecules that act through phosphorylation to sensitize neighboring synapses (Harvey and Svoboda, 2007) and/or 2) activation of dendritic translation and production of plasticity-related proteins (PRPs) that are effectively captured by tagged synapses within a dendritic branch (Govindarajan et al., 2011; Govindarajan et al., 2006). These two mechanisms are not necessarily mutually exclusive and both involve activation of Ras-ERK signaling pathway (Harvey et al., 2008b; Kelleher et al., 2004a). My finding that activation of 2 spines almost saturated the dendritic ERK activity (Figure 5.4) is consistent with the mechanisms of clustered plasticity, suggesting that stimulation of one or two spines produces ERK activity spreading over a long stretch of dendrite. In addition, the failure of clustered spines to induce a nuclear ERK signal (Figure 5.3) suggests a plausible mechanism of how nucleus senses and then ignores the background noise—the co-activity of clustered spines during spontaneous network activity.

I also found that integration between different dendrites, which is required for nuclear ERK activation, can occur even when two stimuli are spaced by 30 min (Figure

5.7). Interestingly, this integration is less effective if the two dendritic branches are adjacent to each other (i.e.  $< 30 \mu\text{m}$  between branch points). These results suggest that adjacent dendritic branches, just like same-branch spines, have overlapping or even shared biochemical signaling pools.

In this study, I also observed that stimulation of distal spines ( $> 200 \mu\text{m}$ ) activates nuclear ERK with a delay of  $\sim 40$  min (Figure 5.6) compared to stimulation of proximal spines ( $50\text{-}200 \mu\text{m}$ ). This suggests that ERK spreading has very slow kinetics. Consistently, nuclear ERK activation is a slow and gradual process, reaching plateau after 30 min or more (Figures 3.5, 3.7, 5.1, 5.2). The slow rate of ERK spreading is consistent with diffusion of signaling molecules from spines to the soma. ERK has a diffusion coefficient ( $D_{eff}$ ) of  $\sim 7 \mu\text{m}^2/\text{s}$  in the cytoplasm (Lidke et al., 2010). Therefore, the estimated time it takes to travel  $100\text{-}200 \mu\text{m}$  by passive diffusion is  $\sim 14\text{-}47$  min ( $t \approx x^2 / 2D_{eff}$ ,  $x$  is the mean distance traveled by the diffusing solute in one direction along one axis after elapsed time  $t$ ). Consistent with a diffusion-driven mechanism, Wiegert et al. reported that ERK trafficking in the dendrite is bidirectional and mediated by passive diffusion (Wiegert et al., 2007). However, diffusion-mediated ERK trafficking is challenged by decay mechanisms such as dilution and dephosphorylation. An amplification mechanism must cooperate with passive diffusion to overcome signal decay and achieve effective synapse-to-nucleus communication. Future experiments may be designed to determine the nature and locale of this amplification mechanism.

Alternatively, the slow kinetics of ERK might be compatible with an importin-mediated retrograde transport which operates on a time scale of minutes (Thompson et al., 2004). Importin-mediated transport is usually accompanied by a loss of transported protein in the dendrites (Karpova et al., 2013; Lai et al., 2008), which was not observed for ERK (Figure 5.4). The present study, however, has not ruled out the possibilities of facilitated diffusion and slow active transport as potential mechanisms for ERK spreading. Furthermore, it has been shown that glutamate-induced nuclear accumulation of ERK is regulated by endocytosis (Trifilieff et al., 2009). Trafficking of ERK in endocytic vesicles may be an efficient way to overcome dephosphorylation over a long distance (Kholodenko, 2003). The slow kinetics of ERK spreading cannot be accounted by fast mechanisms such as  $\text{Ca}^{2+}$  waves and traveling phosphorylated kinase waves (Kholodenko, 2003; Watanabe et al., 2006). In Chapter 7, I discuss in greater detail on how ERK signal could be perpetuated in the face of decay mechanisms.

## **Chapter 6. Nuclear targets for ERK activity increase triggered by sLTP induction at a few spines**

### **6.1 Introduction**

Some of the nuclear targets of ERK signaling pathway during LTP have been proposed, including transcription factors CREB and Elk-1, suggesting a major role for ERK in the regulation of gene expression (Thomas and Huganir, 2004). It is known that ERK mediates phosphorylation of transcription factor CREB at Ser133 in response to growth factor stimulation or LTP induction (Impey et al., 1998; Thomas and Huganir, 2004; Xing et al., 1996). Under basal conditions, CREB sits prebound to cAMP response element (CRE) in the promoter of target genes. Upon phosphorylation at Ser133 by RSK or MSK, the kinases downstream of ERK, CREB binds transcriptional coactivator CREB-binding protein (CBP). This leads to: 1) CBP-mediated recruitment of transcription machinery to promoters of CRE-containing genes, and 2) CBP-catalyzed histone acetylation that renders chromatin more accessible to transcription (West et al., 2001). Therefore, phosphorylation of Ser133 constitutes an essential step in the induction of CRE-mediated gene expression.

Elk-1 is phosphorylated in an ERK-dependent manner in the insular cortex in response to new taste stimuli and in the dentate gyrus in response to LTP induction (Berman et al., 1998; Besnard et al., 2011; Davis et al., 2000). Unlike CREB which is phosphorylated by kinases downstream of ERK, Elk-1 is directly bound and phosphorylated by ERK at multiple phosphorylation sites (Fantz et al., 2001).

Phosphorylation at Ser383, the site crucial for Elk-1's transcriptional activity, leads to recruitment of serum response factor (SRF) and formation of ternary complex at the serum response element (SRE) in the promoter region of target genes. Moreover, activated Elk-1 recruits coactivators that acetylate core histones and relieve repression of transcription through chromatin remodeling (Besnard et al., 2011).

In this chapter, I set out to investigate the functional consequence of nuclear ERK activation induced by multi-spine uncaging. Specifically, I asked whether the sustained ERK activity elicited by sLTP induction at a few spines leads to phosphorylation of transcription factors CREB and Elk-1.

## **6.2 Results**

### **6.2.1 Seven-spine stimulation induces phosphorylation of transcription factors**

To address the question above, I first determined whether sLTP induction at 7 spines (7-spine stimulation) could cause phosphorylation of these transcription factors. This was examined by measuring the phosphorylation state of transcription factors CREB and Elk-1 by immunostaining. Slices were transfected biolistically with mEGFP. After glutamate uncaging at 7 spines of mEGFP-expressing CA1 neurons, the slices were fixed at 45 or 90 min and immunostained for CREB phosphorylated at Ser133 (Figure 6.1 A and B), or Elk-1 phosphorylated at Ser383 (Figure 6.1 C and D), the phosphorylations essential for triggering their transcriptional activity (Gille et al., 1995b; Gonzalez and

Montminy, 1989). Under the basal condition, the level of phosphorylated CREB (pCREB) varied from neuron to neuron perhaps due to spontaneous circuit activity, while that of phosphorylated Elk-1 (pElk-1) was always low (Figure 6.1, A and C). On average, mEGFP-positive, unstimulated neurons show similar level of pCREB and pElk-1 compared to surrounding neurons (Figure 6.1, B and D). However, at 45 and 90 min after uncaging, the levels of pCREB and pElk-1 were ~2 fold higher in uncaged neurons than in surrounding untransfected neurons (Figure 6.1, B and D). These results indicate that stimulation of a few dendritic spines induces, in addition to sustained activation of ERK, sustained phosphorylation of transcription factors.

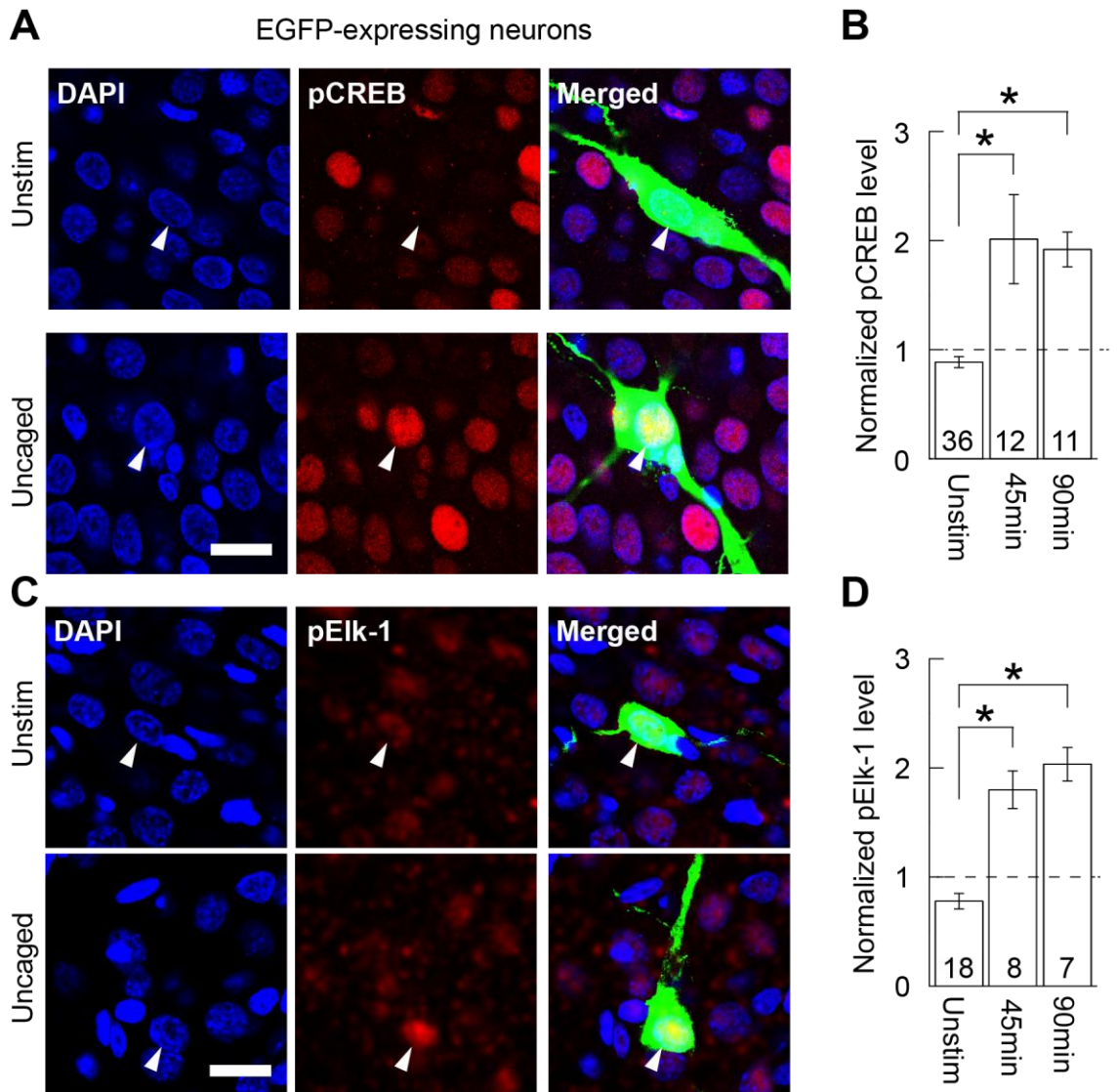


**Figure 6.1 Phosphorylation of CREB and Elk-1 triggered by induction of sLTP at 7 spines**

(A) Immunofluorescent images of phosphorylated CREB (red; “pCREB”) imaged under a confocal microscope. Seven spines of neurons expressing mEGFP (green) were stimulated and the slices were fixed 45 min after stimulation (“Uncaged”). An unstimulated mEGFP neuron in the same slices is also shown (“Unstim”) as negative control. The nuclei were stained with 4',6-diamidino-2-phenylindole (DAPI) (blue). Scale bars, 20  $\mu$ m.

(B) Quantification of the fluorescence intensity of pCREB in the nuclei identified with DAPI. The fluorescence in the nuclei of mEGFP-expressing neurons was normalized to the average fluorescence in nuclei of 5 surrounding untransfected neurons. Stimulated

neurons were always paired with unstimulated neurons in the same slices (see Chapter 2 Material and Methods). The numbers of neurons are indicated at the bottom of the graph. (\*\* $P < 0.001$ , ANOVA followed by post-hoc test using the least significant difference).

(C) Immunofluorescent images of phosphorylated Elk-1 (red; “pElk-1”). Seven spines of neurons expressing mEGFP (green) were stimulated and the slices were fixed 45 min after stimulation (“Uncaged”). An unstimulated mEGFP neuron in the same slices is also shown (“Unstim”) as negative control. The nuclei were stained with DAPI (blue). Images were smoothed with Gaussian filter. Scale bars, 20  $\mu\text{m}$ .

(D) Quantification of the fluorescence intensity of pElk-1 in the nuclei identified with DAPI. Quantification was performed in the same way as in (B). The numbers of neurons are indicated at the bottom of the graph. (\*\* $P < 0.001$ , ANOVA followed by post-hoc test using the least significant difference).

## 6.2.2 Phosphorylation of CREB and Elk-1 is mediated by ERK activity

As shown in the previous sections, sLTP induction at as few as 7 spines led to both sustained ERK activity increase in the nucleus and sustained phosphorylation of transcription factors CREB and Elk-1. It is still unknown whether it is the ERK pathway that mediates the phosphorylation of these transcription factors in response to 7-spine uncaging. Indeed, CREB sits at the crossroad of several signaling pathways and can be phosphorylated at Ser133 by different kinases including PKA, CaMKIV and ERK *in vivo* and by even more pathways *in vitro* (West et al., 2001). To test the hypothesis that ERK mediates sustained phosphorylation of CREB and Elk-1 in response to sLTP induction at a few spines, I assessed the levels of pCREB and pElk-1 in the presence and absence of ERK inhibitor FR180204. In the nuclei of unstimulated mEGFP neurons (“Unstim”, Figure 6.2), inhibition of ERK by FR180204 did not affect the levels of pCREB and pElk-1. This suggests that the spontaneous phosphorylation of CREB occasionally observed in

untransfected neurons (Figure 6.1 A) might be mediated by other signaling pathways such as CaMKIV or PKA (West et al., 2001). In contrast, the strong phosphorylation of CREB and Elk-1 induced by 7-spine uncaging was completely abolished by FR180204 (“Uncaged”, Figure 6.2 A-B), indicating that ERK activation triggered by sLTP induction at a few spines leads to CREB and Elk-1 phosphorylation.

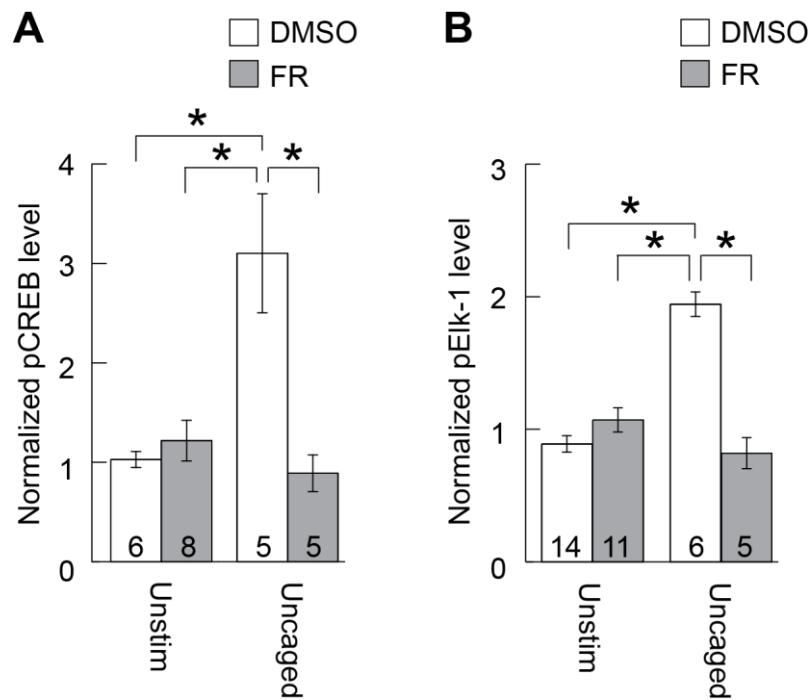


**Figure 6.2 Phosphorylation of CREB and pElk-1 induced by 7-spine stimulation depends on ERK activity**

Effect of ERK inhibitor FR180204 on the levels of pCREB (A) and pElk-1 (B) in mEGFP neurons that were either unstimulated and used as negative control (“Unstim”), or stimulated by inducing sLTP sequentially at 7 spines (“Uncaged”). The immunofluorescence in the nuclei of mEGFP-expressing neurons was normalized to the average immunofluorescence in nuclei of 5 surrounding untransfected neurons. The numbers of neurons are indicated at the bottom of the graph. \* $P < 0.05$ , ANOVA followed by post-hoc test using the least significant difference.

## 6.3 Discussion

### 6.3.1 ERK-mediated CREB phosphorylation is triggered by activating a few spines

Long-term maintenance of LTP, learning and memory all requires *de novo* gene expression. In the case of hippocampal LTP, it has been shown that the late phase is blocked by transcription inhibitors, suggesting a critical role for gene induction in modifying synaptic function (Nguyen et al., 1994). CREB-mediated gene transcription has been implicated in both LTP and memory (Barco et al., 2003). The mechanisms of CREB activation have been extensively studied in neurons. As reported by Impey and colleagues, the ERK-Rsk1 pathway mediates Ca<sup>2+</sup>-mediated CREB-dependent transcription in a PKA-dependent manner, whereas CaMKIV is largely dispensable. More importantly, high-frequency stimulation-induced LTP (HFS-LTP) in CA1 neurons is associated with CRE-mediated gene expression as detected by CRE-LacZ transgenic mice. Both the late phase of LTP and CRE-LacZ gene expression were abolished by inhibiting ERK pathway, suggesting that ERK pathway is the predominant CREB-activating pathway in neurons (Impey et al., 1998). Using a shorter stimulation (3 min instead of 4 hr of KCl), another group has revealed a transient phase of CREB phosphorylation mediated by CaM kinase pathway that is followed by a sustained phase mediated by ERK pathway (Wu et al., 2001b).

Structural plasticity (sLTP) is a form of long-term synaptic plasticity that can be induced at individual spines by repetitive glutamate uncaging (Matsuzaki et al., 2004).

Maintenance of the structural changes during sLTP, at least for the first hour, is independent of *de novo* gene expression (Tanaka et al., 2008). However, it is unknown whether more enduring structural changes (for hours) require new gene expression. Also, it has been unclear whether nuclear events could be triggered by inducing sLTP in the absence of global calcium rise. In the present study, I have shown that phosphorylation of CREB could be triggered by inducing sLTP at a few spines, in an ERK-dependent manner (Figures 6.1-6.2). These results, in line with the previous finding that the ERK pathway mediates CREB phosphorylation during conventional LTP (Impey et al., 1998), suggesting that the ERK pathway is the primary signaling pathway responsible for CREB-mediated transcription in some forms of synaptic plasticity. Consistent with these *ex vivo* studies, an *in vivo* study has shown that hippocampus-dependent fear conditioning is associated with ERK-mediated CREB phosphorylation (Trifilieff et al., 2006). My results also suggest that sequential activation of as few as 7 spines, without causing a global Ca<sup>2+</sup> rise, might be sufficient for activating new gene transcription.

However, an important consideration is that phosphorylation of the transcription factor CREB at Ser133 does not necessarily lead to its activation or downstream transcription. Several additional mechanisms exist for regulating CREB-mediated gene transcription. First, CREB could be phosphorylated at several other sites in addition to Ser133. For example, Ser142 is phosphorylated together with Ser133 by CaM kinase in

response to calcium elevation (Lonze and Ginty, 2002). Phosphorylation of Ser142 poses a physical hindrance for interaction between CREB and CBP, thus favoring an alternative CBP-independent CREB pathway (Kornhauser et al., 2002; Parker et al., 1998; Wu and McMurray, 2001). Second, CREB is subject to modulation by other posttranslational modifications. For example, CREB is acetylated by its coactivator CBP and such acetylation negatively regulates the transcriptional activity of CREB (Lu et al., 2003) Third, the activities of coactivators are also subject to modulation. For example, CBP can be phosphorylated at Ser439 or Ser301 and its transcription-activating ability is dependent on its phosphorylation (Impey et al., 2002; Zanger et al., 2001). In fact, CREB Ser133 phosphorylation is dissociable from CREB-CBP-activated transcription. CBP activation requires nuclear  $Ca^{2+}$  and CaM kinase IV or cAMP. It has been shown that activation of Ras-ERK signaling pathway, although sufficient to induce CREB Ser133 phosphorylation and CBP recruitment, fails to activate CREB/CBP-mediated transcription (Chawla et al., 1998; Hardingham et al., 1999). In addition to the positive modulation through phosphorylation, CBP is also negatively modulated through methylation at its arginine residues (Xu et al., 2001). Finally, because CREB is not the only binding partner for the coactivators, competition with other nuclear proteins for vacant coactivators provides an extra layer of control for CREB-mediated transcription. Taken together, it is still unclear whether CREB-mediated gene transcription is induced by sLTP induction at a few spines.

## 6.2.2 ERK-mediated Elk-1 phosphorylation is triggered by activating a few spines

Although Elk-1 is a substrate of several MAPKs including ERK and p38 kinase, several studies have demonstrated that ERK signaling pathway mediates Elk-1 phosphorylation in response to neuronal activation and synaptic plasticity. Elk-1 is phosphorylated by ERK upon electrical stimulation of the corticostriatal pathway *in vivo* or upon glutamate stimulation in striatal slices (Sgambato et al., 1998; Vanhoutte et al., 1999). ERK-mediated Elk-1 phosphorylation is also found in hippocampal neurons after induction of LTP (Davis et al., 2000) or contextual fear conditioning (Sananbenesi et al., 2002). Interestingly, ERK-dependent phosphorylation of Elk-1 is also observed in both NMDAR-dependent LTD *in vivo* or mGluR-LTD (Lindecke et al., 2006; Thiels et al., 2002). The functional significance of Elk-1-mediated transcription in bidirectional synaptic plasticity is still undefined, although one of its target genes, *Zif268*, has been found to be crucial to the late phase of LTP and memory (Jones et al., 2001)

In the present study, I determined whether induction of sLTP at a few dendritic spines was sufficient to cause Elk-1 phosphorylation, a prerequisite for SRE-mediated transcription. I found that phosphorylation of Elk-1 was triggered by inducing sLTP at a few spines, in an ERK-dependent manner (Figures 6.1-6.2). These results, being in line with the previous findings discussed above, imply that ERK plays an important role in regulating SRE-controlled genes in neurons.

The caveat for CREB phosphorylation also applies here: Elk-1 phosphorylation at Ser383 does not guarantee transcription of SRE-containing genes. SRE-mediated transcription is regulated by additional mechanisms. First, just like CREB, Elk-1 could be phosphorylated at multiple sites. For example, serum- and glucocorticoid-inducible kinase 1 (SGK1) phosphorylates Elk-1 at Ser159 and Thr160, abolishing its transcriptional activity (Tyan et al., 2008). Second, Elk-1 is also subject to other posttranslational modifications. Small ubiquitin-like modifier (SUMO) conjugation promotes nuclear export of Elk-1, thus shutting off Elk-1-mediated transcriptional activation (Salinas et al., 2004). Third, SRF, Elk-1's binding partner in the ternary complex, is also regulated by phosphorylation events that alter its affinities for DNA and Elk-1 (Posern and Treisman, 2006). Fourth, in the same way that CREB competes with other nuclear proteins for CBP, Elk-1 also competes with other ternary complex factors (TCFs) or myocardin-related transcription factors (MRTFs) for binding to SRF (O'Sullivan et al., 2010; Posern and Treisman, 2006). Finally, phosphorylation of Elk-1 at Ser383 could lead to recruitment of corepressor complexes that possess intrinsic histone deacetylase activities (HDAC). This in turn leads to compaction of chromatin and repression of transcription (Yang et al., 2001).

In contrast to CREB, Elk-1 might be phosphorylated in the cytoplasm where it resides in its resting state in mature neurons (Besnard et al., 2011). Therefore, phosphorylation of Elk-1 (Figure 6.1 C, D) and nuclear ERK activity increase (Figures

3.5-3.6) are, instead of causally related, temporally correlated processes that are both downstream of cytoplasmic ERK activation. In fact, it has been proposed that ERK2 and Elk-1 are recruited to a protein complex that translocates into the nucleus following glutamate treatment (Trifilieff et al., 2009). This type of cytoplasm-to-nucleus translocation of protein complex comprising ERK and its substrate has also been reported recently (Karpova et al., 2013), and may be a common theme in synaptic plasticity. Future experiments are needed to determine if translocation of ERK-Elk-1 complex occurs in response to 7-spine stimulation.

### **6.3.3 Future directions**

Although I have demonstrated that ERK activity increase triggered by activating 7 spines leads to phosphorylation of transcription factors, at sites critical for their activation, it remains unclear whether gene transcription is induced. Therefore, future experiments may include monitoring synthesis of new mRNA by *in situ* hybridization. The role of ERK in gene induction might be determined by assessing the effect of ERK inhibitor on new mRNA synthesis. Genes that contain CRE and/or SRE sites in their promoter regions and are implicated in synaptic plasticity, such as *c-fos* and *Zif268*, are primary candidates to begin with (Tischmeyer and Grimm, 1999). Because dendritic targeting and local translation of mRNA may play an important role in synaptic

plasticity and memory formation (Sutton and Schuman, 2006), ideally the subcellular localization of new transcripts should also be examined.

Assuming that transcription is induced by 7-spine stimulation, it still remains unknown whether translation is induced. Therefore, it would be interesting to monitor new protein synthesis in response to glutamate uncaging at a few spines, in the absence and presence of ERK inhibitor. The most straightforward approach is to use immunohistochemistry with antibodies against proteins of interest, although this method suffers from poor spatiotemporal resolution. Novel methods have been developed to visualize translation of a specific mRNA, even in the dendrites and synapses (Martin and Zukin, 2006). For example, in a pioneering study by Schuman lab, GFP sequence was flanked by the 5' and 3' regions of CaMKII and delivered biolistically into neurons. Newly synthesized fluorescent protein, as a surrogate for CaMKII, was detected in real time in the soma as well as dendrites in response to BDNF stimulation (Aakalu et al., 2001).

In addition to transcriptional activation, ERK has been found to mediate acetylation and phosphorylation of histone H3 in contextual fear conditioning (Chwang et al., 2006b; Levenson et al., 2004a). It would be interesting to determine whether these histone H3 modifications are triggered by 7-spine stimulation in an ERK-dependent manner, using antibodies against phospho-H3 and acetyl-H3.

## Chapter 7. General discussions and future directions

In the present study, I have examined the spatiotemporal dynamics of ERK in response to structural plasticity (sLTP) induction at individual spines. Remarkably, I found that inducing sLTP at as few as three spines is sufficient to produce a significant increase in ERK activity in the neuronal nucleus which is about a hundred microns away from and 2,000-fold larger in volume than the stimulated spines (Adams and Dudek, 2005). Because global firing is inhibited by TTX, the nuclear ERK signal elicited by activating a few spines implies the existence of synapse-to-nucleus communication, as well as an amplification mechanism that ensures the effectiveness of this communication. The spatiotemporal integration required for nuclear ERK activation was also investigated. The present data have revealed that although sustained dendritic ERK activation is induced by stimulation a single dendrite, nuclear ERK activation requires integration between different dendrites. This requirement for more than one dendrite is partially explained by the observation that the biochemical input from a single dendritic branch could be saturated by stimulating 2 spines. A threshold mechanism must exist, the nature of which remains to be determined in the future. Furthermore, the ERK activity increase induced by uncaging at a few spines seems to have nuclear functions- phosphorylation of transcription factors. Whether nuclear ERK induced by uncaging has

additional nuclear functions (e.g. histone H3 phosphorylation) and further impacts on gene expression remains to be elucidated.

### **Why ERK activity is long-lasting?**

ERK activation in the neuron might be transient or sustained, depending on the type of stimuli and neurons. Fear conditioning training upregulates ERK activity in CA1 neurons *in vivo* which peaks around 1 hr and returns to baseline within 3-4 hr (Chwang et al., 2006a). Less physiological stimulations, such as BDNF and KCl, also induce gradual and sustained ERK activation (Wiegert et al., 2007; Wu et al., 2001a). In contrast, ERK activation induced by high-frequency stimulation (HFS) or theta-burst stimulation was transient, returning to baseline within ~30 min (English and Sweatt, 1997; Harvey et al., 2008a). The duration of ERK activation is a critical determinant of its biological outcome. For example, in PC12 cells, NGF-induced sustained ERK activity favors differentiation whereas EGF-induced transient ERK activity favors proliferation (Pellegrino and Stork, 2006). In the present study, I have found that uncaging-induced ERK activation in the nucleus and dendrites is gradual and sustained, persisting for more than 70 min. The persistence of ERK activity is intriguing, considering the transient durations of its upstream activators: calcium transients cease within 1 s after completion of uncaging (Figure 4.3) and Ras activity returns to baseline within 5 min (Harvey et al., 2008b). Here, I speculate on the potential mechanisms that might account for the

sustained ERK activation following induction of sLTP at a few spines. These mechanisms are not mutually exclusive and might be working together.

### **No activation or inactivation of phosphatases**

Although ERK is activated through phosphorylation of its threonine and tyrosine residues exclusively by kinase MEK, it is inactivated by three classes of protein phosphatases: dual-specificity phosphatases, serine/threonine phosphatases, and protein tyrosine phosphatases (Alessi et al., 1995; Camps et al., 2000; Pulido et al., 1998). The duration of ERK activation is tightly controlled by a balance of kinases and phosphatases. In the case of glutamate stimulation, ERK activation is terminated by striatal-enriched protein tyrosine phosphatase (STEP) which is activated by calcineurin through dephosphorylation (Paul et al., 2003). Activity of phosphatases such as calcineurin and PP1 is dependent on moderate calcium signals which may result from spontaneous firing (Li et al., 2012). However, the tight balance between kinases and phosphatases might be tilted towards kinases in our system. Phosphatases might be inactive due to lack of moderate  $Ca^{2+}$  transients, an effect caused by inclusion of TTX throughout the experiment. To test this hypothesis, ERK activity can be measured in neurons subject to sLTP induction (strong  $Ca^{2+}$  signal) and then sLTD induction (moderate  $Ca^{2+}$  signal)(Oh et al., 2013). A reversal of ERK activation by sLTD induction would indicate that the observed sustained activity of ERK is due to phosphatase inhibition in our experimental system.

### **Positive feedback loop of kinases**

Computational biologists have proposed that a positive feedback loop that involves reciprocal activation of ERK and PKC accounts for sustained activation of ERK (Ajay and Bhalla, 2007; Kuroda et al., 2001; Markevich et al., 2006). Recently, the existence of such a positive feedback loop has been confirmed experimentally in cerebellar LTD (Tanaka and Augustine, 2008; Yamamoto et al., 2012). Given that PKC is also activated by glutamate uncaging (Matsuzaki et al., 2004), it is possible that the same positive feedback loop is also involved in the persistent ERK activation induced by sLTP induction at a few spines. As discussed above, this possibility could be tested by disrupting the loop without affecting sLTP induction, for example by PLA<sub>2</sub> inhibition or delayed PKC inhibition.

### **Positive feedback from BDNF**

In a recent study, Maharana et al. has demonstrated that KCl-induced sustained ERK activation is susceptible to inhibitions of protein synthesis, gene transcription, and receptor tyrosine kinase (Maharana et al., 2013). More remarkably, sustained ERK activation is also prevented by anti-BDNF antibodies. Therefore, a positive feedback loop mediated by BDNF synthesis underlies sustained ERK activation induced by KCl. It is possible that this BDNF-mediated positive feedback is also involved in uncaging-induced ERK activation. Moreover, given that facts that BDNF mRNA is localized in

dendrites (Tongiorgi et al., 1997) and that ERK activity is an integral part of dendritic translation (Kelleher et al., 2004a), it is also possible that a local BDNF synthesis around the stimulated spine contributes to sustained ERK activation in the nucleus and dendrites. To test this hypothesis, the effect of receptor tyrosine kinase inhibitor or anti-BDNF antibodies on ERK activation in response to multi-spine uncaging should be assessed.

### **Protection by bound proteins**

Transport of phosphorylated kinases over long distances is critical to axon-to-soma signaling after nerve injury. How is the phosphorylated state protected during long-distance transport in the face of constitutive phosphatase activity in neurons? This question has been elegantly addressed in the case of retrograde transport of phosphorylated ERK in axons (Perlson et al., 2005). Upon activation at injured nerve ends, ERK is retrogradely transported to the soma through association with molecular motor dynein and importin  $\beta$ . Association of ERK with intermediate filament vimentin is crucial for preservation of its phosphorylation state and its downstream actions in the nucleus. Vimentin protects ERK phosphorylation by providing a steric hindrance against phosphatases (Perlson et al., 2006). Furthermore, a recent study has found that physical protection by associated proteins might also play a role in dendritic trafficking of phosphorylated ERK (Karpova et al., 2013). Upon synaptic NMDAR activation, ERK binds and phosphorylates a novel postsynaptic protein Jacob, which in turn recruits

intermediate filament  $\alpha$ -internexin. The binding of  $\alpha$ -internexin protects both pERK and phospho-Jacob from dephosphorylation, ensuring the nuclear accumulation and actions of these phosphoproteins. It is plausible that the ERK activation induced by multi-spine uncaging is protected by steric hindrance posed by bound proteins. It is also plausible that the multi-spine uncaging-induced ERK propagation and nuclear activation involve formation of a trimeric complex with Jacob and  $\alpha$ -internexin. In fact, ERK activation in this study and Jacob activation (Karpova et al., 2013) seem to share the same NMDAR dependence and slow time course. In the future, these possibilities could be addressed by examining the spatiotemporal kinetics of Jacob and  $\alpha$ -internexin upon multi-spine uncaging. Moreover, it remains unknown whether nuclear ERK activation induced by uncaging at a few spines is impaired by blocking the interactions of ERK with these proteins.

### **ERK pathway as a synapse-to-nucleus signal**

The work presented in this dissertation illuminates the mechanisms of synapse-to-nucleus signaling during LTP. Previously, two models have been proposed (Adams and Dudek, 2005; Hagenston and Bading, 2011): one is that biochemical signals relay information from activated synapses to the nucleus (Deisseroth et al., 2003; Martin et al., 1997; Meffert et al., 2003; Thompson et al., 2004; Worley et al., 1993). In the alternative model, action potentials at the soma induced by strong synaptic stimulation directly increase somatic  $\text{Ca}^{2+}$  via VGCC activation, leading to gene transcription (Adams and

Dudek, 2005; Dudek and Fields, 2002). Under the present experimental condition, the second mechanism is unlikely to be involved, because low frequency glutamate uncaging at individual spines under inhibition of action potentials produces only a small somatic depolarization ( $< 1$  mV) (Bloodgood and Sabatini, 2007). Furthermore, activation of VGCCs is not required for nuclear ERK activation (Figure 4.1). Taken together, my results strongly suggest that biochemical mechanism exists to transmit signal from synapses to the nucleus. Because activation of mGluRs and internal  $\text{Ca}^{2+}$  stores are required (Figure 4.1), mGluR-mediated  $\text{Ca}^{2+}$  waves may play an important role in the synapse-to-nucleus signaling (Hagenston et al., 2008; Nakamura et al., 1999). Alternatively, trafficking of signaling proteins may mediate the synapse-to-nucleus communication. Such kind of synapse-to-nucleus signaling moieties have been previously reported. For instance, BAPTA-sensitive and EGTA-insensitive local  $\text{Ca}^{2+}$  elevation resulted from glutamate, NMDA or KCl application is sufficient to cause translocation of transcription factor NF- $\kappa$ B from distal processes into the nucleus (Meffert et al., 2003). Another reported synapse-to-nucleus messenger is Jacob, a recently identified caldendrin-binding protein. In response to LTP-inducing tetanic stimuli, Jacob senses the calcium increase upon activation of NMDARs and translocates from dendrites into the nucleus in an ERK-dependent way (Behnisch et al., 2011; Dieterich et al., 2008; Karpova et al., 2013). As Ras-MEK signaling is required for nuclear ERK activation (Figure 4.1) and Ras activity is known to spread over  $\sim 10$   $\mu\text{m}$  upon single

spine stimulation (Harvey et al., 2008b), downstream ERK may travel further and invade the nucleus following multi-spine stimulation.

## References

- Aakalu, G., Smith, W.B., Nguyen, N., Jiang, C., and Schuman, E.M. (2001). Dynamic visualization of local protein synthesis in hippocampal neurons. *Neuron* 30, 489-502.
- Abel, T., Nguyen, P.V., Barad, M., Deuel, T.A., Kandel, E.R., and Bourtchouladze, R. (1997). Genetic demonstration of a role for PKA in the late phase of LTP and in hippocampus-based long-term memory. *Cell* 88, 615-626.
- Adams, J.P., Anderson, A.E., Varga, A.W., Dineley, K.T., Cook, R.G., Pfaffinger, P.J., and Sweatt, J.D. (2000). The A-type potassium channel Kv4.2 is a substrate for the mitogen-activated protein kinase ERK. *J Neurochem* 75, 2277-2287.
- Adams, J.P., and Dudek, S.M. (2005). Late-phase long-term potentiation: getting to the nucleus. *Nat Rev Neurosci* 6, 737-743.
- Adesnik, H., and Nicoll, R.A. (2007). Conservation of Glutamate Receptor 2-Containing AMPA Receptors during Long-Term Potentiation. *The Journal of Neuroscience* 27, 4598-4602.
- Ajay, S.M., and Bhalla, U.S. (2007). A propagating ERKII switch forms zones of elevated dendritic activation correlated with plasticity. *HFSP J* 1, 49-66.
- Alarcón, J.M., Malleret, G., Touzani, K., Vronskaya, S., Ishii, S., Kandel, E.R., and Barco, A. (2004). Chromatin Acetylation, Memory, and LTP Are Impaired in CBP+/- Mice: A Model for the Cognitive Deficit in Rubinstein-Taybi Syndrome and Its Amelioration. *Neuron* 42, 947-959.
- Alessi, D.R., Gomez, N., Moorhead, G., Lewis, T., Keyse, S.M., and Cohen, P. (1995). Inactivation of p42 MAP kinase by protein phosphatase 2A and a protein tyrosine phosphatase, but not CL100, in various cell lines. *Current biology : CB* 5, 283-295.
- Alford, S., Frenguelli, B.G., Schofield, J.G., and Collingridge, G.L. (1993). Characterization of Ca<sup>2+</sup> signals induced in hippocampal CA1 neurones by the synaptic activation of NMDA receptors. *J Physiol* 469, 693-716.
- Andersen, P. (2007). *The hippocampus book* (Oxford; New York: Oxford University Press).
- Araya, R., Eisenthal, K.B., and Yuste, R. (2006a). Dendritic spines linearize the summation of excitatory potentials. *Proc Natl Acad Sci U S A* 103, 18799-18804.

- Araya, R., Jiang, J., Eisenthal, K.B., and Yuste, R. (2006b). The spine neck filters membrane potentials. *Proc Natl Acad Sci U S A* 103, 17961-17966.
- Atkins, C.M., Selcher, J.C., Petraitis, J.J., Trzaskos, J.M., and Sweatt, J.D. (1998). The MAPK cascade is required for mammalian associative learning. *Nat Neurosci* 1, 602-609.
- Bading, H., Ginty, D.D., and Greenberg, M.E. (1993). Regulation of gene expression in hippocampal neurons by distinct calcium signaling pathways. *Science (New York, NY)* 260, 181-186.
- Bading, H., Segal, M.M., Sucher, N.J., Dudek, H., Lipton, S.A., and Greenberg, M.E. (1995). N-methyl-d-aspartate receptors are critical for mediating the effects of glutamate on intracellular calcium concentration and immediate early gene expression in cultured hippocampal neurons. *Neuroscience* 64, 653-664.
- Bagni, C., Tassone, F., Neri, G., and Hagerman, R. (2012). Fragile X syndrome: causes, diagnosis, mechanisms, and therapeutics. *The Journal of clinical investigation* 122, 4314-4322.
- Bailey, C.H., and Chen, M. (1988). Long-term memory in *Aplysia* modulates the total number of varicosities of single identified sensory neurons. *Proceedings of the National Academy of Sciences* 85, 2373-2377.
- Bailey, C.H., Kaang, B.-K., Chen, M., Martin, K.C., Lim, C.-S., Casadio, A., and Kandel, E.R. (1997). Mutation in the Phosphorylation Sites of MAP Kinase Blocks Learning-Related Internalization of apCAM in *Aplysia* Sensory Neurons. *Neuron* 18, 913-924.
- Bailey, C.H., and Kandel, E.R. (1993). Structural changes accompanying memory storage. *Annu Rev Physiol* 55, 397-426.
- Ballif, B.A., Arnaud, L., Arthur, W.T., Guris, D., Imamoto, A., and Cooper, J.A. (2004). Activation of a Dab1/CrkL/C3G/Rap1 pathway in Reelin-stimulated neurons. *Current biology : CB* 14, 606-610.
- Balschun, D., Manahan-Vaughan, D., Wagner, T., Behnisch, T., Reymann, K.G., and Wetzell, W. (1999). A Specific Role for Group I mGluRs in Hippocampal LTP and Hippocampus-Dependent Spatial Learning. *Learning & Memory* 6, 138-152.
- Bannerman, D.M., Good, M.A., Butcher, S.P., Ramsay, M., and Morris, R.G. (1995). Distinct components of spatial learning revealed by prior training and NMDA receptor blockade. *Nature* 378, 182-186.

- Barco, A., Pittenger, C., and Kandel, E.R. (2003). CREB, memory enhancement and the treatment of memory disorders: promises, pitfalls and prospects. *Expert Opinion on Therapeutic Targets* 7, 101-114.
- Behnisch, T., Matsushita, S., and Knopfel, T. (2004). Imaging of gene expression during long-term potentiation. *Neuroreport* 15, 2039-2043.
- Behnisch, T., and Reymann, K.G. (1995). Thapsigargin blocks long-term potentiation induced by weak, but not strong tetanisation in rat hippocampal CA1 neurons. *Neuroscience letters* 192, 185-188.
- Behnisch, T., YuanXiang, P., Bethge, P., Parvez, S., Chen, Y., Yu, J., Karpova, A., Frey, J.U., Mikhaylova, M., and Kreutz, M.R. (2011). Nuclear Translocation of Jacob in Hippocampal Neurons after Stimuli Inducing Long-Term Potentiation but Not Long-Term Depression. *PLoS ONE* 6, e17276.
- Berman, D.E., Hazvi, S., Rosenblum, K., Seger, R., and Dudai, Y. (1998). Specific and Differential Activation of Mitogen-Activated Protein Kinase Cascades by Unfamiliar Taste in the Insular Cortex of the Behaving Rat. *The Journal of Neuroscience* 18, 10037-10044.
- Besnard, a., Galan, B., Vanhoutte, p., and Caboche, J. (2011). Elk-1 a transcription factor with multiple facets in the brain. *Frontiers in neuroscience* 5.
- Bjork, R.A., and Allen, T.W. (1970). The spacing effect: Consolidation or differential encoding? *Journal of Verbal Learning and Verbal Behavior* 9, 567-572.
- Blendy, J.A., Kaestner, K.H., Schmid, W., Gass, P., and Schutz, G. (1996). Targeting of the CREB gene leads to up-regulation of a novel CREB mRNA isoform. *EMBO J* 15, 1098-1106.
- Bliss, T.V., and Collingridge, G.L. (1993). A synaptic model of memory: long-term potentiation in the hippocampus. *Nature* 361, 31-39.
- Bliss, T.V.P., and Lømo, T. (1973). Long-lasting potentiation of synaptic transmission in the dentate area of the anaesthetized rabbit following stimulation of the perforant path. *J Physiol* 232, 331-356.
- Bloodgood, B.L., Giessel, A.J., and Sabatini, B.L. (2009). Biphasic Synaptic Ca Influx Arising from Compartmentalized Electrical Signals in Dendritic Spines. *PLoS Biol* 7, e1000190.

Bloodgood, B.L., and Sabatini, B.L. (2005). Neuronal activity regulates diffusion across the neck of dendritic spines. *Science* 310, 866-869.

Bloodgood, B.L., and Sabatini, B.L. (2007). Nonlinear regulation of unitary synaptic signals by CaV(2.3) voltage-sensitive calcium channels located in dendritic spines. *Neuron* 53, 249-260.

Blum, S., and Dash, P.K. (2009). MAP Kinase Signaling in Learning and Memory. In *Encyclopedia of Neuroscience*, R.S. Editor-in-Chief: Larry, ed. (Oxford: Academic Press), pp. 657-662.

Boehm, J., Kang, M.-G., Johnson, R.C., Esteban, J., Huganir, R.L., and Malinow, R. (2006). Synaptic Incorporation of AMPA Receptors during LTP Is Controlled by a PKC Phosphorylation Site on GluR1. *Neuron* 51, 213-225.

Borrelli, E., Nestler, E.J., Allis, C.D., and Sassone-Corsi, P. (2008). Decoding the Epigenetic Language of Neuronal Plasticity. *Neuron* 60, 961-974.

Bortolotto, Z.A., Fitzjohn, S.M., and Collingridge, G.L. (1999). Roles of metabotropic glutamate receptors in LTP and LTD in. *Curr Opin Neurobiol* 9, 299-304.

Bourtchuladze, R., Frenguelli, B., Blendy, J., Cioffi, D., Schutz, G., and Silva, A.J. (1994). Deficient long-term memory in mice with a targeted mutation of the cAMP-responsive element-binding protein. *Cell* 79, 59-68.

Branco, T., and Häusser, M. (2010). The single dendritic branch as a fundamental functional unit in the nervous system. *Curr Opin Neurobiol* 20, 494-502.

Burack, W.R., and Shaw, A.S. (2005). Live Cell Imaging of ERK and MEK. *Journal of Biological Chemistry* 280, 3832-3837.

Busetto, G., Higley, M.J., and Sabatini, B.L. (2008). Developmental presence and disappearance of postsynaptically silent synapses on dendritic spines of rat layer 2/3 pyramidal neurons. *J Physiol* 586, 1519-1527.

Camps, M., Nichols, A., and Arkinstall, S. (2000). Dual specificity phosphatases: a gene family for control of MAP kinase function. *FASEB J* 14, 6-16.

Canagarajah, B.J., Khokhlatchev, A., Cobb, M.H., and Goldsmith, E.J. (1997). Activation mechanism of the MAP kinase ERK2 by dual phosphorylation. *Cell* 90, 859-869.

- Cavus, I., and Teyler, T. (1996). Two forms of long-term potentiation in area CA1 activate different signal transduction cascades. *Journal of neurophysiology* 76, 3038-3047.
- Chang, F.L., and Greenough, W.T. (1984). Transient and enduring morphological correlates of synaptic activity and efficacy change in the rat hippocampal slice. *Brain Res* 309, 35-46.
- Chao, T.S., Byron, K.L., Lee, K.M., Villereal, M., and Rosner, M.R. (1992). Activation of MAP kinases by calcium-dependent and calcium-independent pathways. Stimulation by thapsigargin and epidermal growth factor. *Journal of Biological Chemistry* 267, 19876-19883.
- Chawla, S., Hardingham, G.E., Quinn, D.R., and Bading, H. (1998). CBP: A Signal-Regulated Transcriptional Coactivator Controlled by Nuclear Calcium and CaM Kinase IV. *Science* 281, 1505-1509.
- Chen, S., Xu, Y., Xu, B., Guo, M., Zhang, Z., Liu, L., Ma, H., Chen, Z., Luo, Y., Huang, S., *et al.* (2011). CaMKII is involved in cadmium activation of MAPK and mTOR pathways leading to neuronal cell death. *J Neurochem* 119, 1108-1118.
- Cheung, E.C.C., and Slack, R.S. (2004). Emerging Role for ERK as a Key Regulator of Neuronal Apoptosis. *Sci STKE* 2004, pe45-.
- Chévere-Torres, I., Kaphzan, H., Bhattacharya, A., Kang, A., Maki, J.M., Gambello, M.J., Arbiser, J.L., Santini, E., and Klann, E. (2012). Metabotropic glutamate receptor-dependent long-term depression is impaired due to elevated ERK signaling in the  $\Delta$ RG mouse model of tuberous sclerosis complex. *Neurobiology of Disease* 45, 1101-1110.
- Chung, K.C., Sung, J.Y., Ahn, W., Rhim, H., Oh, T.H., Lee, M.G., and Ahn, Y.S. (2001). Intracellular Calcium Mobilization Induces Immediate Early Genepip92 via Src and Mitogen-activated Protein Kinase in Immortalized Hippocampal Cells. *Journal of Biological Chemistry* 276, 2132-2138.
- Chwang, W.B., Arthur, J.S., Schumacher, A., and Sweatt, J.D. (2007). The nuclear kinase mitogen- and stress-activated protein kinase 1 regulates hippocampal chromatin remodeling in memory formation. *The Journal of neuroscience : the official journal of the Society for Neuroscience* 27, 12732-12742.
- Chwang, W.B., O'Riordan, K.J., Levenson, J.M., and Sweatt, J.D. (2006a). ERK/MAPK regulates hippocampal histone phosphorylation following contextual fear conditioning. *Learn Mem* 13, 322-328.

Chwang, W.B., O’Riordan, K.J., Levenson, J.M., and Sweatt, J.D. (2006b). ERK/MAPK regulates hippocampal histone phosphorylation following contextual fear conditioning. *Learning & Memory* 13, 322-328.

Cole, A.J., Saffen, D.W., Baraban, J.M., and Worley, P.F. (1989). Rapid increase of an immediate early gene messenger RNA in hippocampal neurons by synaptic NMDA receptor activation. *Nature* 340, 474-476.

Costa, R.M., Federov, N.B., Kogan, J.H., Murphy, G.G., Stern, J., Ohno, M., Kucherlapati, R., Jacks, T., and Silva, A.J. (2002). Mechanism for the learning deficits in a mouse model of neurofibromatosis type 1. *Nature* 415, 526-530.

Cracco, J.B., Serrano, P., Moskowitz, S.I., Bergold, P.J., and Sacktor, T.C. (2005). Protein synthesis-dependent LTP in isolated dendrites of CA1 pyramidal cells. *Hippocampus* 15, 551-556.

Davis, S., Vanhoutte, P., Pagès, C., Caboche, J., and Laroche, S. (2000). The MAPK/ERK Cascade Targets Both Elk-1 and cAMP Response Element-Binding Protein to Control Long-Term Potentiation-Dependent Gene Expression in the Dentate Gyrus In Vivo. *The Journal of Neuroscience* 20, 4563-4572.

De Roo, M., Klausner, P., and Muller, D. (2008). LTP promotes a selective long-term stabilization and clustering of dendritic spines. *PLoS Biol* 6, e219.

de Rooij, J., Zwartkruis, F.J., Verheijen, M.H., Cool, R.H., Nijman, S.M., Wittinghofer, A., and Bos, J.L. (1998). Epac is a Rap1 guanine-nucleotide-exchange factor directly activated by cyclic AMP. *Nature* 396, 474-477.

Deadwyler, S.A., Dunwiddie, T., and Lynch, G. (1987). A critical level of protein synthesis is required for long-term potentiation. *Synapse* 1, 90-95.

Deisseroth, K., Mermelstein, P.G., Xia, H., and Tsien, R.W. (2003). Signaling from synapse to nucleus: the logic behind the mechanisms. *Curr Opin Neurobiol* 13, 354-365.

Derkach, V., Barria, A., and Soderling, T.R. (1999). Ca<sup>2+</sup>/calmodulin-kinase II enhances channel conductance of  $\alpha$ -amino-3-hydroxy-5-methyl-4-isoxazolepropionate type glutamate receptors. *Proceedings of the National Academy of Sciences* 96, 3269-3274.

Dieterich, D.C., Karpova, A., Mikhaylova, M., Zdobnova, I., König, I., Landwehr, M., Kreutz, M., Smalla, K.-H., Richter, K., Landgraf, P., *et al.* (2008). Caldendrin–Jacob: A Protein Liaison That Couples NMDA Receptor Signalling to the Nucleus. *PLoS Biol* 6, e34.

- Downward, J., Graves, J.D., Warne, P.H., Rayter, S., and Cantrell, D.A. (1990). Stimulation of p21ras upon T-cell activation. *Nature* 346, 719-723.
- Dudek, S.M., and Fields, R.D. (2001). Mitogen-activated protein kinase/extracellular signal-regulated kinase activation in somatodendritic compartments: roles of action potentials, frequency, and mode of calcium entry. *The Journal of neuroscience : the official journal of the Society for Neuroscience* 21, RC122.
- Dudek, S.M., and Fields, R.D. (2002). Somatic action potentials are sufficient for late-phase LTP-related cell signaling. *Proc Natl Acad Sci U S A* 99, 3962-3967.
- Dudman, J.T., Tsay, D., and Siegelbaum, S.A. (2007). A role for synaptic inputs at distal dendrites: instructive signals for hippocampal long-term plasticity. *Neuron* 56, 866-879.
- Ebinu, J.O., Bottorff, D.A., Chan, E.Y.W., Stang, S.L., Dunn, R.J., and Stone, J.C. (1998). RasGRP, a Ras Guanyl Nucleotide- Releasing Protein with Calcium- and Diacylglycerol-Binding Motifs. *Science* 280, 1082-1086.
- Emptage, N., Bliss, T.V.P., and Fine, A. (1999). Single Synaptic Events Evoke NMDA Receptor-Mediated Release of Calcium from Internal Stores in Hippocampal Dendritic Spines. *Neuron* 22, 115-124.
- Engert, F., and Bonhoeffer, T. (1997). Synapse specificity of long-term potentiation breaks down at short distances. *Nature* 388, 279-284.
- Engert, F., and Bonhoeffer, T. (1999). Dendritic spine changes associated with hippocampal long-term synaptic plasticity. *Nature* 399, 66-70.
- English, J.D., and Sweatt, J.D. (1996). Activation of p42 Mitogen-activated Protein Kinase in Hippocampal Long Term Potentiation. *Journal of Biological Chemistry* 271, 24329-24332.
- English, J.D., and Sweatt, J.D. (1997). A Requirement for the Mitogen-activated Protein Kinase Cascade in Hippocampal Long Term Potentiation. *Journal of Biological Chemistry* 272, 19103-19106.
- Fantz, D.A., Jacobs, D., Glossip, D., and Kornfeld, K. (2001). Docking Sites on Substrate Proteins Direct Extracellular Signal-regulated Kinase to Phosphorylate Specific Residues. *Journal of Biological Chemistry* 276, 27256-27265.

- Farnsworth, C.L., Freshney, N.W., Rosen, L.B., Ghosh, A., Greenberg, M.E., and Feig, L.A. (1995). Calcium activation of Ras mediated by neuronal exchange factor Ras-GRF. *Nature* 376, 524-527.
- Fifkova, E., and Anderson, C.L. (1981). Stimulation-induced changes in dimensions of stalks of dendritic spines in the dentate molecular layer. *Exp Neurol* 74, 621-627.
- Fitzjohna, S.M., Irving, A.J., Palmer, M.J., Harvey, J., Lodge, D., and Collingridge, G.L. (1996). Activation of group I mGluRs potentiates NMDA responses in rat hippocampal slices. *Neuroscience letters* 203, 211-213.
- Fitzpatrick, J.S., Hagenston, A.M., Hertle, D.N., Gipson, K.E., Bertetto-D'Angelo, L., and Yeckel, M.F. (2009). Inositol-1,4,5-trisphosphate receptor-mediated Ca<sup>2+</sup> waves in pyramidal neuron dendrites propagate through hot spots and cold spots. *J Physiol* 587, 1439-1459.
- Frey, U., Frey, S., Schollmeier, F., and Krug, M. (1996). Influence of actinomycin D, a RNA synthesis inhibitor, on long-term potentiation in rat hippocampal neurons in vivo and in vitro. *J Physiol* 490, 703-711.
- Frey, U., Huang, Y.Y., and Kandel, E.R. (1993). Effects of cAMP simulate a late stage of LTP in hippocampal CA1 neurons. *Science* 260, 1661-1664.
- Frey, U., Krug, M., Reymann, K.G., and Matthies, H. (1988). Anisomycin, an inhibitor of protein synthesis, blocks late phases of LTP phenomena in the hippocampal CA1 region in vitro. *Brain Res* 452, 57-65.
- Fujii, S., Matsumoto, M., Igarashi, K., Kato, H., and Mikoshiba, K. (2000). Synaptic Plasticity in Hippocampal CA1 Neurons of Mice Lacking Type 1 Inositol-1,4,5-Trisphosphate Receptors. *Learning & Memory* 7, 312-320.
- Fukuda, M., Gotoh, I., Gotoh, Y., and Nishida, E. (1996). Cytoplasmic localization of mitogen-activated protein kinase kinase directed by its NH<sub>2</sub>-terminal, leucine-rich short amino acid sequence, which acts as a nuclear export signal. *J Biol Chem* 271, 20024-20028.
- Fukuda, M., Gotoh, Y., and Nishida, E. (1997). Interaction of MAP kinase with MAP kinase kinase: its possible role in the control of nucleocytoplasmic transport of MAP kinase. *EMBO J* 16, 1901-1908.
- Futatsugi, A., Kato, K., Ogura, H., Li, S.-T., Nagata, E., Kuwajima, G., Tanaka, K., Itohara, S., and Mikoshiba, K. (1999). Facilitation of NMDAR-Independent LTP and

Spatial Learning in Mutant Mice Lacking Ryanodine Receptor Type 3. *Neuron* 24, 701-713.

Gardoni, F., Caputi, A., Cimino, M., Pastorino, L., Cattabeni, F., and Di Luca, M. (1998). Calcium/Calmodulin-Dependent Protein Kinase II Is Associated with NR2A/B Subunits of NMDA Receptor in Postsynaptic Densities. *Journal of Neurochemistry* 71, 1733-1741.

Gasparini, S., Migliore, M., and Magee, J.C. (2004). On the initiation and propagation of dendritic spikes in CA1 pyramidal neurons. *The Journal of neuroscience : the official journal of the Society for Neuroscience* 24, 11046-11056.

Geinisman, Y., deToledo-Morrell, L., and Morrell, F. (1991). Induction of long-term potentiation is associated with an increase in the number of axospinous synapses with segmented postsynaptic densities. *Brain Res* 566, 77-88.

Gille, H., Strahl, T., and Shaw, P.E. (1995a). Activation of ternary complex factor Elk-1 by stress-activated protein kinases. *Current biology : CB* 5, 1191-1200.

Gille, H., Strahl, T., and Shaw, P.E. (1995b). Activation of ternary complex factor Elk-1 by stress-activated protein kinases. *Current biology : CB* 5, 1191-1200.

Giovannini, M.G., Blitzer, R.D., Wong, T., Asoma, K., Tsokas, P., Morrison, J.H., Iyengar, R., and Landau, E.M. (2001). Mitogen-activated protein kinase regulates early phosphorylation and delayed expression of Ca<sup>2+</sup>/calmodulin-dependent protein kinase II in long-term potentiation. *The Journal of neuroscience : the official journal of the Society for Neuroscience* 21, 7053-7062.

Gold, P.E. (2008). Protein synthesis inhibition and memory: formation vs amnesia. *Neurobiol Learn Mem* 89, 201-211.

Goldin, M., and Segal, M. (2003). Protein kinase C and ERK involvement in dendritic spine plasticity in cultured rodent hippocampal neurons. *European Journal of Neuroscience* 17, 2529-2539.

Gonzalez, G.A., and Montminy, M.R. (1989). Cyclic AMP stimulates somatostatin gene transcription by phosphorylation of CREB at serine 133. *Cell* 59, 675-680.

Govindarajan, A., Israely, I., Huang, S.-Y., and Tonegawa, S. (2011). The Dendritic Branch Is the Preferred Integrative Unit for Protein Synthesis-Dependent LTP. *Neuron* 69, 132-146.

- Govindarajan, A., Kelleher, R.J., and Tonegawa, S. (2006). A clustered plasticity model of long-term memory engrams. *Nat Rev Neurosci* 7, 575-583.
- Gray, E.E., Fink, A.E., Sariñana, J., Vissel, B., and O'Dell, T.J. (2007). Long-Term Potentiation in the Hippocampal CA1 Region Does Not Require Insertion and Activation of GluR2-Lacking AMPA Receptors. *Journal of neurophysiology* 98, 2488-2492.
- Gray, E.G. (1959). Electron microscopy of synaptic contacts on dendrite spines of the cerebral cortex. *Nature* 183, 1592-1593.
- Grewal, S.S., York, R.D., and Stork, P.J. (1999). Extracellular-signal-regulated kinase signalling in neurons. *Curr Opin Neurobiol* 9, 544-553.
- Guzowski, J.F., Lyford, G.L., Stevenson, G.D., Houston, F.P., McGaugh, J.L., Worley, P.F., and Barnes, C.A. (2000). Inhibition of Activity-Dependent Arc Protein Expression in the Rat Hippocampus Impairs the Maintenance of Long-Term Potentiation and the Consolidation of Long-Term Memory. *The Journal of Neuroscience* 20, 3993-4001.
- Habas, A., Kharebava, G., Szatmari, E., and Hetman, M. (2006). NMDA neuroprotection against a phosphatidylinositol-3 kinase inhibitor, LY294002 by NR2B-mediated suppression of glycogen synthase kinase-3 $\beta$ -induced apoptosis. *J Neurochem* 96, 335-348.
- Hagenston, A.M., and Bading, H. (2011). Calcium Signaling in Synapse-to-Nucleus Communication. *Cold Spring Harbor Perspectives in Biology* 3.
- Hagenston, A.M., Fitzpatrick, J.S., and Yeckel, M.F. (2008). mGluR-Mediated Calcium Waves that Invade the Soma Regulate Firing in Layer V Medial Prefrontal Cortical Pyramidal Neurons. *Cerebral Cortex* 18, 407-423.
- Hardingham, G.E., Arnold, F.J., and Bading, H. (2001). A calcium microdomain near NMDA receptors: on switch for ERK-dependent synapse-to-nucleus communication. *Nat Neurosci* 4, 565-566.
- Hardingham, G.E., Chawla, S., Cruzalegui, F.H., and Bading, H. (1999). Control of Recruitment and Transcription-Activating Function of CBP Determines Gene Regulation by NMDA Receptors and L-Type Calcium Channels. *Neuron* 22, 789-798.
- Harnett, M.T., Makara, J.K., Spruston, N., Kath, W.L., and Magee, J.C. (2012). Synaptic amplification by dendritic spines enhances input cooperativity. *Nature* 491, 599-602.

- Harris, K.M., and Kater, S.B. (1994). Dendritic spines: cellular specializations imparting both stability and flexibility to synaptic function. *Annu Rev Neurosci* 17, 341-371.
- Harvey, C.D., Ehrhardt, A.G., Cellurale, C., Zhong, H., Yasuda, R., Davis, R.J., and Svoboda, K. (2008a). A genetically encoded fluorescent sensor of ERK activity. *Proceedings of the National Academy of Sciences* 105, 19264-19269.
- Harvey, C.D., and Svoboda, K. (2007). Locally dynamic synaptic learning rules in pyramidal neuron dendrites. *Nature* 450, 1195-1200.
- Harvey, C.D., Yasuda, R., Zhong, H., and Svoboda, K. (2008b). The spread of Ras activity triggered by activation of a single dendritic spine. *Science* 321, 136-140.
- Hayashi, Y., Shi, S.-H., Esteban, J.A., Piccini, A., Poncer, J.-C., and Malinow, R. (2000). Driving AMPA Receptors into Synapses by LTP and CaMKII: Requirement for GluR1 and PDZ Domain Interaction. *Science* 287, 2262-2267.
- Hernandez, A.I., Blace, N., Crary, J.F., Serrano, P.A., Leitges, M., Libien, J.M., Weinstein, G., Tcherapanov, A., and Sacktor, T.C. (2003). Protein Kinase M $\zeta$  Synthesis from a Brain mRNA Encoding an Independent Protein Kinase C $\zeta$  Catalytic Domain. *Journal of Biological Chemistry* 278, 40305-40316.
- Hetman, M., Hsuan, S.-L., Habas, A., Higgins, M.J., and Xia, Z. (2002). ERK1/2 Antagonizes Glycogen Synthase Kinase-3 $\beta$ -induced Apoptosis in Cortical Neurons. *Journal of Biological Chemistry* 277, 49577-49584.
- Hoffman, D.A., and Johnston, D. (1998). Downregulation of transient K<sup>+</sup> channels in dendrites of hippocampal CA1 pyramidal neurons by activation of PKA and PKC. *The Journal of neuroscience : the official journal of the Society for Neuroscience* 18, 3521-3528.
- Hoffman, D.A., Magee, J.C., Colbert, C.M., and Johnston, D. (1997). K<sup>+</sup> channel regulation of signal propagation in dendrites of hippocampal pyramidal neurons. *Nature* 387, 869-875.
- Horgan, A.M., and Stork, P.J.S. (2003). Examining the mechanism of Erk nuclear translocation using green fluorescent protein. *Experimental Cell Research* 285, 208-220.
- Hou, L., Antion, M.D., Hu, D., Spencer, C.M., Paylor, R., and Klann, E. (2006). Dynamic Translational and Proteasomal Regulation of Fragile X Mental Retardation Protein Controls mGluR-Dependent Long-Term Depression. *Neuron* 51, 441-454.

Hu, H., Qin, Y., Bochorishvili, G., Zhu, Y., van Aelst, L., and Zhu, J.J. (2008). Ras Signaling Mechanisms Underlying Impaired GluR1-Dependent Plasticity Associated with Fragile X Syndrome. *The Journal of Neuroscience* 28, 7847-7862.

Huang, Y.Y., and Kandel, E.R. (1994). Recruitment of long-lasting and protein kinase A-dependent long-term potentiation in the CA1 region of hippocampus requires repeated tetanization. *Learn Mem* 1, 74-82.

Impey, S., Fong, A.L., Wang, Y., Cardinaux, J.R., Fass, D.M., Obrietan, K., Wayman, G.A., Storm, D.R., Soderling, T.R., and Goodman, R.H. (2002). Phosphorylation of CBP mediates transcriptional activation by neural activity and CaM kinase IV. *Neuron* 34, 235-244.

Impey, S., Mark, M., Villacres, E.C., Poser, S., Chavkin, C., and Storm, D.R. (1996). Induction of CRE-mediated gene expression by stimuli that generate long-lasting LTP in area CA1 of the hippocampus. *Neuron* 16, 973-982.

Impey, S., Obrietan, K., Wong, S.T., Poser, S., Yano, S., Wayman, G., Deloulme, J.C., Chan, G., and Storm, D.R. (1998). Cross Talk between ERK and PKA Is Required for Ca<sup>2+</sup> Stimulation of CREB-Dependent Transcription and ERK Nuclear Translocation. *Neuron* 21, 869-883.

Jacob, S.N., Choe, C.-U., Uhlen, P., DeGray, B., Yeckel, M.F., and Ehrlich, B.E. (2005). Signaling Microdomains Regulate Inositol 1,4,5-Trisphosphate-Mediated Intracellular Calcium Transients in Cultured Neurons. *The Journal of Neuroscience* 25, 2853-2864.

Jonas, P., Racca, C., Sakmann, B., Seeburg, P.H., and Monyer, H. (1994). Differences in Ca<sup>2+</sup> permeability of AMPA-type glutamate receptor channels in neocortical neurons caused by differential GluR-B subunit expression. *Neuron* 12, 1281-1289.

Jones, M.W., Errington, M.L., French, P.J., Fine, A., Bliss, T.V., Garel, S., Charnay, P., Bozon, B., Laroche, S., and Davis, S. (2001). A requirement for the immediate early gene *Zif268* in the expression of late LTP and long-term memories. *Nat Neurosci* 4, 289-296.

Joyal, J.L., Burks, D.J., Pons, S., Matter, W.F., Vlahos, C.J., White, M.F., and Sacks, D.B. (1997). Calmodulin Activates Phosphatidylinositol 3-Kinase. *Journal of Biological Chemistry* 272, 28183-28186.

Judkewitz, B., Roth, A., and Häusser, M. (2006). Dendritic Enlightenment: Using Patterned Two-Photon Uncaging to Reveal the Secrets of the Brain's Smallest Dendrites. *Neuron* 50, 180-183.

- Kang, H., Sun, L.D., Atkins, C.M., Soderling, T.R., Wilson, M.A., and Tonegawa, S. (2001). An Important Role of Neural Activity-Dependent CaMKIV Signaling in the Consolidation of Long-Term Memory. *Cell* 106, 771-783.
- Karpova, A., Mikhaylova, M., Bera, S., Bar, J., Reddy, P.P., Behnisch, T., Rankovic, V., Spilker, C., Bethge, P., Sahin, J., *et al.* (2013). Encoding and Transducing the Synaptic or Extrasynaptic Origin of NMDA Receptor Signals to the Nucleus. *Cell* 152, 1119-1133.
- Kawasaki, H., Springett, G.M., Mochizuki, N., Toki, S., Nakaya, M., Matsuda, M., Housman, D.E., and Graybiel, A.M. (1998). A family of cAMP-binding proteins that directly activate Rap1. *Science* 282, 2275-2279.
- Kelleher, R.J., 3rd, Govindarajan, A., Jung, H.Y., Kang, H., and Tonegawa, S. (2004a). Translational control by MAPK signaling in long-term synaptic plasticity and memory. *Cell* 116, 467-479.
- Kelleher, R.J., 3rd, Govindarajan, A., and Tonegawa, S. (2004b). Translational regulatory mechanisms in persistent forms of synaptic plasticity. *Neuron* 44, 59-73.
- Kelly, M.T., Crary, J.F., and Sacktor, T.C. (2007). Regulation of Protein Kinase M $\zeta$  Synthesis by Multiple Kinases in Long-Term Potentiation. *The Journal of Neuroscience* 27, 3439-3444.
- Kerchner, G.A., and Nicoll, R.A. (2008). Silent synapses and the emergence of a postsynaptic mechanism for LTP. *Nat Rev Neurosci* 9, 813-825.
- Kholodenko, B.N. (2003). Four-dimensional organization of protein kinase signaling cascades: the roles of diffusion, endocytosis and molecular motors. *J Exp Biol* 206, 2073-2082.
- Kleindienst, T., Winnubst, J., Roth-Alpermann, C., Bonhoeffer, T., and Lohmann, C. (2011). Activity-Dependent Clustering of Functional Synaptic Inputs on Developing Hippocampal Dendrites. *Neuron* 72, 1012-1024.
- Koester, H.J., and Sakmann, B. (1998). Calcium dynamics in single spines during coincident pre- and postsynaptic activity depend on relative timing of back-propagating action potentials and subthreshold excitatory postsynaptic potentials. *Proceedings of the National Academy of Sciences* 95, 9596-9601.
- Kolch, W. (2005). Coordinating ERK/MAPK signalling through scaffolds and inhibitors. *Nat Rev Mol Cell Biol* 6, 827-837.

Kolch, W., Heidecker, G., Kochs, G., Hummel, R., Vahidi, H., Mischak, H., Finkenzeller, G., Marme, D., and Rapp, U.R. (1993). Protein kinase C[alpha] activates RAF-1 by direct phosphorylation. *Nature* 364, 249-252.

Komatsu, N., Aoki, K., Yamada, M., Yukinaga, H., Fujita, Y., Kamioka, Y., and Matsuda, M. (2011). Development of an optimized backbone of FRET biosensors for kinases and GTPases. *Molecular biology of the cell* 22, 4647-4656.

Komiyama, N.H., Watabe, A.M., Carlisle, H.J., Porter, K., Charlesworth, P., Monti, J., Strathdee, D.J., O'Carroll, C.M., Martin, S.J., Morris, R.G., *et al.* (2002). SynGAP regulates ERK/MAPK signaling, synaptic plasticity, and learning in the complex with postsynaptic density 95 and NMDA receptor. *The Journal of neuroscience : the official journal of the Society for Neuroscience* 22, 9721-9732.

Kornhauser, J.M., Cowan, C.W., Shaywitz, A.J., Dolmetsch, R.E., Griffith, E.C., Hu, L.S., Haddad, C., Xia, Z., and Greenberg, M.E. (2002). CREB transcriptional activity in neurons is regulated by multiple, calcium-specific phosphorylation events. *Neuron* 34, 221-233.

Korzus, E., Rosenfeld, M.G., and Mayford, M. (2004). CBP Histone Acetyltransferase Activity Is a Critical Component of Memory Consolidation. *Neuron* 42, 961-972.

Kotecha, S.A., Jackson, M.F., Al-Mahrouki, A., Roder, J.C., Orser, B.A., and MacDonald, J.F. (2003). Co-stimulation of mGluR5 and N-Methyl-D-aspartate Receptors Is Required for Potentiation of Excitatory Synaptic Transmission in Hippocampal Neurons. *Journal of Biological Chemistry* 278, 27742-27749.

Kovalchuk, Y., Eilers, J., Lisman, J., and Konnerth, A. (2000). NMDA Receptor-Mediated Subthreshold Ca<sup>2+</sup> Signals in Spines of Hippocampal Neurons. *The Journal of Neuroscience* 20, 1791-1799.

Krapivinsky, G., Krapivinsky, L., Manasian, Y., Ivanov, A., Tyzio, R., Pellegrino, C., Ben-Ari, Y., Clapham, D.E., and Medina, I. (2003). The NMDA Receptor Is Coupled to the ERK Pathway by a Direct Interaction between NR2B and RasGRF1. *Neuron* 40, 775-784.

Krug, M., Lossner, B., and Ott, T. (1984). Anisomycin blocks the late phase of long-term potentiation in the dentate gyrus of freely moving rats. *Brain Res Bull* 13, 39-42.

Kuroda, S., Schweighofer, N., and Kawato, M. (2001). Exploration of signal transduction pathways in cerebellar long-term depression by kinetic simulation. *The Journal of neuroscience : the official journal of the Society for Neuroscience* 21, 5693-5702.

- Lai, K.-O., Zhao, Y., Ch'ng, T.H., and Martin, K.C. (2008). Importin-mediated retrograde transport of CREB2 from distal processes to the nucleus in neurons. *Proceedings of the National Academy of Sciences* 105, 17175-17180.
- Larkum, M.E., Watanabe, S., Nakamura, T., Lasser-Ross, N., and Ross, W.N. (2003). Synaptically activated Ca<sup>2+</sup> waves in layer 2/3 and layer 5 rat neocortical pyramidal neurons. *J Physiol* 549, 471-488.
- Lee, K.S., Schottler, F., Oliver, M., and Lynch, G. (1980). Brief bursts of high-frequency stimulation produce two types of structural change in rat hippocampus. *Journal of neurophysiology* 44, 247-258.
- Lee, S.J., Escobedo-Lozoya, Y., Szatmari, E.M., and Yasuda, R. (2009). Activation of CaMKII in single dendritic spines during long-term potentiation. *Nature* 458, 299-304.
- Legendre, P., and Westbrook, G.L. (1990). The inhibition of single N-methyl-D-aspartate-activated channels by zinc ions on cultured rat neurones. *J Physiol* 429, 429-449.
- Levenson, J.M., O'Riordan, K.J., Brown, K.D., Trinh, M.A., Molfese, D.L., and Sweatt, J.D. (2004a). Regulation of Histone Acetylation during Memory Formation in the Hippocampus. *Journal of Biological Chemistry* 279, 40545-40559.
- Levenson, J.M., O'Riordan, K.J., Brown, K.D., Trinh, M.A., Molfese, D.L., and Sweatt, J.D. (2004b). Regulation of histone acetylation during memory formation in the hippocampus. *J Biol Chem* 279, 40545-40559.
- Levenson, J.M., and Sweatt, J.D. (2006). Epigenetic mechanisms: a common theme in vertebrate and invertebrate memory formation. *Cell Mol Life Sci* 63, 1009-1016.
- Li, L., Stefan, M.I., and Le Novère, N. (2012). Calcium Input Frequency, Duration and Amplitude Differentially Modulate the Relative Activation of Calcineurin and CaMKII. *PLoS ONE* 7, e43810.
- Li, M., Xia, T., Jiang, C.-S., Li, L.-J., Fu, J.-L., and Zhou, Z.-C. (2003). Cadmium directly induced the opening of membrane permeability pore of mitochondria which possibly involved in cadmium-triggered apoptosis. *Toxicology* 194, 19-33.
- Lidke, D.S., Huang, F., Post, J.N., Rieger, B., Wilsbacher, J., Thomas, J.L., Pouysségur, J., Jovin, T.M., and Lenormand, P. (2010). ERK Nuclear Translocation Is Dimerization-independent but Controlled by the Rate of Phosphorylation. *Journal of Biological Chemistry* 285, 3092-3102.

- Lindecke, A., Korte, M., Zagrebelsky, M., Horejschi, V., Elvers, M., Widera, D., Prullage, M., Pfeiffer, J., Kaltschmidt, B., and Kaltschmidt, C. (2006). Long-term depression activates transcription of immediate early transcription factor genes: involvement of serum response factor/Elk-1. *Eur J Neurosci* 24, 555-563.
- Ling, D.S., Benardo, L.S., Serrano, P.A., Blace, N., Kelly, M.T., Crary, J.F., and Sacktor, T.C. (2002). Protein kinase Mzeta is necessary and sufficient for LTP maintenance. *Nat Neurosci* 5, 295-296.
- Link, W., Konietzko, U., Kauselmann, G., Krug, M., Schwanke, B., Frey, U., and Kuhl, D. (1995). Somatodendritic expression of an immediate early gene is regulated by synaptic activity. *Proc Natl Acad Sci U S A* 92, 5734-5738.
- Lisman, J., Schulman, H., and Cline, H. (2002). The molecular basis of CaMKII function in synaptic and behavioural memory. *Nat Rev Neurosci* 3, 175-190.
- Lisman, J., Yasuda, R., and Raghavachari, S. (2012). Mechanisms of CaMKII action in long-term potentiation. *Nat Rev Neurosci* 13, 169-182.
- Lonze, B.E., and Ginty, D.D. (2002). Function and regulation of CREB family transcription factors in the nervous system. *Neuron* 35, 605-623.
- Lu, Q., Hutchins, A.E., Doyle, C.M., Lundblad, J.R., and Kwok, R.P. (2003). Acetylation of cAMP-responsive element-binding protein (CREB) by CREB-binding protein enhances CREB-dependent transcription. *J Biol Chem* 278, 15727-15734.
- Lu, Y.M., Roder, J.C., Davidow, J., and Salter, M.W. (1998). Src Activation in the Induction of Long-Term Potentiation in CA1 Hippocampal Neurons. *Science* 279, 1363-1368.
- Lynch, G., Larson, J., Kelso, S., Barrionuevo, G., and Schottler, F. (1983). Intracellular injections of EGTA block induction of hippocampal long-term potentiation. *Nature* 305, 719-721.
- Magee, J.C. (2000). Dendritic integration of excitatory synaptic input. *Nat Rev Neurosci* 1, 181-190.
- Magee, J.C., and Cook, E.P. (2000). Somatic EPSP amplitude is independent of synapse location in hippocampal pyramidal neurons. *Nat Neurosci* 3, 895-903.

- Maharana, C., Sharma, K.P., and Sharma, S.K. (2013). Feedback Mechanism in Depolarization-Induced Sustained Activation of Extracellular Signal-Regulated Kinase in the Hippocampus. *Sci Rep* 3.
- Malenka, R.C., Kauer, J.A., Zucker, R.S., and Nicoll, R.A. (1988). Postsynaptic Calcium Is Sufficient for Potentiation of Hippocampal Synaptic Transmission. *Science* 242, 81-84.
- Maletic-Savatic, M., Malinow, R., and Svoboda, K. (1999). Rapid dendritic morphogenesis in CA1 hippocampal dendrites induced by synaptic activity. *Science* 283, 1923-1927.
- Malinow, R., Otmakhov, N., Blum, K.I., and Lisman, J. (1994). Visualizing hippocampal synaptic function by optical detection of Ca<sup>2+</sup> entry through the N-methyl-D-aspartate channel. *Proceedings of the National Academy of Sciences* 91, 8170-8174.
- Malinow, R., Schulman, H., and Tsien, R. (1989). Inhibition of postsynaptic PKC or CaMKII blocks induction but not expression of LTP. *Science* 245, 862-866.
- Man, H.-Y., Wang, Q., Lu, W.-Y., Ju, W., Ahmadian, G., Liu, L., D'Souza, S., Wong, T.P., Taghibiglou, C., Lu, J., *et al.* (2003). Activation of PI3-Kinase Is Required for AMPA Receptor Insertion during LTP of mEPSCs in Cultured Hippocampal Neurons. *Neuron* 38, 611-624.
- Mao, L., Yang, L., Arora, A., Choe, E.S., Zhang, G., Liu, Z., Fibuch, E.E., and Wang, J.Q. (2005a). Role of Protein Phosphatase 2A in mGluR5-regulated MEK/ERK Phosphorylation in Neurons. *Journal of Biological Chemistry* 280, 12602-12610.
- Mao, L., Yang, L., Tang, Q., Samdani, S., Zhang, G., and Wang, J.Q. (2005b). The Scaffold Protein Homer1b/c Links Metabotropic Glutamate Receptor 5 to Extracellular Signal-Regulated Protein Kinase Cascades in Neurons. *The Journal of Neuroscience* 25, 2741-2752.
- Markevich, N.I., Tsyganov, M.A., Hoek, J.B., and Kholodenko, B.N. (2006). Long-range signaling by phosphoprotein waves arising from bistability in protein kinase cascades. *Mol Syst Biol* 2, 61.
- Martin, K.C., Michael, D., Rose, J.C., Barad, M., Casadio, A., Zhu, H., and Kandel, E.R. (1997). MAP Kinase Translocates into the Nucleus of the Presynaptic Cell and Is Required for Long-Term Facilitation in Aplysia. *Neuron* 18, 899-912.
- Martin, K.C., and Zukin, R.S. (2006). RNA Trafficking and Local Protein Synthesis in Dendrites: An Overview. *The Journal of Neuroscience* 26, 7131-7134.

- Martin, S.J., Grimwood, P.D., and Morris, R.G.M. (2000). Synaptic Plasticity and Memory: An Evaluation of the Hypothesis. *Annual Review of Neuroscience* 23, 649-711.
- Matsuzaki, M., Ellis-Davies, G.C., Nemoto, T., Miyashita, Y., Iino, M., and Kasai, H. (2001). Dendritic spine geometry is critical for AMPA receptor expression in hippocampal CA1 pyramidal neurons. *Nat Neurosci* 4, 1086-1092.
- Matsuzaki, M., Honkura, N., Ellis-Davies, G.C., and Kasai, H. (2004). Structural basis of long-term potentiation in single dendritic spines. *Nature* 429, 761-766.
- Matsuzaki, M., and Kasai, H. (2011). Two-Photon Uncaging Microscopy. *Cold Spring Harbor Protocols* 2011, pdb.prot5620.
- Matthies, H. (1974). The biochemical basis of learning and memory. *Life sciences* 15, 2017-2031.
- Matthies, H. (1989). Neurobiological aspects of learning and memory. *Annu Rev Psychol* 40, 381-404.
- Matthies, H., Frey, U., Reymann, K., Krug, M., Jork, R., and Schroeder, H. (1990). Different mechanisms and multiple stages of LTP. *Advances in experimental medicine and biology* 268, 359-368.
- Matthies, H., and Reymann, K.G. (1993). Protein kinase A inhibitors prevent the maintenance of hippocampal long-term potentiation. *Neuroreport* 4, 712-714.
- Mayer, M.L., Vyklicky, L., and Westbrook, G.L. (1989). Modulation of excitatory amino acid receptors by group IIB metal cations in cultured mouse hippocampal neurones. *J Physiol* 415, 329-350.
- McAllister, A.K. (2000). Biolistic Transfection of Neurons. *Sci STKE* 2000, pl1-.
- McClatchey, A.I. (2007). Neurofibromatosis. *Annual Review of Pathology: Mechanisms of Disease* 2, 191-216.
- McHugh, T.J., Blum, K.I., Tsien, J.Z., Tonegawa, S., and Wilson, M.A. (1996). Impaired Hippocampal Representation of Space in CA1-Specific NMDAR1 Knockout Mice. *Cell* 87, 1339-1349.
- Meffert, M.K., Chang, J.M., Wiltgen, B.J., Fanselow, M.S., and Baltimore, D. (2003). NF- $\kappa$ B functions in synaptic signaling and behavior. *Nat Neurosci* 6, 1072-1078.

- Messaoudi, E., Kanhema, T., Soule, J., Tiron, A., Dagyte, G., da Silva, B., and Bramham, C.R. (2007). Sustained Arc/Arg3.1 synthesis controls long-term potentiation consolidation through regulation of local actin polymerization in the dentate gyrus in vivo. *The Journal of neuroscience : the official journal of the Society for Neuroscience* 27, 10445-10455.
- Miyawaki, A. (2003). Visualization of the Spatial and Temporal Dynamics of Intracellular Signaling. *Developmental Cell* 4, 295-305.
- Mochida, H., Sato, K., Sasaki, S., Yazawa, I., Kamino, K., and Momose-Sato, Y. (2001). Effects of anisomycin on LTP in the hippocampal CA1: long-term analysis using optical recording. *NeuroReport* 12, 987-991.
- Morozov, A., Muzzio, I.A., Bourtchouladze, R., Van-Strien, N., Lapidus, K., Yin, D., Winder, D.G., Adams, J.P., Sweatt, J.D., and Kandel, E.R. (2003). Rap1 couples cAMP signaling to a distinct pool of p42/44MAPK regulating excitability, synaptic plasticity, learning, and memory. *Neuron* 39, 309-325.
- Morris, R.G.M., Anderson, E., Lynch, G.S., and Baudry, M. (1986). Selective impairment of learning and blockade of long-term potentiation by an N-methyl-D-aspartate receptor antagonist, AP5. *Nature* 319, 774-776.
- Moser, M.-B., Trommald, M., Egeland, T., and Andersen, P. (1997). Spatial training in a complex environment and isolation alter the spine distribution differently in rat CA1 pyramidal cells. *The Journal of Comparative Neurology* 380, 373-381.
- Muller, W., and Connor, J.A. (1991). Dendritic spines as individual neuronal compartments for synaptic Ca<sup>2+</sup> responses. *Nature* 354, 73-76.
- Murakoshi, H., Lee, S.-J., and Yasuda, R. (2008). Highly sensitive and quantitative FRET-FLIM imaging in single dendritic spines using improved non-radiative YFP. *Brain Cell Biol* 36, 31-42.
- Murakoshi, H., Wang, H., and Yasuda, R. (2011). Local, persistent activation of Rho GTPases during plasticity of single dendritic spines. *Nature* 472, 100-104.
- Muslimov, I.A., Nimmrich, V., Hernandez, A.I., Tcherepanov, A., Sacktor, T.C., and Tiedge, H. (2004). Dendritic Transport and Localization of Protein Kinase M $\zeta$  mRNA. *Journal of Biological Chemistry* 279, 52613-52622.

- Nakamura, T., Barbara, J.G., Nakamura, K., and Ross, W.N. (1999). Synergistic release of Ca<sup>2+</sup> from IP<sub>3</sub>-sensitive stores evoked by synaptic activation of mGluRs paired with backpropagating action potentials. *Neuron* 24, 727-737.
- Nakamura, T., Lasser-Ross, N., Nakamura, K., and Ross, W.N. (2002). Spatial Segregation and Interaction of Calcium Signalling Mechanisms in Rat Hippocampal CA1 Pyramidal Neurons. *J Physiol* 543, 465-480.
- Nayak, A., Zastrow, D.J., Lickteig, R., Zahniser, N.R., and Browning, M.D. (1998). Maintenance of late-phase LTP is accompanied by PKA-dependent increase in AMPA receptor synthesis. *Nature* 394, 680-683.
- Neyman, S., and Manahan-Vaughan, D. (2008). Metabotropic glutamate receptor 1 (mGluR1) and 5 (mGluR5) regulate late phases of LTP and LTD in the hippocampal CA1 region in vitro. *European Journal of Neuroscience* 27, 1345-1352.
- Nguyen, P.V., Abel, T., and Kandel, E.R. (1994). Requirement of a critical period of transcription for induction of a late phase of LTP. *Science* 265, 1104-1107.
- Nguyen, P.V., and Kandel, E.R. (1997). Brief theta-burst stimulation induces a transcription-dependent late phase of LTP requiring cAMP in area CA1 of the mouse hippocampus. *Learning & Memory* 4, 230-243.
- Nikonenko, I., Boda, B., Steen, S., Knott, G., Welker, E., and Muller, D. (2008). PSD-95 promotes synaptogenesis and multiinnervated spine formation through nitric oxide signaling. *The Journal of cell biology* 183, 1115-1127.
- Nimchinsky, E.A., Sabatini, B.L., and Svoboda, K. (2002). STRUCTURE AND FUNCTION OF DENDRITIC SPINES. *Annual Review of Physiology* 64, 313-353.
- Nishiyama, M., Hong, K., Mikoshiba, K., Poo, M.M., and Kato, K. (2000). Calcium stores regulate the polarity and input specificity of synaptic modification. *Nature* 408, 584-588.
- Niswender, C.M., and Conn, P.J. (2010). Metabotropic Glutamate Receptors: Physiology, Pharmacology, and Disease. *Annual Review of Pharmacology and Toxicology* 50, 295-322.
- Noguchi, J., Matsuzaki, M., Ellis-Davies, G.C., and Kasai, H. (2005). Spine-neck geometry determines NMDA receptor-dependent Ca<sup>2+</sup> signaling in dendrites. *Neuron* 46, 609-622.
- O'Brien, J.A., and Lummis, S.C. (2006). Biolistic transfection of neuronal cultures using a hand-held gene gun. *Nat Protoc* 1, 977-981.

O'Riordan, K.J., Huang, I.C., Pizzi, M., Spano, P., Boroni, F., Egli, R., Desai, P., Fitch, O., Malone, L., Ahn, H.J., *et al.* (2006). Regulation of nuclear factor kappaB in the hippocampus by group I metabotropic glutamate receptors. *The Journal of neuroscience : the official journal of the Society for Neuroscience* 26, 4870-4879.

O'Sullivan, N.C., Pickering, M., Di Giacomo, D., Loscher, J.S., and Murphy, K.J. (2010). Mkl Transcription Cofactors Regulate Structural Plasticity in Hippocampal Neurons. *Cerebral Cortex* 20, 1915-1925.

Oh, W.C., Hill, T.C., and Zito, K. (2013). Synapse-specific and size-dependent mechanisms of spine structural plasticity accompanying synaptic weakening. *Proceedings of the National Academy of Sciences* 110, E305-E312.

Oliet, S.H., Malenka, R.C., and Nicoll, R.A. (1997). Two distinct forms of long-term depression coexist in CA1 hippocampal pyramidal cells. *Neuron* 18, 969-982.

Ortiz, J., Harris, H.W., Guitart, X., Terwilliger, R.Z., Haycock, J.W., and Nestler, E.J. (1995). Extracellular signal-regulated protein kinases (ERKs) and ERK kinase (MEK) in brain: Regional distribution and regulation by chronic morphine. *Journal of Neuroscience* 15, 1285-1297.

Otani, S., Marshall, C.J., Tate, W.P., Goddard, G.V., and Abraham, W.C. (1989). Maintenance of long-term potentiation in rat dentate gyrus requires protein synthesis but not messenger RNA synthesis immediately post-tetanization. *Neuroscience* 28, 519-526.

Otmakhov, N., Tao-Cheng, J.-H., Carpenter, S., Asrican, B., Dosemeci, A., Reese, T.S., and Lisman, J. (2004). Persistent Accumulation of Calcium/Calmodulin-Dependent Protein Kinase II in Dendritic Spines after Induction of NMDA Receptor-Dependent Chemical Long-Term Potentiation. *The Journal of Neuroscience* 24, 9324-9331.

Parker, D., Jhala, U.S., Radhakrishnan, I., Yaffe, M.B., Reyes, C., Shulman, A.I., Cantley, L.C., Wright, P.E., and Montminy, M. (1998). Analysis of an Activator:Coactivator Complex Reveals an Essential Role for Secondary Structure in Transcriptional Activation. *Molecular Cell* 2, 353-359.

Patterson, M., and Yasuda, R. (2011). Signalling pathways underlying structural plasticity of dendritic spines. *British Journal of Pharmacology* 163, 1626-1638.

Patterson, M.A., Szatmari, E.M., and Yasuda, R. (2010). AMPA receptors are exocytosed in stimulated spines and adjacent dendrites in a Ras-ERK-dependent manner during

long-term potentiation. *Proceedings of the National Academy of Sciences* 107, 15951-15956.

Paul, S., Nairn, A.C., Wang, P., and Lombroso, P.J. (2003). NMDA-mediated activation of the tyrosine phosphatase STEP regulates the duration of ERK signaling. *Nat Neurosci* 6, 34-42.

Pellegrino, M.J., and Stork, P.J.S. (2006). Sustained activation of extracellular signal-regulated kinase by nerve growth factor regulates c-fos protein stabilization and transactivation in PC12 cells. *J Neurochem* 99, 1480-1493.

Perkinton, M.S., Sihra, T.S., and Williams, R.J. (1999). Ca(2+)-permeable AMPA receptors induce phosphorylation of cAMP response element-binding protein through a phosphatidylinositol 3-kinase-dependent stimulation of the mitogen-activated protein kinase signaling cascade in neurons. *The Journal of neuroscience : the official journal of the Society for Neuroscience* 19, 5861-5874.

Perlson, E., Hanz, S., Ben-Yaakov, K., Segal-Ruder, Y., Seger, R., and Fainzilber, M. (2005). Vimentin-dependent spatial translocation of an activated MAP kinase in injured nerve. *Neuron* 45, 715-726.

Perlson, E., Michaelevski, I., Kowalsman, N., Ben-Yaakov, K., Shaked, M., Seger, R., Eisenstein, M., and Fainzilber, M. (2006). Vimentin binding to phosphorylated Erk sterically hinders enzymatic dephosphorylation of the kinase. *J Mol Biol* 364, 938-944.

Pettit, D.L., Perlman, S., and Malinow, R. (1994). Potentiated transmission and prevention of further LTP by increased CaMKII activity in postsynaptic hippocampal slice neurons. *Science* 266, 1881-1885.

Plant, K., Pelkey, K.A., Bortolotto, Z.A., Morita, D., Terashima, A., McBain, C.J., Collingridge, G.L., and Isaac, J.T. (2006). Transient incorporation of native GluR2-lacking AMPA receptors during hippocampal long-term potentiation. *Nat Neurosci* 9, 602-604.

Pockett, S., Slack, J.R., and Peacock, S. (1993). Cyclic AMP and long-term potentiation in the CA1 region of rat hippocampus. *Neuroscience* 52, 229-236.

Pologruto, T.A., Sabatini, B.L., and Svoboda, K. (2003). ScanImage: Flexible software for operating laser-scanning microscopes. *Biomed Eng Online* 2, 13.

Posern, G., and Treisman, R. (2006). Actin together: serum response factor, its cofactors and the link to signal transduction. *Trends in cell biology* 16, 588-596.

Power, J.M., and Sah, P. (2002). Nuclear Calcium Signaling Evoked by Cholinergic Stimulation in Hippocampal CA1 Pyramidal Neurons. *The Journal of Neuroscience* 22, 3454-3462.

Pulido, R., Zuniga, A., and Ullrich, A. (1998). PTP-SL and STEP protein tyrosine phosphatases regulate the activation of the extracellular signal-regulated kinases ERK1 and ERK2 by association through a kinase interaction motif. *EMBO J* 17, 7337-7350.

Raymond, C.R., and Redman, S.J. (2002). Different Calcium Sources Are Narrowly Tuned to the Induction of Different Forms of LTP. *Journal of neurophysiology* 88, 249-255.

Raymond, C.R., and Redman, S.J. (2006). Spatial segregation of neuronal calcium signals encodes different forms of LTP in rat hippocampus. *J Physiol* 570, 97-111.

Raymond, C.R., Thompson, V.L., Tate, W.P., and Abraham, W.C. (2000). Metabotropic glutamate receptors trigger homosynaptic protein synthesis to prolong long-term potentiation. *The Journal of neuroscience : the official journal of the Society for Neuroscience* 20, 969-976.

Redondo, R.L., and Morris, R.G. (2011). Making memories last: the synaptic tagging and capture hypothesis. *Nat Rev Neurosci* 12, 17-30.

Regehr, W.G., and Tank, D.W. (1990). Postsynaptic NMDA receptor-mediated calcium accumulation in hippocampal CA1 pyramidal cell dendrites. *Nature* 345, 807-810.

Reymann, K.G., Matthies, H.K., Schulzeck, K., and Matthies, H. (1989). N-methyl-D-aspartate receptor activation is required for the induction of both early and late phases of long-term potentiation in rat hippocampal slices. *Neuroscience letters* 96, 96-101.

Roberson, E.D., English, J.D., Adams, J.P., Selcher, J.C., Kondratieck, C., and Sweatt, J.D. (1999). The mitogen-activated protein kinase cascade couples PKA and PKC to cAMP response element binding protein phosphorylation in area CA1 of hippocampus. *The Journal of neuroscience : the official journal of the Society for Neuroscience* 19, 4337-4348.

Rongo, C., and Kaplan, J.M. (1999). CaMKII regulates the density of central glutamatergic synapses in vivo. *Nature* 402, 195-199.

Rotenberg, A., Mayford, M., Hawkins, R.D., Kandel, E.R., and Muller, R.U. (1996). Mice Expressing Activated CaMKII Lack Low Frequency LTP and Do Not Form Stable Place Cells in the CA1 Region of the Hippocampus. *Cell* 87, 1351-1361.

- Sabatini, B.L., Maravall, M., and Svoboda, K. (2001). Ca<sup>2+</sup> signaling in dendritic spines. *Curr Opin Neurobiol* 11, 349-356.
- Sabatini, B.L., Oertner, T.G., and Svoboda, K. (2002). The Life Cycle of Ca<sup>2+</sup> Ions in Dendritic Spines. *Neuron* 33, 439-452.
- Sacktor, T.C., Osten, P., Valsamis, H., Jiang, X., Naik, M.U., and Sublette, E. (1993). Persistent activation of the zeta isoform of protein kinase C in the maintenance of long-term potentiation. *Proceedings of the National Academy of Sciences* 90, 8342-8346.
- Sajikumar, S., Navakkode, S., Sacktor, T.C., and Frey, J.U. (2005). Synaptic Tagging and Cross-Tagging: The Role of Protein Kinase M $\zeta$  in Maintaining Long-Term Potentiation But Not Long-Term Depression. *The Journal of Neuroscience* 25, 5750-5756.
- Salinas, S., Briancon-Marjollet, A., Bossis, G., Lopez, M.A., Piechaczyk, M., Jariel-Encontre, I., Debant, A., and Hipskind, R.A. (2004). SUMOylation regulates nucleocytoplasmic shuttling of Elk-1. *The Journal of cell biology* 165, 767-773.
- Sananbenesi, F., Fischer, A., Schrick, C., Spiess, J., and Radulovic, J. (2002). Phosphorylation of hippocampal Erk-1/2, Elk-1, and p90-Rsk-1 during contextual fear conditioning: interactions between Erk-1/2 and Elk-1. *Mol Cell Neurosci* 21, 463-476.
- Sanhueza, M., Fernandez-Villalobos, G., Stein, I.S., Kasumova, G., Zhang, P., Bayer, K.U., Otmakhov, N., Hell, J.W., and Lisman, J. (2011). Role of the CaMKII/NMDA Receptor Complex in the Maintenance of Synaptic Strength. *The Journal of Neuroscience* 31, 9170-9178.
- Sanna, P.P., Cammalleri, M., Berton, F., Simpson, C., Lutjens, R., Bloom, F.E., and Francesconi, W. (2002). Phosphatidylinositol 3-Kinase Is Required for the Expression But Not for the Induction or the Maintenance of Long-Term Potentiation in the Hippocampal CA1 Region. *The Journal of Neuroscience* 22, 3359-3365.
- Schiller, J., Major, G., Koester, H.J., and Schiller, Y. (2000). NMDA spikes in basal dendrites of cortical pyramidal neurons. *Nature* 404, 285-289.
- Schiller, J., Schiller, Y., and Clapham, D.E. (1998). NMDA receptors amplify calcium influx into dendritic spines during associative pre- and postsynaptic activation. *Nat Neurosci* 1, 114-118.
- Schmitt, J.M., Guire, E.S., Saneyoshi, T., and Soderling, T.R. (2005). Calmodulin-Dependent Kinase Kinase/Calmodulin Kinase I Activity Gates Extracellular-Regulated Kinase-Dependent Long-Term Potentiation. *The Journal of Neuroscience* 25, 1281-1290.

Schneider, A., Mehmood, T., Pannetier, S., and Hanauer, A. (2011). Altered ERK/MAPK signaling in the hippocampus of the *mrsk2\_KO* mouse model of Coffin-Lowry syndrome. *Journal of Neurochemistry* 119, 447-459.

Schrader, L.A., Birnbaum, S.G., Nadin, B.M., Ren, Y., Bui, D., Anderson, A.E., and Sweatt, J.D. (2006). ERK/MAPK regulates the Kv4.2 potassium channel by direct phosphorylation of the pore-forming subunit. *Am J Physiol Cell Physiol* 290, C852-861.

Sekine, K., Kawauchi, T., Kubo, K., Honda, T., Herz, J., Hattori, M., Kinashi, T., and Nakajima, K. (2012). Reelin controls neuronal positioning by promoting cell-matrix adhesion via inside-out activation of integrin  $\alpha 5\beta 1$ . *Neuron* 76, 353-369.

Selcher, J.C., Weeber, E.J., Christian, J., Nekrasova, T., Landreth, G.E., and Sweatt, J.D. (2003). A Role for ERK MAP Kinase in Physiologic Temporal Integration in Hippocampal Area CA1. *Learning & Memory* 10, 26-39.

Serrano, P., Yao, Y., and Sacktor, T.C. (2005). Persistent Phosphorylation by Protein Kinase M $\zeta$  Maintains Late-Phase Long-Term Potentiation. *The Journal of Neuroscience* 25, 1979-1984.

Sevetson, B.R., Kong, X., and Lawrence, J.C. (1993). Increasing cAMP attenuates activation of mitogen-activated protein kinase. *Proceedings of the National Academy of Sciences* 90, 10305-10309.

Sgambato, V., Pages, C., Rogard, M., Besson, M.J., and Caboche, J. (1998). Extracellular signal-regulated kinase (ERK) controls immediate early gene induction on corticostriatal stimulation. *The Journal of neuroscience : the official journal of the Society for Neuroscience* 18, 8814-8825.

Sheng, M., and Hoogenraad, C.C. (2007). The postsynaptic architecture of excitatory synapses: a more quantitative view. *Annu Rev Biochem* 76, 823-847.

Silva, A., Stevens, C., Tonegawa, S., and Wang, Y. (1992a). Deficient hippocampal long-term potentiation in alpha-calcium-calmodulin kinase II mutant mice. *Science* 257, 201-206.

Silva, A.J., Frankland, P.W., Marowitz, Z., Friedman, E., Laszlo, G.S., Cioffi, D., Jacks, T., and Bourtchuladze, R. (1997). A mouse model for the learning and memory deficits associated with neurofibromatosis type I. *Nat Genet* 15, 281-284.

Silva, A.J., Paylor, R., Wehner, J.M., and Tonegawa, S. (1992b). Impaired Spatial Learning in  $\alpha$ -Calcium-Calmodulin Kinase II Mutant Mice. *Science* 257, 206-211.

- Smith, M.A., Ellis-Davies, G.C., and Magee, J.C. (2003). Mechanism of the distance-dependent scaling of Schaffer collateral synapses in rat CA1 pyramidal neurons. *J Physiol* 548, 245-258.
- Sorra, K.E., and Harris, K.M. (1998). Stability in synapse number and size at 2 hr after long-term potentiation in hippocampal area CA1. *The Journal of neuroscience : the official journal of the Society for Neuroscience* 18, 658-671.
- Spacek, J., and Harris, K.M. (1997). Three-dimensional organization of smooth endoplasmic reticulum in hippocampal CA1 dendrites and dendritic spines of the immature and mature rat. *The Journal of neuroscience : the official journal of the Society for Neuroscience* 17, 190-203.
- Spruston, N. (2008). Pyramidal neurons: dendritic structure and synaptic integration. *Nat Rev Neurosci* 9, 206-221.
- Squire, L.R. (1992). Memory and the hippocampus: a synthesis from findings with rats, monkeys, and humans. *Psychol Rev* 99, 195-231.
- Stanton, P., and Sarvey, J. (1984). Blockade of long-term potentiation in rat hippocampal CA1 region by inhibitors of protein synthesis. *The Journal of Neuroscience* 4, 3080-3088.
- Steward, O., and Schuman, E.M. (2001). Protein synthesis at synaptic sites on dendrites. *Annu Rev Neurosci* 24, 299-325.
- Stoppini, L., Buchs, P.A., and Muller, D. (1991). A simple method for organotypic cultures of nervous tissue. *Journal of Neuroscience Methods* 37, 173-182.
- Strack, S., and Colbran, R.J. (1998). Autophosphorylation-dependent Targeting of Calcium/ Calmodulin-dependent Protein Kinase II by the NR2B Subunit of the N-Methyl- d-aspartate Receptor. *Journal of Biological Chemistry* 273, 20689-20692.
- Sun, P., Lou, L., and Maurer, R.A. (1996). Regulation of activating transcription factor-1 and the cAMP response element-binding protein by Ca<sup>2+</sup>/calmodulin-dependent protein kinases type I, II, and IV. *J Biol Chem* 271, 3066-3073.
- Sutton, M.A., and Schuman, E.M. (2006). Dendritic protein synthesis, synaptic plasticity, and memory. *Cell* 127, 49-58.
- Svoboda, K., Tank, D.W., and Denk, W. (1996). Direct measurement of coupling between dendritic spines and shafts. *Science* 272, 716-719.

- Sweatt, J.D. (2001). The neuronal MAP kinase cascade: a biochemical signal integration system subserving synaptic plasticity and memory. *J Neurochem* 76, 1-10.
- Sweatt, J.D. (2004). Mitogen-activated protein kinases in synaptic plasticity and memory. *Curr Opin Neurobiol* 14, 311-317.
- Takahashi, N., Kitamura, K., Matsuo, N., Mayford, M., Kano, M., Matsuki, N., and Ikegaya, Y. (2012). Locally synchronized synaptic inputs. *Science* 335, 353-356.
- Tanaka, J., Horiike, Y., Matsuzaki, M., Miyazaki, T., Ellis-Davies, G.C., and Kasai, H. (2008). Protein synthesis and neurotrophin-dependent structural plasticity of single dendritic spines. *Science* 319, 1683-1687.
- Tanaka, K., and Augustine, G.J. (2008). A positive feedback signal transduction loop determines timing of cerebellar long-term depression. *Neuron* 59, 608-620.
- Thiels, E., Kanterewicz, B.I., Norman, E.D., Trzaskos, J.M., and Klann, E. (2002). Long-term depression in the adult hippocampus in vivo involves activation of extracellular signal-regulated kinase and phosphorylation of Elk-1. *The Journal of neuroscience : the official journal of the Society for Neuroscience* 22, 2054-2062.
- Thomas, G.M., and Huganir, R.L. (2004). MAPK cascade signalling and synaptic plasticity. *Nat Rev Neurosci* 5, 173-183.
- Thompson, K.R., Otis, K.O., Chen, D.Y., Zhao, Y., O'Dell, T.J., and Martin, K.C. (2004). Synapse to nucleus signaling during long-term synaptic plasticity; a role for the classical active nuclear import pathway. *Neuron* 44, 997-1009.
- Tian, L., Hires, S.A., Mao, T., Huber, D., Chiappe, M.E., Chalasani, S.H., Petreanu, L., Akerboom, J., McKinney, S.A., Schreier, E.R., *et al.* (2009). Imaging neural activity in worms, flies and mice with improved GCaMP calcium indicators. *Nat Methods* 6, 875-881.
- Tischmeyer, W., and Grimm, R. (1999). Activation of immediate early genes and memory formation. *Cell Mol Life Sci* 55, 564-574.
- Tongiorgi, E., Righi, M., and Cattaneo, A. (1997). Activity-dependent dendritic targeting of BDNF and TrkB mRNAs in hippocampal neurons. *The Journal of neuroscience : the official journal of the Society for Neuroscience* 17, 9492-9505.

Trifilieff, P., Herry, C., Vanhoutte, P., Caboche, J., Desmedt, A., Riedel, G., Mons, N., and Micheau, J. (2006). Foreground contextual fear memory consolidation requires two independent phases of hippocampal ERK/CREB activation. *Learn Mem* 13, 349-358.

Trifilieff, P., Lavaur, J., Pascoli, V., Kappès, V., Brami-Cherrier, K., Pagès, C., Micheau, J., Caboche, J., and Vanhoutte, P. (2009). Endocytosis controls glutamate-induced nuclear accumulation of ERK. *Molecular and Cellular Neuroscience* 41, 325-336.

Tsien, J.Z., Huerta, P.T., and Tonegawa, S. (1996). The Essential Role of Hippocampal CA1 NMDA Receptor Dependent Synaptic Plasticity in Spatial Memory. *Cell* 87, 1327-1338.

Tsokas, P., Grace, E.A., Chan, P., Ma, T., Sealfon, S.C., Iyengar, R., Landau, E.M., and Blitzer, R.D. (2005). Local protein synthesis mediates a rapid increase in dendritic elongation factor 1A after induction of late long-term potentiation. *The Journal of neuroscience : the official journal of the Society for Neuroscience* 25, 5833-5843.

Tyan, S.W., Tsai, M.C., Lin, C.L., Ma, Y.L., and Lee, E.H. (2008). Serum- and glucocorticoid-inducible kinase 1 enhances zif268 expression through the mediation of SRF and CREB1 associated with spatial memory formation. *J Neurochem* 105, 820-832.

Van Harreveld, A., and Fifkova, E. (1975). Swelling of dendritic spines in the fascia dentata after stimulation of the perforant fibers as a mechanism of post-tetanic potentiation. *Exp Neurol* 49, 736-749.

Vanhoutte, P., Barnier, J.V., Guibert, B., Pages, C., Besson, M.J., Hipskind, R.A., and Caboche, J. (1999). Glutamate induces phosphorylation of Elk-1 and CREB, along with c-fos activation, via an extracellular signal-regulated kinase-dependent pathway in brain slices. *Mol Cell Biol* 19, 136-146.

Varga, A.W., Anderson, A.E., Adams, J.P., Vogel, H., and Sweatt, J.D. (2000). Input-Specific Immunolocalization of Differentially Phosphorylated Kv4.2 in the Mouse Brain. *Learning & Memory* 7, 321-332.

Vickers, C.A., Dickson, K.S., and Wyllie, D.J.A. (2005). Induction and maintenance of late-phase long-term potentiation in isolated dendrites of rat hippocampal CA1 pyramidal neurones. *J Physiol* 568, 803-813.

Volk, L.J., Bachman, J.L., Johnson, R., Yu, Y., and Huganir, R.L. (2013). PKM-zeta is not required for hippocampal synaptic plasticity, learning and memory. *Nature* 493, 420-423.

- Vossler, M.R., Yao, H., York, R.D., Pan, M.G., Rim, C.S., and Stork, P.J. (1997). cAMP activates MAP kinase and Elk-1 through a B-Raf- and Rap1-dependent pathway. *Cell* 89, 73-82.
- Wang, L., and Proud, C.G. (2002). Ras/Erk Signaling Is Essential for Activation of Protein Synthesis by Gq Protein-Coupled Receptor Agonists in Adult Cardiomyocytes. *Circulation Research* 91, 821-829.
- Wang, X., Snape, M., Klann, E., Stone, J.G., Singh, A., Petersen, R.B., Castellani, R.J., Casadesus, G., Smith, M.A., and Zhu, X. (2012). Activation of the extracellular signal-regulated kinase pathway contributes to the behavioral deficit of fragile x-syndrome. *Journal of Neurochemistry* 121, 672-679.
- Watanabe, S., Hong, M., Lasser-Ross, N., and Ross, W.N. (2006). Modulation of calcium wave propagation in the dendrites and to the soma of rat hippocampal pyramidal neurons. *J Physiol* 575, 455-468.
- Wenthold, R.J., Petralia, R.S., Blahos, J., II, and Niedzielski, A.S. (1996). Evidence for multiple AMPA receptor complexes in hippocampal CA1/CA2 neurons. *The Journal of neuroscience : the official journal of the Society for Neuroscience* 16, 1982-1989.
- West, A.E., Chen, W.G., Dalva, M.B., Dolmetsch, R.E., Kornhauser, J.M., Shaywitz, A.J., Takasu, M.A., Tao, X., and Greenberg, M.E. (2001). Calcium regulation of neuronal gene expression. *Proceedings of the National Academy of Sciences* 98, 11024-11031.
- Wiegert, J.S., Bengtson, C.P., and Bading, H. (2007). Diffusion and not active transport underlies and limits ERK1/2 synapse-to-nucleus signaling in hippocampal neurons. *J Biol Chem* 282, 29621-29633.
- Winder, D.G., Martin, K.C., Muzzio, I.A., Rohrer, D., Chruscinski, A., Kobilka, B., and Kandel, E.R. (1999). ERK plays a regulatory role in induction of LTP by theta frequency stimulation and its modulation by beta-adrenergic receptors. *Neuron* 24, 715-726.
- Wood, M.A., Kaplan, M.P., Park, A., Blanchard, E.J., Oliveira, A.M.M., Lombardi, T.L., and Abel, T. (2005). Transgenic mice expressing a truncated form of CREB-binding protein (CBP) exhibit deficits in hippocampal synaptic plasticity and memory storage. *Learning & Memory* 12, 111-119.
- Worley, P., Bhat, R., Baraban, J., Erickson, C., McNaughton, B., and Barnes, C. (1993). Thresholds for synaptic activation of transcription factors in hippocampus: correlation with long-term enhancement. *The Journal of Neuroscience* 13, 4776-4786.

- Wu, G.-Y., Deisseroth, K., and Tsien, R.W. (2001a). Spaced stimuli stabilize MAPK pathway activation and its effects on dendritic morphology. *Nat Neurosci* 4, 151-158.
- Wu, G.-Y., Deisseroth, K., and Tsien, R.W. (2001b). Activity-dependent CREB phosphorylation: convergence of a fast, sensitive calmodulin kinase pathway and a slow, less sensitive mitogen-activated protein kinase pathway. *Proc Natl Acad Sci U S A* 98, 2808-2813.
- Wu, J., Dent, P., Jelinek, T., Wolfman, A., Weber, M., and Sturgill, T. (1993). Inhibition of the EGF-activated MAP kinase signaling pathway by adenosine 3',5'-monophosphate. *Science* 262, 1065-1069.
- Wu, S.-P., Lu, K.-T., Chang, W.-C., and Gean, P.-W. (1999). Involvement of mitogen-activated protein kinase in hippocampal long-term potentiation. *Journal of Biomedical Science* 6, 409-417.
- Wu, X., and McMurray, C.T. (2001). Calmodulin kinase II attenuation of gene transcription by preventing cAMP response element-binding protein (CREB) dimerization and binding of the CREB-binding protein. *J Biol Chem* 276, 1735-1741.
- Xing, J., Ginty, D.D., and Greenberg, M.E. (1996). Coupling of the RAS-MAPK pathway to gene activation by RSK2, a growth factor-regulated CREB kinase. *Science* 273, 959-963.
- Xu, W., Chen, H., Du, K., Asahara, H., Tini, M., Emerson, B.M., Montminy, M., and Evans, R.M. (2001). A Transcriptional Switch Mediated by Cofactor Methylation. *Science* 294, 2507-2511.
- Yamamoto, Y., Lee, D., Kim, Y., Lee, B., Seo, C., Kawasaki, H., Kuroda, S., and Tanaka-Yamamoto, K. (2012). Raf Kinase Inhibitory Protein is Required for Cerebellar Long-Term Synaptic Depression by Mediating PKC-Dependent MAPK Activation. *The Journal of Neuroscience* 32, 14254-14264.
- Yang, L., Mao, L., Tang, Q., Samdani, S., Liu, Z., and Wang, J.Q. (2004). A Novel Ca<sup>2+</sup>-Independent Signaling Pathway to Extracellular Signal-Regulated Protein Kinase by Coactivation of NMDA Receptors and Metabotropic Glutamate Receptor 5 in Neurons. *The Journal of Neuroscience* 24, 10846-10857.
- Yang, S.H., Vickers, E., Brehm, A., Kouzarides, T., and Sharrocks, A.D. (2001). Temporal recruitment of the mSin3A-histone deacetylase corepressor complex to the ETS domain transcription factor Elk-1. *Mol Cell Biol* 21, 2802-2814.

- Yao, Y., Kelly, M.T., Sajikumar, S., Serrano, P., Tian, D., Bergold, P.J., Frey, J.U., and Sacktor, T.C. (2008). PKM $\zeta$  Maintains Late Long-Term Potentiation by N-Ethylmaleimide-Sensitive Factor/GluR2-Dependent Trafficking of Postsynaptic AMPA Receptors. *The Journal of Neuroscience* 28, 7820-7827.
- Yasuda, H., Barth, A.L., Stellwagen, D., and Malenka, R.C. (2003). A developmental switch in the signaling cascades for LTP induction. *Nat Neurosci* 6, 15-16.
- Yasuda, R. (2006). Imaging spatiotemporal dynamics of neuronal signaling using fluorescence resonance energy transfer and fluorescence lifetime imaging microscopy. *Curr Opin Neurobiol* 16, 551-561.
- Yasuda, R., Harvey, C.D., Zhong, H., Sobczyk, A., van Aelst, L., and Svoboda, K. (2006). Supersensitive Ras activation in dendrites and spines revealed by two-photon fluorescence lifetime imaging. *Nat Neurosci* 9, 283-291.
- Yu, X.-M., Askalan, R., Keil, G.J., and Salter, M.W. (1997). NMDA Channel Regulation by Channel-Associated Protein Tyrosine Kinase Src. *Science* 275, 674-678.
- Yuan, L.L., Adams, J.P., Swank, M., Sweatt, J.D., and Johnston, D. (2002). Protein kinase modulation of dendritic K<sup>+</sup> channels in hippocampus involves a mitogen-activated protein kinase pathway. *The Journal of neuroscience : the official journal of the Society for Neuroscience* 22, 4860-4868.
- Yuste, R., and Bonhoeffer, T. (2004). Genesis of dendritic spines: insights from ultrastructural and imaging studies. *Nat Rev Neurosci* 5, 24-34.
- Yuste, R., and Denk, W. (1995). Dendritic spines as basic functional units of neuronal integration. *Nature* 375, 682-684.
- Yuste, R., Majewska, A., Cash, S.S., and Denk, W. (1999). Mechanisms of Calcium Influx into Hippocampal Spines: Heterogeneity among Spines, Coincidence Detection by NMDA Receptors, and Optical Quantal Analysis. *The Journal of Neuroscience* 19, 1976-1987.
- Zanger, K., Radovick, S., and Wondisford, F.E. (2001). CREB Binding Protein Recruitment to the Transcription Complex Requires Growth Factor-Dependent Phosphorylation of Its GF Box. *Molecular Cell* 7, 551-558.
- Zhao, M., Adams, J.P., and Dudek, S.M. (2005). Pattern-dependent role of NMDA receptors in action potential generation: consequences on extracellular signal-regulated

kinase activation. *The Journal of neuroscience : the official journal of the Society for Neuroscience* 25, 7032-7039.

Zhu, J.J., Qin, Y., Zhao, M., Van Aelst, L., and Malinow, R. (2002). Ras and Rap control AMPA receptor trafficking during synaptic plasticity. *Cell* 110, 443-455.

## Biography

### Shenyu Zhai

#### Birthplace

Lanzhou, China

October 14, 1984

#### Education

##### **Ph.D. in Neurobiology**

Duke University, Durham, NC

August 2007 - May, 2013

##### **B.Sc. in Biochemistry**

The Chinese University of Hong Kong, Hong Kong, China

August 2002 - July 2007

#### Publications

- **Zhai, S.G.**, Park, E., Yasuda, R. (2013) Nuclear ERK signaling triggered by activation of a few dendritic spines. (Submitted)
- Chan, C.M., Tsoi, H., Chan, W.M., **Zhai, S.**, Wong, C.O., Yao, X., Chan, W.Y., Tsui, S.K., Chan, H.Y. (2009) The ion channel activity of the SARS-coronavirus 3a protein is linked to its pro-apoptotic function. *Int J Biochem Cell Biol.* 41(11):2232-9.

#### Awards and Honors

Duke University Graduate School Fellowship	2007-present
Duke University Graduate School Conference Travel Fellowship	2007-2009
CUHK Mainland China Undergraduate Scholarship	2002-2007
CUHK Liu Po Shan Scholarship	2004-2005
CUHK Dean's List Honor	2004-2005
CUHK Wu Chung Scholarship	2003-2004
CUHK Dean's List Honor	2003-2004